Development and Demonstration of Rapid Repair of Levee Breaching Technology

Donald Resio[1], Stanley Boc, Stephen Maynord, Donald Ward, and David Abraham

Duane Dudeck[2] and Brian Welsh

[1] Coastal & Hydraulics Laboratory, Engr. Res. and Dev. Ctr., Vicksburg, MS 39180-6199

[2] Oceaneering International, Inc., Hanover, MD 21076

Table of Contents

Preface

In 2007 the Department of Homeland Security provided initial funding for the development and demonstration of a Rapid Repair of Levee Breaching (RRLB). The initial concept development and testing was accomplished at the facilities of the Coastal and Hydraulics Laboratory (CHL), U.S, Amy Engineer Research and Development Center, Vicksburg, MS. Additional large scale testing were completed at the Hydraulic Engineering Research Unit in Stillwater, OK in September 2008.

This work represents original concepts that rely on the incompressibility of water and the use of fabrics and are measured against four key metrics. This study is of interest to not only the sponsors but also State and Local government agencies that work within the flood fighting arena.

Funding for this work was provided by The Homeland Security Advanced Research Projects Agency (HSARPA) and Southeast Region Research Inititative (SERRI).

This report was prepared by Dr. Donald Resio, Mr. Stanley Boc, Dr. Stephen Maynord, Dr. Donald Ward, Mr. David Abraham of CHL and Mr. Dwayne Dudeck and Brain Welsh of Oceaneering Inc.

The authors wish to thank Dr. Greg Hanson and his colleagues of the Hydraulic Engineering Research Unit in Stillwater OK.

Chapter 1

Introduction

The Department of Homeland Security (DHS) Directorate of Science and Technology (S&T) is tasked with researching and organizing the scientific, engineering, and technological resources of the United States and leveraging these existing resources into technological tools to help protect the homeland. As part of this task, in July of 2007, the Homeland Security Advanced Research Projects Agency (HSARPA) funded the initial phase of a project to develop and demonstrate concepts for Rapid Repair of Levee Breaches (RRLB). This first phase of the DHS-funded work showed good promise for several of the concepts under investigation; and in June of 2008, supplemental funding from the Southeast Region Research Initiative (SERRI) was provided to enable a second phase of this work in which some of these concepts were demonstrated at a large-scale facility in Stillwater, Oklahoma.

This report documents the work conducted under both phases of the DHS funding referenced above. The sections contained in this report are as follows:

1. Introduction;
2. Overview of the development approach;
3. Breaches in nature;
4. Discharge through a breach;
5. Small-scale (1:50) model concept testing and development;
6. Intermediate-scale (1:16) testing and development;
7. Large-scale model testing and demonstration;
8. Extrapolation to larger breaches; and
9. Conclusions and "Road Ahead."

As will be described in Chapter 3, levee breaches can occur very quickly in nature. Due to the nature of where they occur and the typical coincident conditions

related to the ongoing flooding, they can be very difficult to reach by overland routes. A prime example of the austerity of breach locations in terms of access and working conditions can be found in the breach in the 17th Street floodwall during Hurricane Katrina. At this site, the only method deemed feasible for repairing the breach, due to lack of ground accessibility and the high velocities of water moving through the breach, was to drop heavy (2000-lb) sand bags from a helicopter (Figure 1.1). This procedure took many days to complete. Since the water level in Lake Pontchartrain stayed high for several days (Figure 1.2), this allowed huge quantities of additional water to flow into the Metro New Orleans area, even after the hurricane had passed. As shown by the Interagency Performance Evaluation Taskforce (IPET) study, water flows into the Metro area from breaches in the 17th Street and London Avenue Canals (Figure 1.4) after noon local time on 29 August was much greater than the amount that entered during the storm itself. As can be seen in Figure 1.5, water levels within the Metro area of New Orleans continued to rise substantially for at least a day and a half following Katrina's passage. From economic analyses conducted by the IPET, this rise in water level contributed to approximately $1.5 Billion of additional direct damages.

Figure 1.1 *Helicopter deploying sandbags at the 17th St. Canal following Hurricane Katrina*

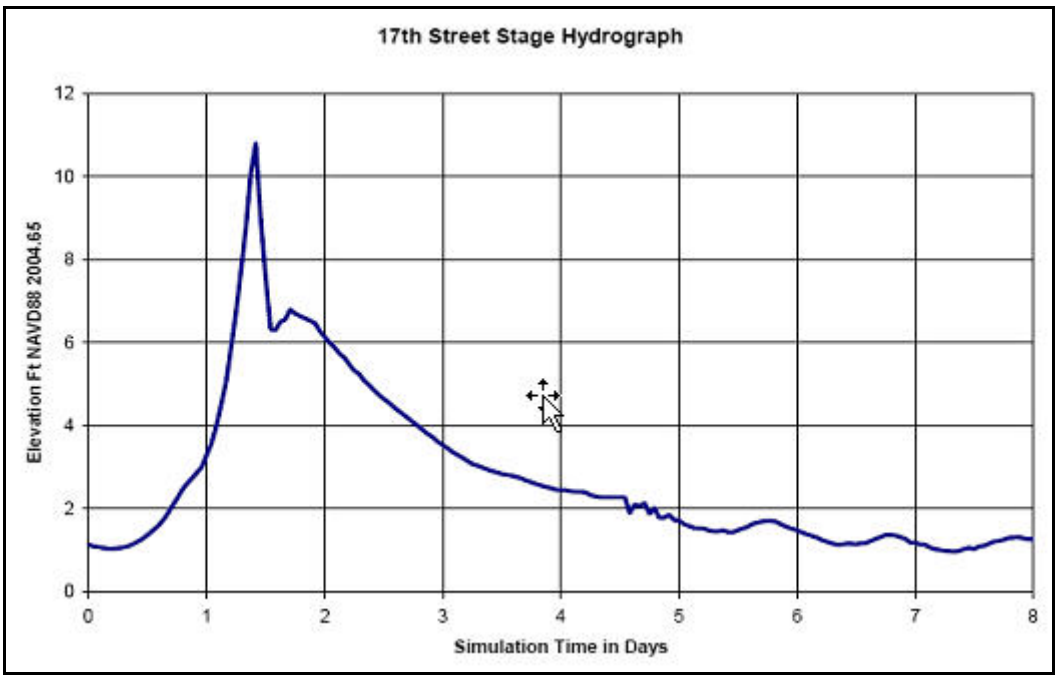

Figure 1.2 *Hydrograph of water levels from ADCIRC simulations for water levels during Hurricane Katrina.*

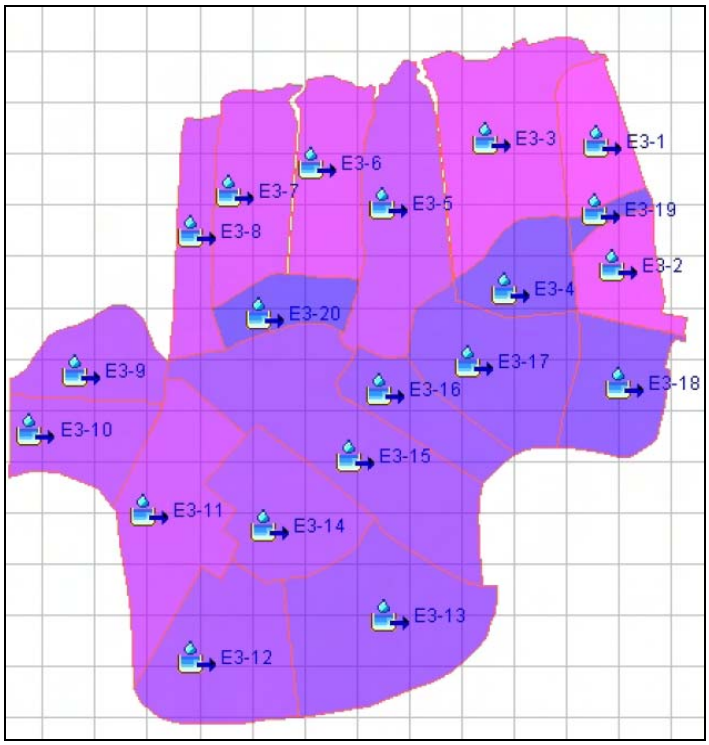

Figure 1.3 *Definitions of basins used in IPET study of flooding within the New Orleans area. The numbers following the hyphens denote sub-basin designations.*

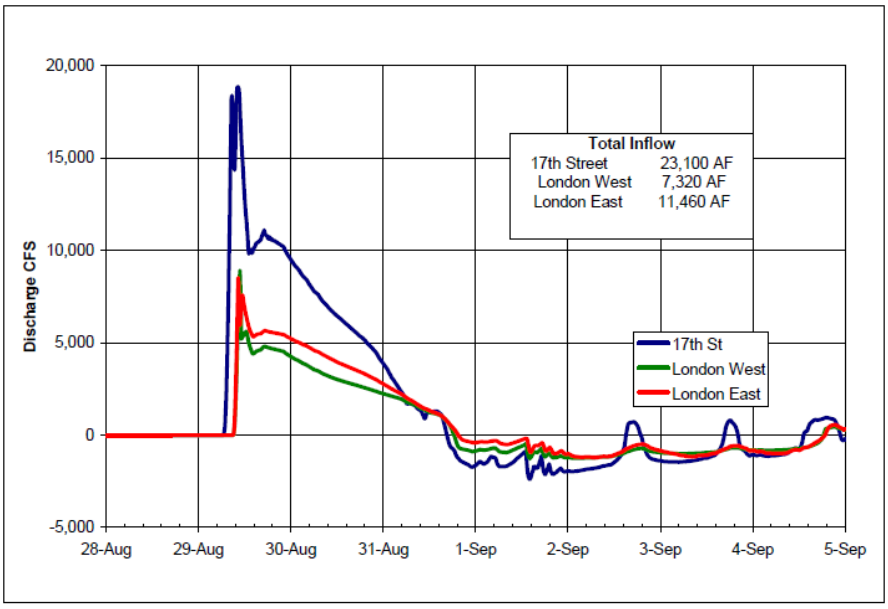

Figure 1.4 *Calculated flows through the breach in the 17th Street Canal and through the two breaches in the London Avenue Canal during the Hurricane Katrina flooding event, from results of the interior drainage study of IPET.*

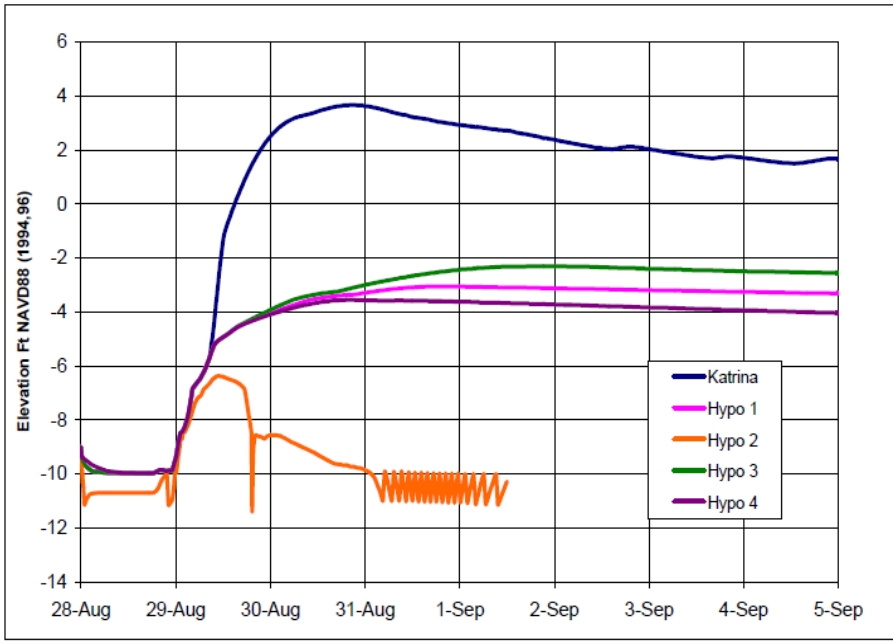

Figure 1.5 *Calculated Water-Surface Elevations in Storage Area 7 during the Katrina flooding event.*

From this example, we see that simply waiting for flow through breaches to subside or using slow repair methods can be an extremely costly decision in terms of allowing enormous additional direct damages. In the post-Katrina example cited here, the helicopter-lifted sandbags did not seal the breach until after the time that the water levels in Lake Pontchartrain had subsided to a level where significant flow was no longer coming into Metro New Orleans. The need for quickly closing a levee breach is also driven by the potentially fast vertical and lateral growth rates of breaches. As will be shown in Chapter 3 of this report, breach widths can grow at rates of 10's of feet to 100's of feet per hour, which can turn a small, repairable breach into a large, unrepairable breach in a matter of just a few hours.

From discussions in the previous paragraph, we see that the first critical metric for breach repair must be the time in which a system can be effectively deployed. As a nominal guideline for deployment time, the project team set a 6-hour time limit on the total time to deploy an effective rapid levee repair system. This time should include all time following the notice to proceed with the repairs up to the time that flow through the breach is halted. This obviously places some constraints on the availability of a system to deploy in the area where it is needed. This type of a constraint could be met by pre-positioning rapid levee repair systems in an area where they might be needed, either permanently or on a temporary basis.

Given the austerity of the physical settings along most levee areas in terms of land accessibility, which is usually greatly exacerbated during flooding events , it is highly unlikely that levee-repair systems that depend on land-based deployments can offer an effective solution in a timely manner. Furthermore, given the relative slowness of travel for ship-borne systems and problems at many sites with accessibility by marine routes (for example, access to the 17th Street Canal Breach and the London Avenue Breaches by a barge was blocked by debris and other obstructions), deployment by water may be impractical in many situations. These considerations dictate that the optimal deployment should be via airborne lift, with a likely requirement for on-ground personnel for assistance. Implicitly, this metric places some relatively stringent constraints on the

weight of the repair system, since practical limits for the lift capacity for helicopters is in the 20,000-30,000 pound range.

A second key metric for deployment of a rapid levee repair system is to be effectively deployable into a breach while the water is flowing through it. As shown in Chapter 4 of this report, flows through breaches depend primarily on the depth of the breach and the head difference between the water levels on either side of the breach. In extreme situations, such as simulated in that Chapter, we see that velocities in excess of 20 feet per second are expected. From this information, we expect that the transient forces on a rapid levee repair system will likely be much greater than the static forces. However, this should not be taken as implying that the static forces will be small. Thus, as will be discussed in Chapter 2, the levee repair system must be capable of withstanding and supporting very large forces across the breach. Another complication, related to actively closing a breach while water is flowing through it, is that the shape of the breach periphery can be relatively irregular and can change quickly during the closure procedure. This introduces some problems with sealing around the edges of a breach if a rigid structure is utilized in the closure.

A third metric for deployment is the amount of force that the rapid levee repair system imparts to the levees on either side of the breach. It is highly likely that the levees adjacent to the breach will be compromised somewhat by the same flooding that is causing the breach; therefore, very little reserve holding power will be available in such levees. Because of this, deployment systems and methods which minimize forces on adjacent levees will be considered to be superior to those which do not. From the previous paragraph, we see that this metric will be best met by systems which can distribute the deceleration of the flow over some amount of time rather than instantaneously stopping the flow.

A final metric that will be utilized here involves a measure of the repair system's complexity. In general, the more complex a system is, the more likely it is to fail. Repair systems that require extensive sequences of operations in series will always be very

difficult to field in severe environmental conditions such as levee breaches. Likewise, a system with many different system components will usually be more prone to failure than a system with only one or two components, simply due to the possibility of failure on any single component and difficulties in mechanically linking system components together in a high-force environment.

The metrics we have introduced here are realistic but at first glance appear extremely difficult to achieve. Having to survive and support very large forces, while still being lightweight, is a definite challenge. Keeping the system simple and yet with components that are deployable from airlift is another challenge. However, as will be seen subsequently in this report, having a set of difficult challenges such as these often provides focus for an approach to a solution. It should also be recognized that this project was oriented toward finding an innovative, near-term solution. It was not a multi-year effort designed to develop a foundation for answering questions related to rapid levee repair. Instead, it was a project designed to investigate the possibility of innovative approaches that might yield very near-term pay-offs in terms of technologies for effectively repairing levee breaches.

Chapter 2

Overview of the Development Approach

In this chapter, we will provide an overview of the different elements of this study. In particular, we will provide a foundation for understanding the nature of the problem of levee breach closure. It offers a brief perspective on the different requirements that must be met in order to stop the flow through a breach and the methods available for this. The theoretical foundations for much of this work are already established, so we will not go into extensive derivations for equations used in this section; however, we will at least attempt to provide sufficient background to understand the basic nature and magnitudes of the forces and problems that must be overcome in the development of effective rapid levee repair technologies.

It is obvious that two critical elements must be met to enable a breach closure. First, the system must be capable of being held in place and not wash through the breach. As an example of this, the weight of the sandbags dropped into the 17th Street Canal breach had to be sufficient to withstand the force of the current passing through the breach without being pushed through the breach. Second, the system must be capable of withstanding the forces acting on it without structural failure, where in this case, structure failure is taken to mean only that it loses its functionality.

Holding the system in place:

The system must be held in place both during emplacement and during the entire interval that it is expected to function in its final position. Means of accomplishing this are expected to involve one or more of the following anchoring methods:

1. ballast – where the weight of the system or system components is sufficient to resist the local forces acting on it;
2. anchoring – where the structure is physically connected into the underlying material in the vicinity of the breach; and

3. support from adjacent and underlying levee sections – where remaining levee sections along the sides and bottom of the breach are utilized to support the system.

As will be seen in the following section of this chapter, loading on anchor locations depends strongly on the number and distribution of "anchoring locations." We use the term anchoring locations here, since we do not want to imply that these are necessarily mechanical anchoring points. It is apparent that each of these methods will have different difficulties and obstacles to overcome and that different methods might work best in some areas, while others would work best in different areas. For example, the ballast anchoring method will rely much less on the geotechnical characteristics of material in the vicinity of the breach since it spreads the loading over the entire contact area underlying the ballast element; whereas, a mechanical anchor, such as one used to anchor ships or a helical anchor, can act more locally on the underlying soils and strata.

It should be noted here that adequate resources required to deploy mechanical anchors capable of holding the immense forces associated with the water flowing through the breach might be unavailable. Typical anchors and anchor handling systems on large ships weigh well in excess of the weight constraints imposed by being helicopter transportable. Furthermore, the holding capacity of such anchors varies substantially depending on the material into which these anchors are imbedded and the procedures used to "set" these anchors. Similarly, deployment of helical anchors into unknown or poorly known underlying materials may not offer very definitive holding capacities; and in situations where the currents are very high, such deployments might be extremely daunting, if not totally impossible. Thus, the use of mechanical anchors might not be very viable for rapid levee breach closures.

The ballast method offers a somewhat different set of challenges, primarily due to the large amount of weight required to resist the force of water passing through the breach. Although the weights of individual sandbags used in the 17th Street Canal closure were already very unwieldy, it should be recognized that the depth of flow over the sill of

this breach during most of the time it was being closed was only about 2 feet. For a large breach with 5 – 15 feet of flow over the sill, the size of the individual sandbags would become larger than available helicopter lift capacity. The implications of this are that the ballast method may also be quite difficult to implement in many cases, even for simplistic deployment scenarios.

A variation on the ballast concept, developed during the early phases of the present study was to use water as the primary source of weight for ballast. This theme will be reiterated several times during this report. The most available material at the site of a breach is water, so rather than bringing different materials to the site, it is advantageous for us to determine ways to effectively utilize water for as many purposes as possible. A simple means to provide very substantial ballast at a site is to fill fabric containers with water up to a level where they protrude above the water level in the vicinity of the breach. Water within the water column is essentially neutrally buoyant and contributes nothing to the ballast; however, all water above the surrounding water level contributes directly to the ballast weight. In this case, only the fabric container and the pumps have to be transported, which is quite feasible.

Forces in the vicinity of a breach:

Let us begin by considering a simple rectangular breach of width W and depth D, within a coordinate system with the breach opening aligned along the x axis, the vertical axis being denoted by z, and the axis perpendicular to the breach denoted by y (Figure 2.1). If water were not flowing through the breach, the static force pressure acting at any point within the water in the breach would be given by

$$p(x,z) = \rho g z \qquad (2.1)$$

where

x is the distance along the breach;
z is the distance from the surface;
ρ is the density of water; and
g is the acceleration due to gravity.

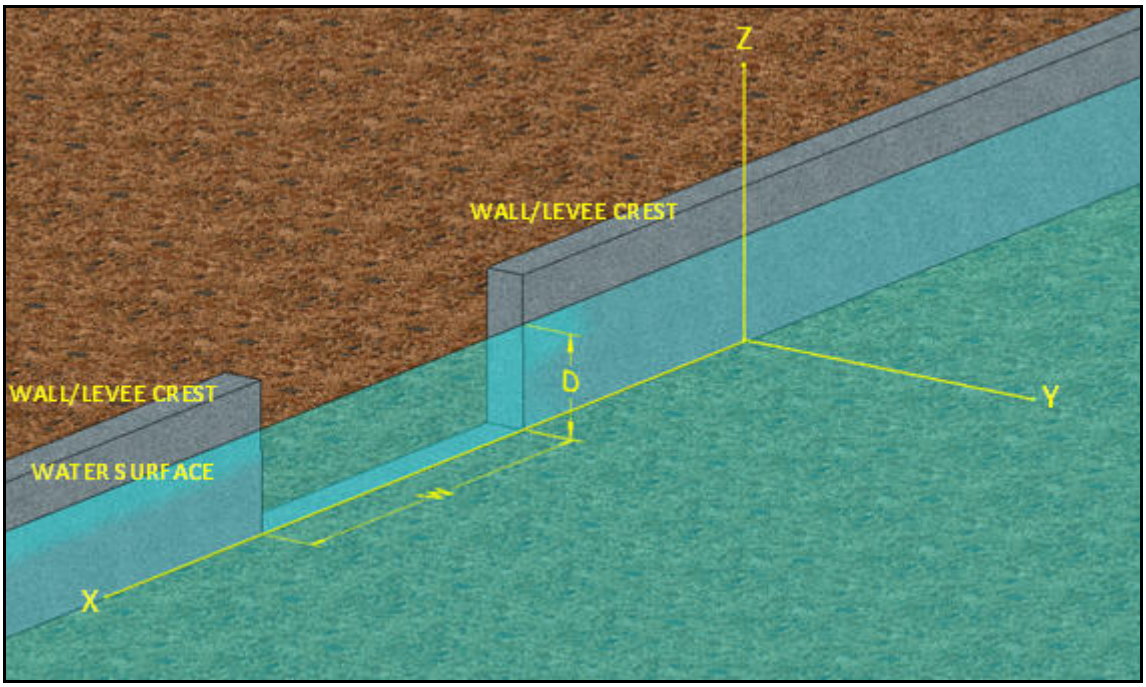

Figure 2.1. *Coordinate system used in this report.*

The total force for a given depth, D, per unit distance, x, along the breach would be obtained by integration over z and would be given by

$$F_y = \frac{\rho g D^2}{2} \tag{2.2}$$

where

F_x is the total force in the y direction per unit distance along the breach.

which shows that the static force is proportional to the square of the depth. Of course the total force acting across the entire width, W, of the breach would be

$$F_{tot} = \frac{\rho g W D^2}{2} \tag{2.3}$$

where

F_{tot} is the total force across the entire breach.

This shows that the total force is linearly dependent on the width of the breach. For a beam that spans the width of the breach to carry the static load of the water, it must be capable of carrying the moment generated by this load. The conventional simple form for the bending stress in such a beam is

$$\sigma = \frac{Mr}{I}$$

where

σ is the unit stress per area at the outer fiber of the beam in bending; 2.4

M is the bending moment;

r is the distance to the outer fiber from the neutral axis; and

I is the moment of inertia of the beam.

Therefore, the beam stress is proportional to the moment carried, which is given by:

$$M = \frac{F_{tot} W}{2} = \frac{\rho g W D^2 W}{4} = \frac{\rho g W^2 D^2}{4} \quad 2.5$$

From this equation we see that the moment that must be carried by the beam will be proportional to the breach width squared. Thus, the size of a breach critically influences the ability to span a breach in the absence of intermediate supports. The gist of this is that scale factors are extremely important in consideration of whether or not a concept that works well in a small-scale model is appropriate for prototype-scale applications.

Returning to the issue of the static force on a surface along the breach, we can calculate from equations 2.3-2.5 that the total force acting across a breach that is 40 feet wide and 15 feet deep will be approximately 281,000 pounds. An estimate of the potential dynamic forces on a structure during a closure can be obtained by examining the response of our hypothetical beam to the dynamic shut-down of the flow. As will be seen

in Chapter 4, extreme flows through the breach can reach velocities of 20 ft/sec or higher. Recognizing that the total deflection (δz) allowed in a beam spanning a 40-ft breach will be only on the order of 0.5 feet, the allowable time for deceleration will be approximately 0.025 seconds ($\frac{\delta z}{V}$ or 0.5 divided by 20), which shows that the sudden insertion of a semi-rigid structure into the breach would induce very large dynamic loads on the structure. In this case if we take the initial dynamic pressure from Bernoulli's Law

$$p_d = \frac{\rho V^2}{2} \qquad 2.6$$

where

p_d is the dynamic pressure at the time the structure is emplaced, and

V is the velocity of the current through the breach.

we see that the total dynamic pressure force over the entire breach opening through which water is flowing is, as expected, approximately the same magnitude as the static force. However, if we attempt to decelerate the flow to zero within 0.025 seconds, the force on our structure will be approximately 40 times greater than the static force. This certainly shows that some care must be taken in how quickly we allow a flow to be decelerated in our proposed levee breach closure systems.

Some Basic Concepts for stopping the flow utilizing fabrics

Many alternative methods for rapid levee repair were considered early in our research program and some of these will be discussed in Chapter 5 on our small-scale model tests. However, it was quickly realized that large structures (gated or non-gated) would be far too heavy to be airlifted into place. On one hand, it might be possible to use barges to transport such structural element; but this did not seem to be a very "universal" solution concept, so it was abandoned, at least in this phase of our work. During considerable discussion of alternatives, concepts which utilized water-filled fabric elements kept emerging as having the best possibilities of success. For the rest of this

chapter, we will address some simple concepts for using fabrics to carry loads in a fashion that might provide a suitable basis for a rapid levee repair system.

Fabrics have been used since ancient times as elements of expedient structures. For the most part, the basic concept has remained the same through the ages – use the fabric to carry tensile loads, while allowing rigid (non-fabric) structural elements to bear the compressive loads as shown in Figure 2.2. In the left-hand panel the structural columns provide the support for the fabrics; while in the right-hand panel, the anchoring into the rock provides the support for the tension.

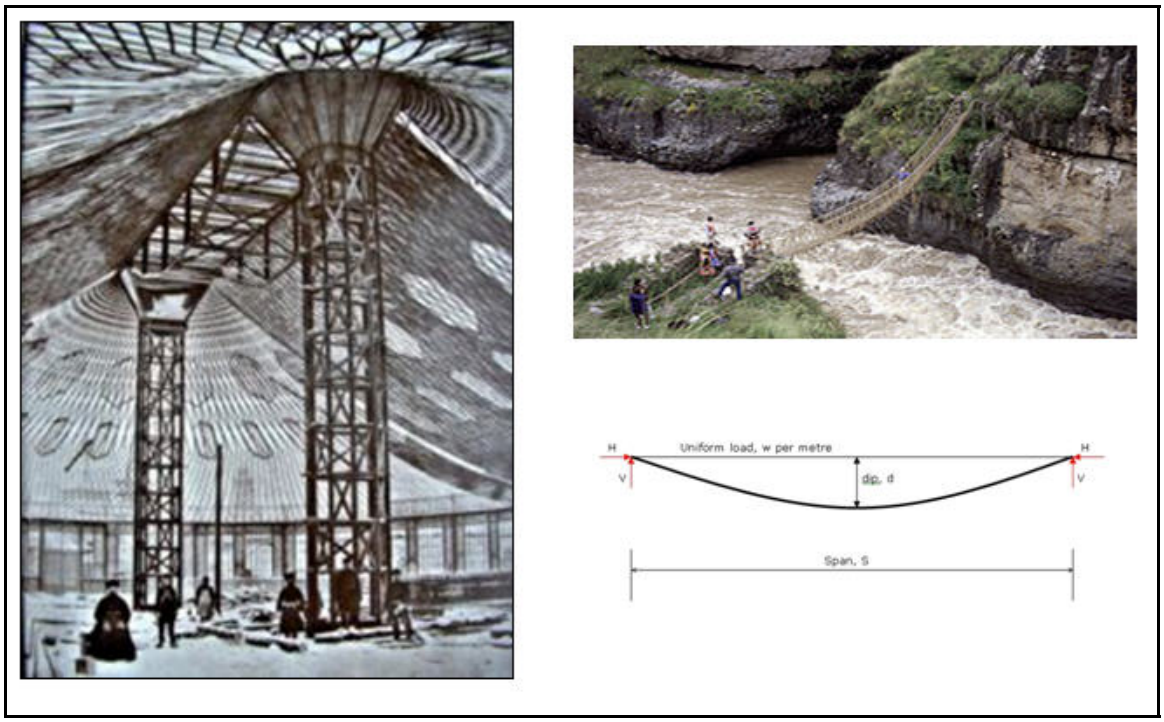

Figure 2.2. *Examples of fabrics in construction. The left hand panel shows the Oval Pavilion from the 1896 World's Fair, while the right-hand panels show the simple idea of using a rope structure to carry a load across a span.*

In the second half of the twentieth century, a new class of fabric structures began to emerge. These structures were based on the pressurization of an enclosed column of air and were typically termed "air-beams" or "inflated membrane structures." Many papers have been written on this topic and such structural elements have become an important part of NASA's space program, where such structural elements afford

significant advantages over rigid materials in many of NASA's mission applications. Some contributions to the application of air-beams to various types of structures and the theory of their deflections under loads can be found in Bulson (1973), Main *et al.* (1994), Cavallaro *et al.* (2007), and Wielgosz *et al.* (2008).

Most of NASA's requirements for air-beams involved relatively modest forces and did not directly treat forces of the magnitudes required for rapid levee repair systems. Fortunately, the principal investigator for the R&D effort described in this report already had extensive experience in the basic extrapolation of this technology to very large forces as the Technical Manager of an Army-sponsored Advanced Technology Demonstration (ATD). This ATD investigated the ability of a floating beam structure to act as an effective breakwater. Appendix A provides a brief description of the overall objective and solution methods examined on that project, which ended in a successful final demonstration.

For a pressurized tube, the bending under a load can be equated to an equivalent elastic beam (equation 2.4) with the substitution of the beams equivalent bending resistance term (EI) into that equation. A first approximation for this equivalency can be written as

$$EI = \frac{F_b D_t^2}{2\varepsilon_b}$$

where

2.7 F_b is the force required to stretch the fabric fibers in the tube to breaking;
ε_b is the fractional amount of stretch at the point of breaking; and
D_t is the diameter of the fabric tube.

A similar type of approximation to the allowable moment that can be carried by a pressurized fabric beam before wrinkling (structural failure) is given by

$$M_w = \frac{\pi P_t D_t^3}{8}$$

where

2.8 M_w is the maximum moment that can be carried before the tube wrinkles; and

P_t is the internal pressure within the tube.

Whereas the bending equation for the tube did not have the internal pressure explicitly within it, the equation for the wrinkling moment does. If we assume that the diameter of the tube will scale approximately as the depth of the water, we can rearrange this equation to solve for the pressure required to support the moment generated by the static load across the breach (for the moment neglecting the dynamic load). Unfortunately, this yields an estimate of almost 300 psi. Such an internal pressure would generate a tension around the perimeter of 54000 pounds per inch along the tube. Thus, the tensile breaking strength of a fabric needed to contain such a pressure would have to exceed 54,000 pounds in order for the tube not to explode. Given that this is well beyond the present "lightweight" fabric strengths and given that we did not even consider the additional effects of the dynamic forces, which would be much larger on such a rigid tube, this does not seem like a viable alternative for rapid levee repair systems. It should also be noted that the rigidity of the tube would make it very difficult to achieve a good seal along the edges of the breach. Consequently, this idea was abandoned.

Although we knew that it would still be possible to utilize fabric systems to generate very large ballast for holding rapid levee repair systems in place, we kept looking at new, more innovative methods of using water-filled tubes for this purpose. Finally, we recognized that a major difference between the focus of all of the NASA-funded work on pressurized fabric beams and the work that we were doing was that we were using water, which is essentially incompressible, while NASA research had focused on air, which is quite compressible. This led us to recognize that a new method of utilizing water-filled tubes was possible, one that was based purely on the resistance of the entire tube to volumetric deformation. This concept will be more thoroughly discussed in Chapter 6.

Chapter 3

Breaches in Nature

Both natural and man-made levees have a long history of breaching in nature. Natural levees, built from sediment deposition when rivers overflow their banks, occasionally breach in what is termed a crevasse. Throughout the US, failures of natural and man-made levees have resulted in lives lost, destroyed infrastructure, and huge economic losses. One example is the Midwest portion of the US containing the Upper Mississippi River, Missouri River, and their tributaries. The Midwest experiences flood events that result in levee failures. Figure 3.1 shows a levee failure on the Pin Oak levee in the Midwest. Figure 3.2 shows the Elm Point levee break from the Midwest.

Figure 3.1. Failure of the Pin Oak levee in Midwest.
Note sand bags atop levee used to fight rising water levels.

Figure 3.2. Failure of the Elm Point levee in Midwest.

Another area where levee failures are of great concern is the Sacramento-San Joaquin River Delta area. Major flood events have occurred in 1950, 1955, 1964, 1986, and 1997. Mount and Twiss (2004) report that the projected subsidence of the Delta indicates that it will "become increasingly difficult and expensive to maintain the Delta levee system." Some areas of the Delta are more than 8 m below sea level. This large amount of subsidence greatly increases the chance of piping related levee failures that will be discussed subsequently. Piping related failures are the major concern in these levees. Figure 3.3 shows the 2004 breach in the levee at the Upper Jones tract in the Sacramento-San Joaquin River Delta.

Figure 3.3. Upper Jones Tract levee Breach in the Sacramento-San Joaquin River Delta.

A third area where concerns about breaching are large is the Herbert Hoover Dike around Lake Okeechobee. According to Bromwell, Dean, and Vick (2006), the dike "in its existing condition (1999) is over 4000 times more likely to fail in any given year from these causes (piping and slope instability) than dams of its kind as a whole". The dike was originally built in response to a hurricane in 1928 that caused loss of life that is second only to the Galveston Hurricane of 1900. Hebert Hoover dike was originally intended to be a levee that has been traditionally viewed as only temporarily retaining water. It now serves more as a dam. "Herbert Hoover Dike was built from local materials by dredges or draglines without concern for material selection or the nature of the foundation soils (primarily muck and porous limestone) on which it was placed" (Bromwell, Dean, and Vick (2006). Piping related failures are the major concern at Herbert Hoover Dike.

The current focus on levee breaches was brought about by the large number of levee and floodwall failures that occurred in the New Orleans area in 2005 as a result of Hurricane Katrina. The specifics of the failures are documented in the IPET report. These failures became the most costly disaster in the history of the US. During Katrina, levees and floodwalls failed as a result of most of the different causes that will be discussed subsequently. Figure 3.4 shows the floodwall failure on the 17th Street Canal.

Figure 3.4. Floodwall failure on 17th Street Canal from Hurricane Katrina in New Orleans.

These examples show that levee breaching and the need to develop methods to rapidly repair levee breaches is a national problem. This chapter examines the various characteristics of levees and levee breaches that are important in developing techniques for rapid repair of levee breaches.

Typical Levee Sections

To develop methods for rapid repair of a levee breach, an evaluation must be made of the various configurations of levees found in nature. Several typical levee sections at projects throughout the nation are presented in the following paragraphs. Levee height can be defined several ways but height above the landside toe is used herein.

Mississippi River- From the headwaters to the Gulf of Mexico, the levees along the Mississippi River vary in size and configuration. In the Memphis District, the typical levee section shown on the Memphis District website is shown in Figure 3.5.

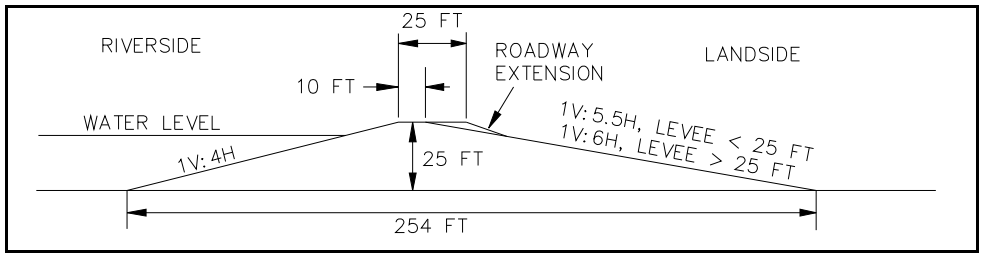

Figure 3.5. Typical levee cross section on Mississippi River in Memphis District.

Sacramento-San Joaquin River Delta- The Sacramento-San Joaquin River Delta has a wide variation in size and configuration of levees. The Delta Risk Management Strategy (DRMS) Phase 1, Topical Area Levee Vulnerability, Draft 2, Prepared by URS Corporation/Jack R. Benjamin and Associates, Inc, June 2007 shows the following ranges of levee characteristics: a) 7-26 ft levee height relative to landside toe, b) 1V:1H-1V:4.5H on riverside, c) 1V:1.5H-1V:5.5H on landside, and d) 11-38 ft crest width. Using averages of the data, the typical levee section used herein for the Sacramento-San Joaquin River Delta has a height of 18 ft, riverside and landside slopes of 1V:3H, and crest width of 20 ft as shown in Figure 3.6.

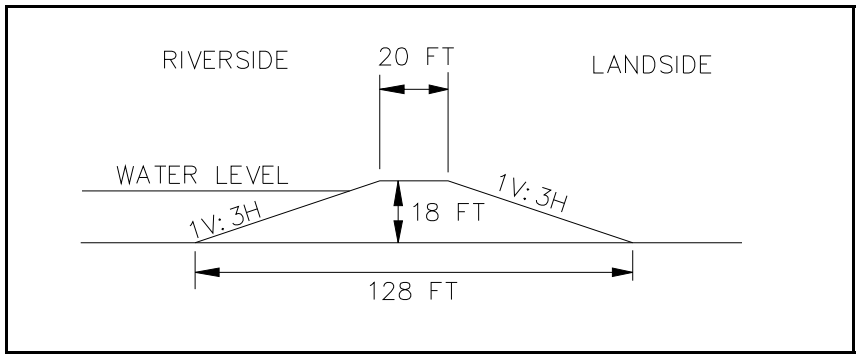

Figure 3.6. Typical levee cross section on Sacramento-San Joaquin River Delta.

Lake Okeechobee/Herbert Hoover Dike- Based on "Report of Expert Review Panel, Technical Evaluation of Herbert Hoover Dike, Lake Okeechobee, Florida", has a crest elevation of 32 to 46 ft with adjacent land elevation of about 10 to 18 ft. Lakeside slopes vary from 1V:10H to 1V:3H and landside slopes vary from 1V:5H to 1V:2H. Based on personal communication with Sam Honeycutt of the Jacksonville District, a typical levee section on the Herbert Hoover Dike is shown in Figure 3.7.

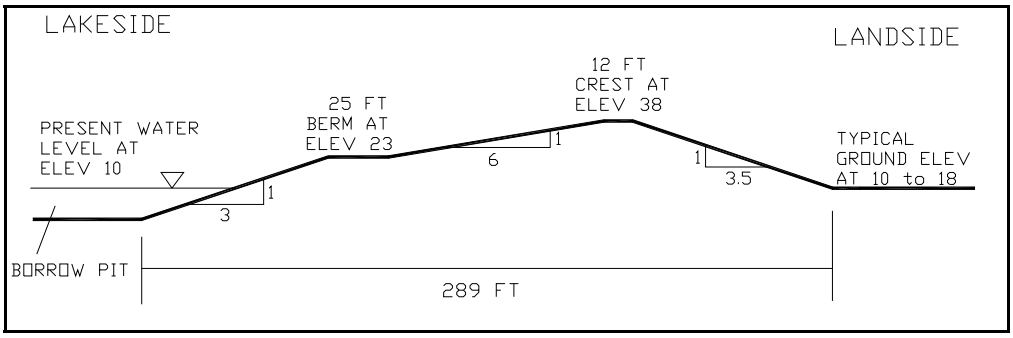

Figure 3.7. Typical levee section on Herbert Hoover Dike.

Lake Pontchartrain at New Orleans- Based on personal communication with Mr. Ellsworth Pilie of the USACE New Orleans District, the typical levee section for Jefferson Parish is shown in Figure 3.8.

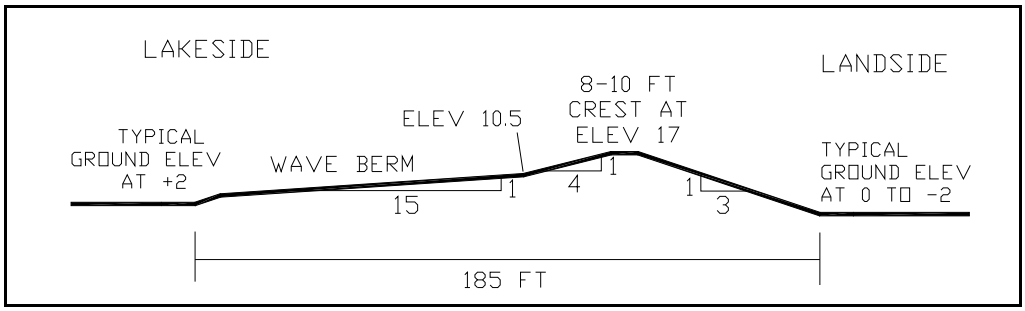

Figure 3.8. Typical levee section on Lake Pontchartrain in Jefferson Parish.

Based on the typical sections presented, some have changing slope on the upstream face that will be a significant problem for sealing the edges of some rapid repair techniques such as barges sunk over the breach.

Causes of Levee Breaches

Levee breaches are caused by excessive forces from the water, weakness in the levee material or the levee foundation, or both. Overtopping of levees by floodwater and waves is the most obvious cause. Seepage through or under a levee is less obvious, far more difficult to predict, and is the major concern in certain areas such as the Sacramento-San Joaquin River Delta and the Herbert Hoover Dike. The different breach causes are discussed in the following paragraphs.

Overtopping- Overtopping occurs when the water level in the river exceeds the crest of the levee or waves spill over the levee. Because of the relatively steep landside slopes of levees shown in the previous levee cross sections, the water moves rapidly down the land side of the levee. If the height and duration of overtopping is small and the slope is covered by a good layer of grass or other protective material, the levee can survive overtopping. For large heights and durations of overtopping and no landside slope protection, a breach is likely to occur. The overtopping flow will find a locally low or locally weak spot at which erosion is initiated. Once initiated, the flow tends to concentrate the erosive forces and the breaching process accelerates. The stages of breach formation will be discussed subsequently. The Scientific Assessment and Strategy Team SAST (2007) reported that eyewitness accounts indicate that the majority of levee

breaches during the 1993 flood on the Missouri River were caused by overtopping. Wave overtopping and breaching of the levee is similar to overtopping from excessive river water level except that a RRLB technique may have to be placed in waves and withstand wave forces. Figures 3.9 and 3.10 show a levee along a river being overtopped over a wide area.

Figure 3.9. Overtopping of a levee over a wide area with a potential breach growing in foreground.

Figure 3.10. Overtopping of the Foley levee in the Midwest.

Piping/Seepage- According to URS/Benjamin and Associates (2007) in their study of Sacramento-San Joaquin River Delta levees, “80% of the past failures can be attributed to seepage induced failures.” Seepage induced failures are also referred to as internal erosion. Levee seepage is broken into underseepage and through seepage. The SAST report states that these two forms of seepage induced levee failure occur in equal numbers in the Sacramento-San Joaquin River Delta levees. The SAST report also states “Under-seepage refers to water flowing under the levee in the underlying foundation materials, often emanating from the bottom of the landside slope and ground surface extending landward from the landside toe of the levee. Through seepage refers to water flowing through the levee prism directly, often emanating from the landside slope of the levee. Both conditions can lead to failures by several mechanisms, including excessive water pressures causing foundation heave and slope instabilities, and immediate and progressive internal erosion, often referred to as piping.” The SAST report goes on to state, “Excessive under-seepage is often accompanied by the formation of sand boils. Boils often look like miniature volcanoes, ejecting water and sediments, usually due to high under seepage pressures. These boils can lead to progressive internal erosion, undermining and levee failure. Boils have been widely observed in all of the historic floods and are believed to have caused significant failures in 1986 and 1997.” Through seepage can result in erosion and instability of the landside slope of the levee and lead to a full breach.

Figure 3.11 shows a ring levee of sand bags around a sand boil on the Kaskaskia River levee. Ring levees are one of the existing rapid repair techniques that have been used for many years with great success. Ring levees are placed only to the level that stops movement of sediment with the water. If placed to a greater height to stop flow, the increased head will likely result in the piping connection blowing out somewhere else. Prior to this picture, the ring levee had reduced the flow and stopped the movement of solid material. Suddenly, the levee foundation material started moving again as shown in the Figure. Efforts to further raise the sand bag levee and stop the material movement were unsuccessful and the full breach formed as shown in Figure 3.12.

Figure 3.11. Sand bag levee around sand boil on Kaskaskia River. Notice that one guy in this picture, who appears to be the oldest guy, has doubts about whether this is going to work because he is wearing a life vest.

Figure 3.12. Kaskaskia River levee breach at location of sand boil.

The SAST (2007) reported 5 factors that contributed to levee breaks in the 1993 flood in the Missouri and Mississippi River. The factors were (1) highly permeable substrata, (2) channel banks subject to high energy flow, (3) levee irregularities, (4) inadequate design, construction, repair and (5) inadequate levee maintenance. Note that the first item suggests underseepage problems and was based on the observation that 72% of the levee breaks in the 1993 flood were associated with areas occupied by one or more active channels within the past 120 years. This finding is contrary to the previously referenced statement from the SAST report that eyewitnesses reported most failures were due to overtopping.

Sliding/foundation stability failure. Although some of these occurred during Hurricane Katrina, foundation stability type failures are infrequent (personal communication, George Sills, ERDC GSL).

River Currents or Waves Failing Levee Section. Note that in the SAST (2007) factors contributing to levee breaks given above, the 2nd item "channel banks subject to high energy flow" occurred at the downstream end of bends and channel banks opposite from tributary flows that deflect flow toward the levee. A levee breach caused by scour of the floodplain adjacent to the levee section could be difficult to perform a RRLB because of deep depths upstream of the breach, swift currents, and likely loss of a portion of the river side of the levee section for a significant distance on each side of the breach. Nationwide, this is likely a failure mechanism of low frequency of occurrence compared to piping and overtopping.

Geometric Stages of a Breach

The delineation of geometric stages of a breach may help understand what RRLB techniques can be employed at different stages of breach formation. The geometric stages of various breach causes differ in the initial stages and become similar in the latter stages. Stages are defined for overtopping and piping type breaches as follows:

Overtopping. Hanson, Cook, and Hunt (2005) have defined the following four stages of breach formation during overtopping. Note that cohesive embankments fail from overtopping in a series of headcuts on the downstream face whereas non-cohesive embankments fail from overtopping by gradual steepening and lowering over most of the downstream face.

(1) Stage 1- starts at beginning of overtopping and ends when erosion of the downstream face has progressed to the downstream edge of the crest. This stage would frequently begin with sheet flow over and down a large length of the levee. The flow would erode a locally weak spot on the downstream face or possibly on the crest. Once the erosion is initiated, turbulence from the eroded area would tend to accelerate the erosion process.

(2) Stage 2- starts at end of stage 1 and ends when erosion has progressed to the upstream edge of the crest. Note that a stage 1 or 2 breach from overtopping has the potential to not result in a full breach if the water level were to recede.

(3) Stage 3- starts at end of stage 2 and ends when the embankment has eroded down to the foundation.

(4) Stage 4- starts at the end of phase 3 and ends when the breach has finished forming. Stage 4 is the widening phase that is likely accompanied by some and possibly a large amount of deepening to form what are called “blue holes” or “blow holes”. One positive factor regarding scour at the breach is the location of the maximum scour. The deepest scour tends to occur near the landside toe of the levee. Significantly less scour is present adjacent to the upstream toe of the levee. That is advantageous because many of the RRLB techniques are proposed for the upstream side of the levee.

Underseepage and Through Seepage- A comparable set of stages for breach formation from piping is not found in the literature. The stages proposed for piping are as follows:

(1) Stage 1- starts when piping first observed but is not moving material from the levee and ends when material starts being removed from the levee or foundation and begins forming a sand boil.

(2) Stage 2- starts at end of stage 1 and ends upon collapse of the crest. During stage 2 is when a ring levee around the sand boil may be effective in stopping the removal of material from the crest and preventing a breach.

(3) Stage 3- starts at end of stage 2 and ends when the embankment has eroded down to the foundation. Similar to stage 3 of overtopping.

(4) Stage 4- starts at the end of phase 3 and ends when the breach has finished forming. Stage 4 is the widening phase that is likely accompanied by some and possibly a large amount of deepening to form what are called “blue holes” or “blow holes”. Same as stage 4 of overtopping.

Estimated Breach Formation Time

An analysis was made of data and predictive methods to determine the time required for breach development. Breach development time is needed to determine how much time is available before a breach becomes too large to be able to achieve a rapid repair. While that critical breach size is not known at this time, a breach width on the order of 200 ft (61 m) is presently considered the maximum width that should be considered in the RRLB study.

No full scale data has been found documenting the formation time of levee breaches. Data is not available to quantify the 4 stages of geometry of breaches. The largest amount of data and predictive techniques are from breaches of earth embankment dams. Earth embankment dams differ from levees in several ways. One of the most significant is that when a dam is breached, the upstream water level starts to drop and discharge reaches a peak as the breach enlarges and then discharge starts to drop as storage in the reservoir is depleted. Tailwater downstream of an earth embankment dam breach generally has little effect on discharge through the breach or the breach dimensions. Reservoir storage tends to limit the size of the earth dam breach. In most levee breaches, the water level in the river or in a large lake such as Lake Pontchartrain either does not drop or drops only a small amount and the discharge and breach size continues to increase until the tailwater

downstream of the levee breach rises to reduce and eventually stop the flow through the breach. Tailwater rise tends to limit the size of levee breaches.

Earth embankment dam breaching data is used herein and provides the best information on development time of levee breaches. Because of the limiting effects of tailwater, the data based on dams may overstate the speed of formation of levee breaches. Most of the studies in dam breaching deal with overtopping failures with much less emphasis on piping failures. The Canadian Electricity Association Technologies Inc (CEATI) Dam Safety Interest Group evaluated models of dam breaching and categorized models for breach formation as empirical, analytical, parametric, and physically based models. The present focus of dam breach modeling being conducted by other researchers is on evaluating several existing physically based models because of the limitations of the first three categories. The analysis presented herein to estimate breach development time is based on existing data and empirical methods. This analysis is not an attempt to develop a new empirical approach for dam breaches. Once physically based models have been further developed and validated, more refined estimates of levee breach development time will be available.

Most of the field data on dam breaches presented subsequently do not distinguish between these two times and the reported time is based on when the breach was first observed until full development of the breach.
Wahl (1998) reports on various empirical relations for breach formation time and presents equations from Von Thun and Gillette (1990) as follows:

3.1 $$t_f = \frac{B}{Ch_w}$$ (erosion resistant, slightly cohesive material)

and

3.2 $$t_f = \frac{B}{Ch_w + 61.0}$$ (highly erodible)

Where t_f is in hours, B is average breach width in meters, C is 4 based on Von Thun and Gillette, and h_w is upstream water surface above breach invert in meters. The Von

Thun and Gillette approach was selected for this levee breach time evaluation because it was the only empirical relation relating breach width, breach depth, and breach time and it follows the expected trend of increasing time for increasing breach width and decreasing time for increasing head. Equation (3.2) for highly erodible embankments was not used because the addition of 61 m to the denominator of equation 3.2 implies a specific limitation of breach width and height for which it is valid.

Prototype data are presented in Table 3.1 showing breach formation time for various dam breaches. Sources are Zech and Soares-Frazao(2007) that includes the Norwegian tests, the CEATI dam breaching database, and the data base in Wahl (1998). Data are limited to dam heights of 30 ft or less to be comparable to most levee heights. The table provides failure cause, breach width, breach depth, failure time, dam composition, the C coefficient based on the Von Thun and Gillette method given by equation 3.1, and rate of failure of the breach. The rate of failure magnitude is calculated for both sides of the breach. Some previous presentations of this parameter have calculated the rate of failure for each side of the breach that is 1/2 of the value presented in Table 3.1.

Hanson, Cook, and Hunt (2005) reported on comprehensive large physical model tests of overtopping of cohesive embankments done by the USDA-ARS in Stillwater, OK. The rate of breach widening was observed to be strongly dependent on the soil material properties. Because these are model test data, the erosion rates are relatively low and their primary value is in validation of physically based models.

Based on Table 3.1, values of C in the Von Thun and Gillette (1990) equation range from 0.7 to 27 with a mean value of 8. The average of the lowest 1/4 of the C values in Table 3.1 is about 2 and should be representative of the more erosion resistant embankments. Since C=2 is close to the value of 4 adopted by Von Thun and Gillette for erosion resistant embankments, an average value of C=3 is adopted herein to use in equation 1 for erosion resistant embankments. The average of the highest 1/4 of the C values in Table 3.1 is about 18 and should be representative of the highly erodible

embankments. It is obvious that these C values represent a huge simplification of breach formation time and are only presented herein to estimate time available to complete a rapid repair. The recommended C values for levee breach times are not recommended for general application to dam breaches. Equation 3.1 is solved for time required to reach a certain breach width for a range of breach heights. Figure 3.13 presents results for erosion resistant embankments and Figure 3.14 presents results for highly erodible embankments. Figures 3.13 and 3.14 should be used to determine approximate upper and lower bounds for the time available to repair a breach. For example, a 100 ft wide breach in a 15 ft high levee will form in less than 0.5 hour in a highly erodible levee (Figure 3.6) and possibly as long as 3.2 hours in an erosion resistant levee (Figure 3.5).

Using the simpler approach of omitting the effects of levee height, the average widening rate of the breach ranges from 0.2 to 6.4 ft/minute with a mean value of 3.3 ft/minute based on the breaches in Table 3.1. The lowest 25% widen at an average rate of 0.5 ft/min and the highest 25% widen at an average rate of 5 ft/min.

Table 3.1. Observed data providing breach formation time.

Location	Failure Cause	Breach Width, ft	Breach Depth, ft	Failure Time, hrs	Dam Composition	C	Failure Rate, ft/minute
Impact:							
Norwegian test 1-02	overtop	69.5 at crest	19.7	0.83-1.17	Homogeneous clay	3.5	0.7
Norwegian test 1B-03	overtop	65.9 top and base	18.7	0.2	Zoned rockfill	18	5.2
Norwegian test 2C-02	overtop	33.1	16.4	0.1	Homogeneous gravel	20	6.4

CEATI:							
Glashutte	overtop	69	26	0.66	Uncertain material properties but compacted	4.0	1.8
Wahl:							
Break Neck Run	?	100	23	3	Rockfill/ earthfill	1.4	0.2
Goose Creek	overtop	179	13.4	0.5	Earthfill	27	6
Grand Rapids	overtop	62	21	0.5	Earthfill with clay corewall	6	3.0
Ireland No. 5	piping	44	17	0.5	Homogeneous earthfill	5.2	1.4
Lake Latonka	piping	129	28.5	3	Homogeneous earthfill	1.5	0.8
Lower Latham	piping	260	23	1.5	Homogeneous earthfill	7.5	3.8
Oakford Park	overtop	75	15.1	1	Earthfill with corewall	5	1.2
Pierce Reservoir	Piping	100	28.5	1	Homogeneous earthfill	3.5	1.6
Prospect	piping	290	14.5	3.5	Homogeneous earthfill	8	3.0
Winston	overtop	65	20	5	Earthfill with corewall	0.7	0.2

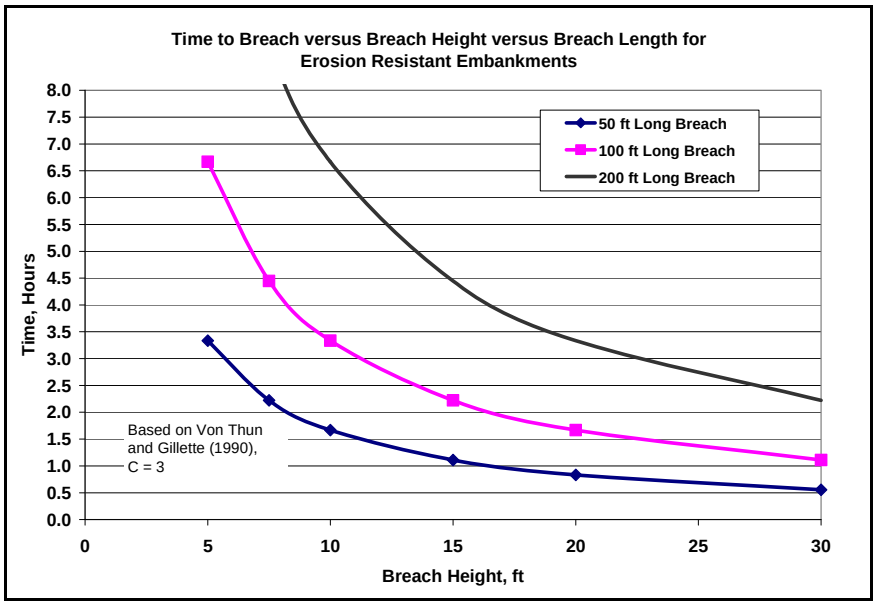

Figure 3.13. Breach time for erosion resistant embankments.

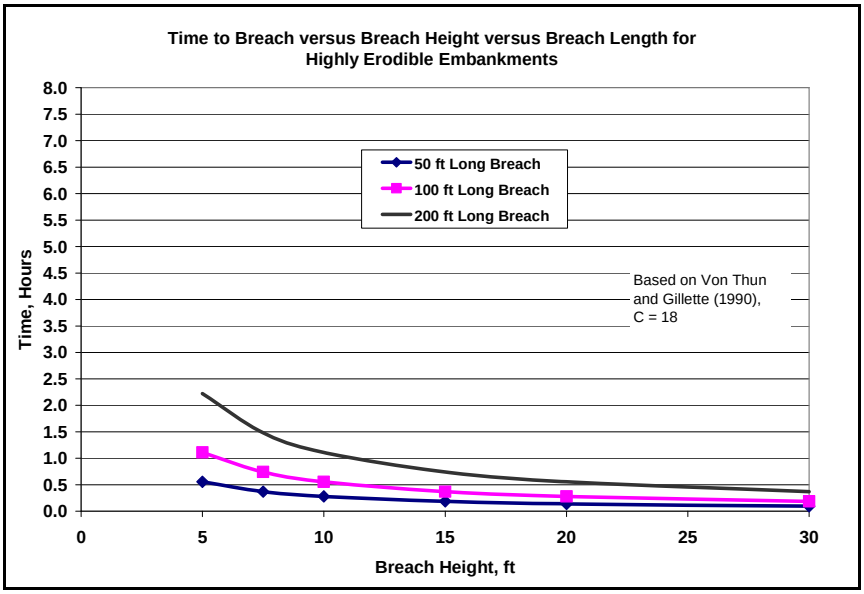

Figure 3.14. Breach time for highly erodible embankments.

Chapter 4

Discharge through a Breach

Numerical Simulation

This section documents a numerical simulation of discharge through a levee breach. The intent was to simulate a worst case scenario of discharge through a breach in order to determine the maximum forces that might be exerted on any object placed in the breach. In order to determine the dynamic hydraulic forces produced by the discharge through the breach, the velocity of the flow must be known. It is expected that the highest velocity will produce the greatest dynamic hydraulic force. Thus a major goal of the numerical simulation was to map the velocity through the breach in both time and space.
Normally a breach forms slowly by overtopping, scouring or piping; but that is not always the case as exemplified by the failure of the Taum Sauk Upper Dam, Missouri, in December of 2005. Figure 4.1 shows a general view of the Taum Sauk Upper Reservoir near Ironton, Missouri just after the breach.

Figure 4.1. *Aerial photo of the Taum Sauk Upper Reservoir, just after breach in December 2005.*

Figure 4.2 shows a closer view of the emptied lake and breach vicinity. In this case the lake wall was overtopped and also suspected of being undermined by seepage. When it collapsed the lake was emptied in a matter of 12 to 15 minutes. It is suspected that the 17th Street breach in New Orleans failed catastrophically after some initial period of overtopping as well. Knowing that such documented cases exist, for this study a worst case scenario was considered as an instantaneous removal of the levee wall, allowing flow to cascade out of the breach.

Figure 4.2. *View of emptied lake and vicinity.*

The conceptual model was staged as water flowing down the Mississippi River. A levee with dimensions similar to large Mississippi River levees is on one side of the model. Opposite the levee is a basin into which the flood waters will flow. Figure 4.3 shows this situation.

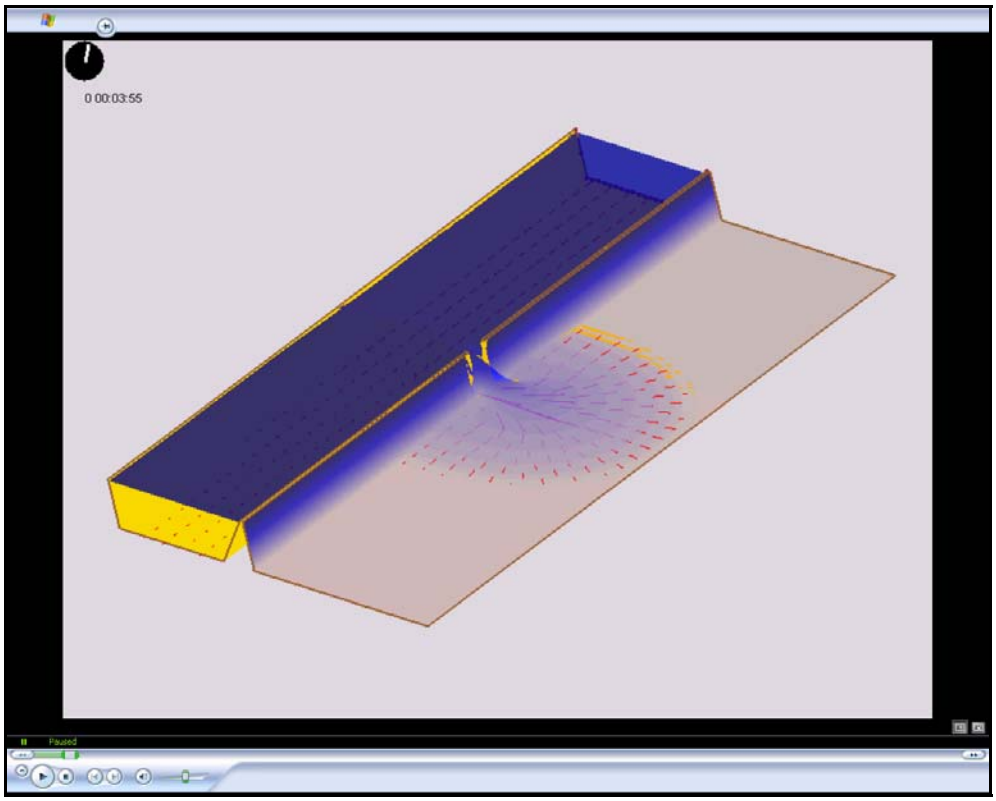

Figure 4.3. *Schematic diagram of computer model of idealized breach.*

The model is 6200 feet in length and about 2760 feet wide. In the Figure the left side represents the river and the right side with the grey-brown floor represents an empty and dry basin into which the water from the breach will flow. The bottom of the simulated river and the ground elevation of the basin are made the same in this model. The simulation initial conditions were set with appropriate discharge in the river to maintain water at a depth of about 24.5 feet. The simulation starts when a 200 foot section of the levee is instantaneously removed. Water falls 24.5 feet across the breach onto the dry ground of the basin. The numerical grid for this simulation is shown in Figure 4.4 as an oblique view with a 5 vertical to 1 horizontal distortion. There are 14134 2-d triangular elements in the grid and 7369 nodes.

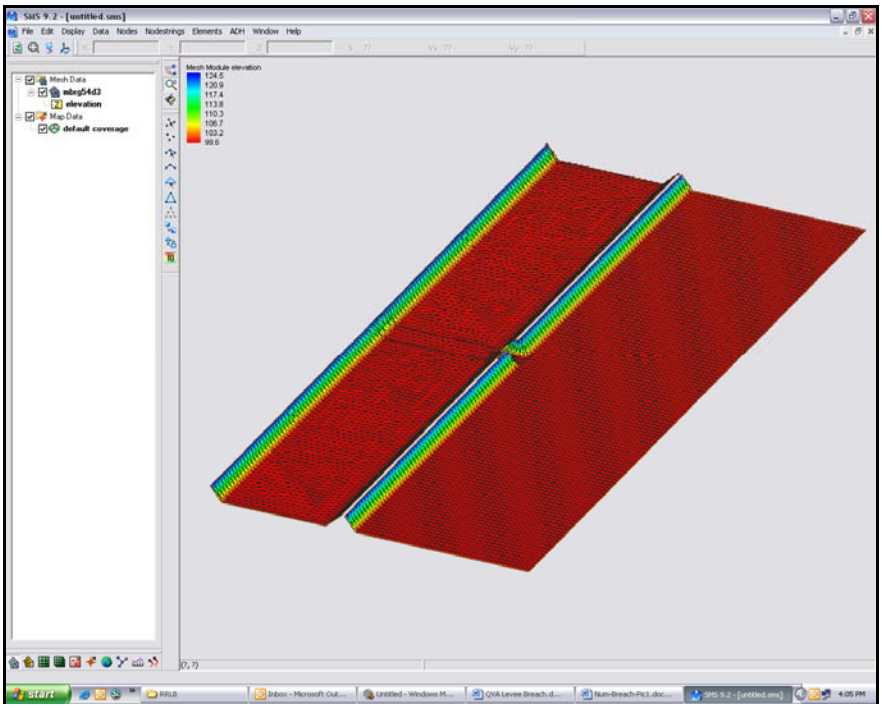

Figure 4.4. *Illustration of nodes used in the idealized breach simulation.*

Flow is into the river at the top and out at the bottom, with lateral flow into the basin. The basin is fully enclosed so as to model the effect of filling on the breach discharge. Figure 4.5 shows a closer view of the 200 foot wide breach opening in the levee wall.

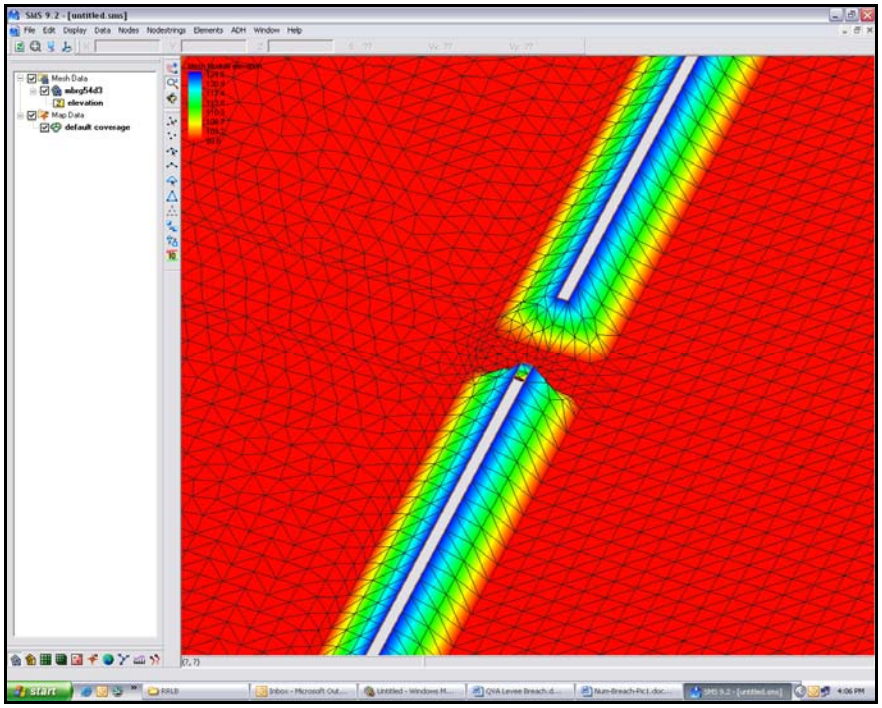

Figure 4.5. *Close-up diagram of nodes in the vicinity of the idealized breach.*

The simulation is noteworthy because the simulation conditions are very extreme. Water will flow from subcritical to supercritical over a large area in an extremely short time, over a relatively large area, and onto a dry surface. Thus any model used to simulate the scenario must be able to model flow transitions, possibly shock capturing, and cell wetting and drying. The model ADH 2-d was selected because of its purported capabilities with regards to these requirements.

The simulation time from the initial time of the breach until the basin was filled was about two hours. Required computation time was about 12.5 days on a PC with a Pentium(R) 4, 3.2 GHz CPU and 1 GB of RAM. At several stages of the simulation, time steps were cut to fractions of a second in order to facilitate convergence. Also the adaptive capability of the model was invoked and necessary. At the initial time of the simulation run, it was not known how long it might take or if it would converge. The run time was very long and future runs of this type should be done on faster, multiple processor computers.

The simulation results show that a maximum velocity of about 22 ft/sec occurred over a period of nearly 12 minutes into the simulation and was located approximately 50 to 250 feet downstream of the levee longitudinal centerline. Figure 4.6 shows a graphic of these results. Figure 4.7 shows a computation of the forces that would be exerted on a flat plate per foot of length for any similar object placed in the flow field at a given location.

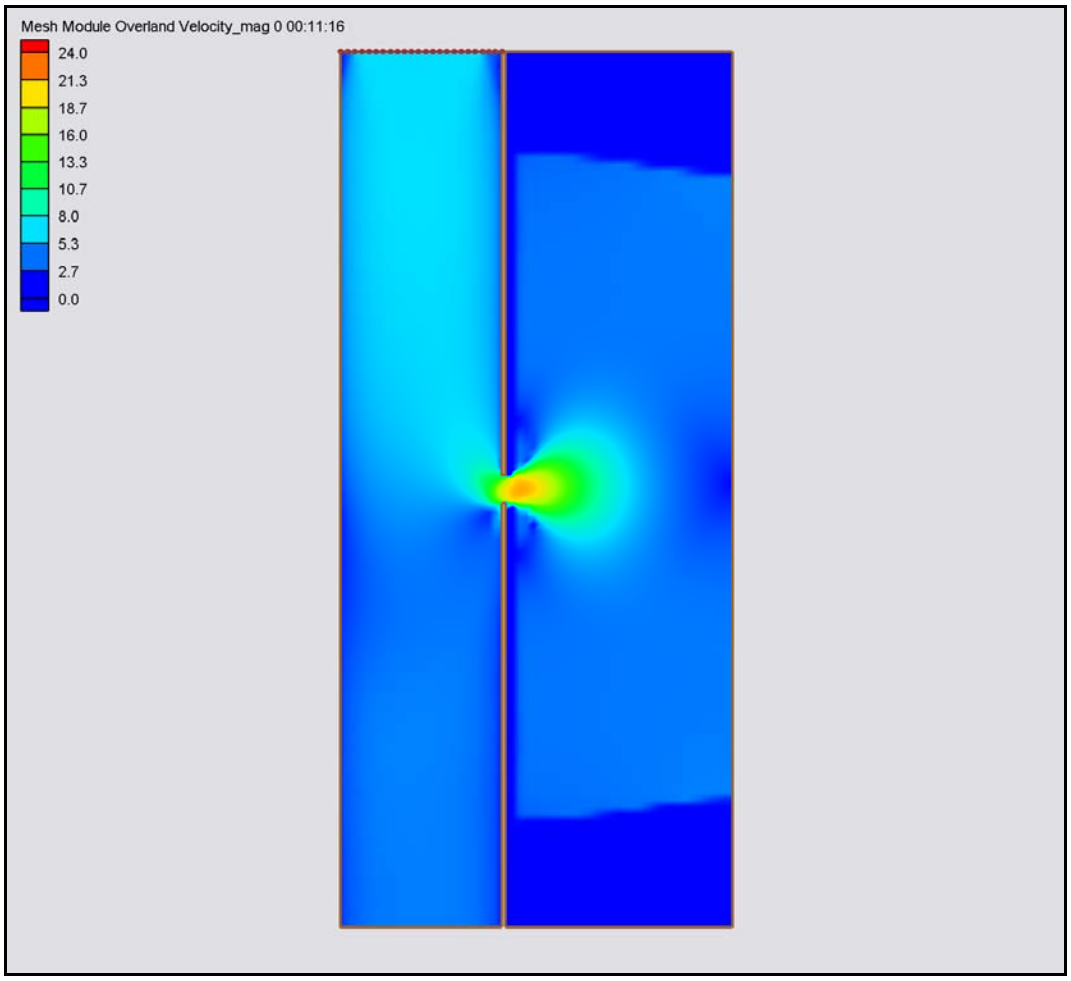

Figure 4.6. *Velocity contours for flows modeled in idealized breach simulation.*

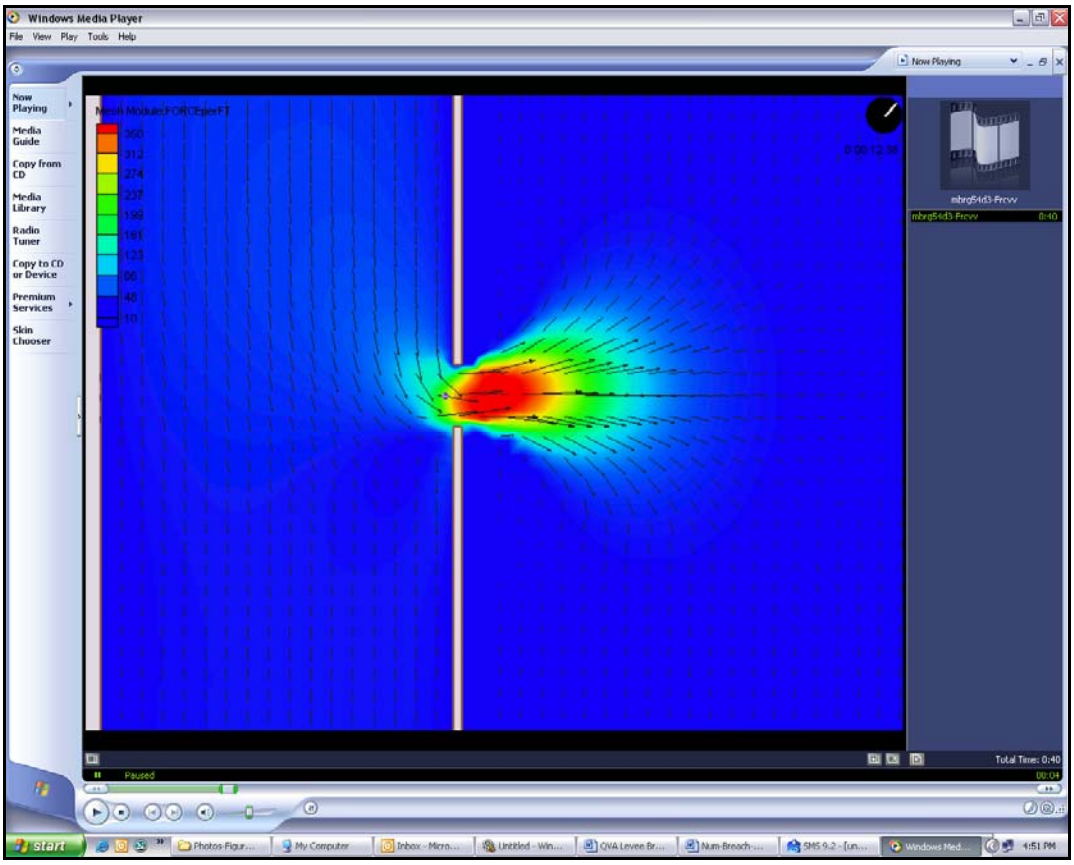

Figure 4.7. *Modeled forces on a flat plate subjected to flows in vicinity of idealized breach.*

These computations were made using equation 4.1 below.

$$F_d = \rho C_d A \frac{V^2}{2}$$

where

4.1 F_d is the force acting on a hypothetical flat plate,

C_d is the coefficient of drag; and

A is the area over which the force is acting.

The emphasis so far has been on the absolute highest velocities and forces occurring in the simulation. However, an object placed upstream of the breach would not necessarily encounter the highest velocities. It is also necessary to consider the direction of velocity in a lateral levee breach. As can be seen in Figure 4.8 the complete velocity vector can have a significant component in the streamwise direction that could seriously

affect the effort to position the closure device. For example, at the centerline of the breach opening and about 150 feet from the levee crest on the river side of the breach, the component of velocity in the breach-direction is 9.5 fps and the streamwise component is 3.3 fps. At the same distance from the levee crest but at the north abutment, the component through the breach is 2.6 fps and the streamwise component is 7.7 fps. So in moving a closure device a distance of only 100 ft in the streamwise direction and being 150 ft away from the levee crest, the velocity components change from 66% streamwise and 33 % breach-direction, to 66% breach-direction and 33% streamwise. This shows clearly that the streamwise components of velocity cannot be ignored when considering the logistics of moving a closure device into place, which will become a very important topic when discussions for the concepts of operations (CONOPS) for deployment are being developed.

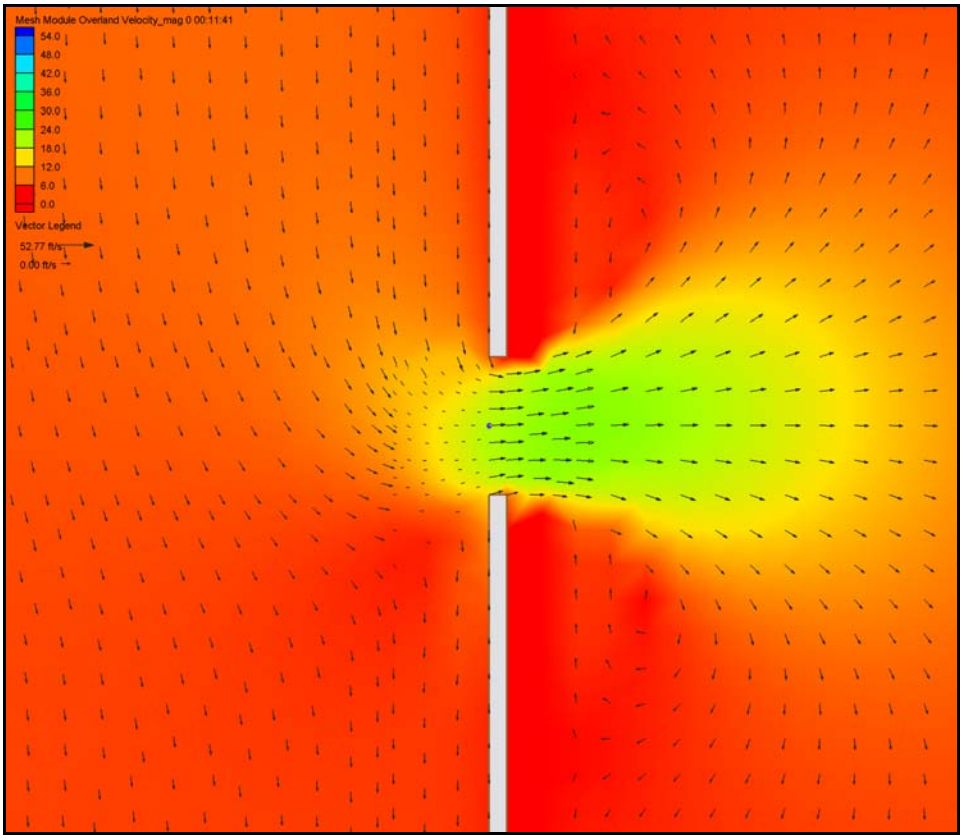

Figure 4.8. *Force vectors (assuming a drag coefficient value of 2) for flow through an idealized breach.*

Chapter 5

Small Scale (1:50) Model Concept Testing and Development

Purpose

Although the project team relatively quickly developed some promising ideas about the potential for application of water-filled fabric components within rapid breach closure systems, we wanted to investigate a much wider range of alternatives before we focused only on this class of structure for RRLB solutions. For this reason, a small scale modeling effort of the RRLB was conducted with the following considerations in mind:

1. Generate new techniques for RRLB;
2. Perform initial evaluation of proposed techniques for RRLB;
3. Identify critical components of proposed techniques and possible deployment alternatives that might enhance the efficiency of the method and its success;
4. Provide information on potential problems related to changes in the flow field, scour potential or head differential; and
5. Provide direct measurements of hydraulic parameters related to the forces.

Methodologies

The tests were also guided by information gleaned by this team's search of the current dam and levee breach literature and our compilation of important factors affecting breach formation described in Chapters 3 and 4 of this report. With these considerations in mind the conceptual methodologies to test were initially listed according to the type of breach which might occur. At this scale, it is very easy to execute almost any option that can be imagined, so there was no attempt at this point to suppress concepts that might be impractical at larger scales. Instead, the small-scale model was used to provide a general learning process for the entire R&D team.

Breach closure systems modeled at small scale

Small Scale Modeling Flume Tests

Facility

An 80 foot long tilting flume was used to provide a simulated levee breach and flow for testing of various closure methods discussed above. The flume cross section is 3 feet wide and one foot deep. The facility has pumps that can supply up to 5.5 cfs of flow capacity. In order to maintain a constant water level during the closure tests, a special side-weir-overflow device was constructed to fit within the flume. A simulated levee was constructed separately, but made to fit exactly within the confines of this overflow device. The flume, overflow device and simulated levee are all shown in figure 5.1.

Figure 5.1. *Photo of flow through small-scale (1:50) breach.*

The model scale was 1 foot in the model to 50 feet in the prototype. The model levee was constructed to represent a Sacramento River Delta levee. Such a levee has about 1 to 3 side slope ratio and is less than 20 feet in height. The modeled breach represented a 50

foot breach in the prototype. When flow calibration was complete, testing of closure methods could begin.

Four breach closure methods or combinations of methods were tested in the small scale model during December 2007 and continuing into January 2008. They were placed into the simulated fully developed breach.

The methods that were tested were:

1. Rectangular gated structure floated into place, with and without a tarp. Figure 5.2 shows the gated structure just after placement. The gates are still open.

Figure 5.2. *Photo of gated structure test in 1:50 scale flume.*

After gate closures, significant flow continued along the device perimeter. A tarp was used in combination with the gated structure to see how this would work in conjunction with it. The slow residual velocities allowed positioning of the tarp, and actually helped move and seal the tarp against the structure. The result was an almost complete reduction of flow through the breach as shown in figure 5.3.

Figure 5.3. *Test of a gated structure combined with a tarp showing almost no residual flow.*

2. Barge floated into place with ballast on one side. A sealing fabric bag was added on the upstream side of the barge. Figure 5.4 shows barge driven up the levee embankment, and having a simulated fabric bag placed against its upstream side. Significant flow reduction occurred.

Figure 5.4. *Idealized barge floated into position on small-scale levee and ballasted with water.*

3. Simulated cable net placed over the breach with tarp placed upstream of the breach. This is shown in Figure 5.5.

Figure 5.5. *Photo of performance of a net anchored on either side of a breach combined with a tarp in the 1:50 scale model.*

4. Geo-textile fabric bags filled with water. For these tests, water-filled plastic bags were tested in anchored and un-anchored configurations. Bags anchored on each end and filled in place are shown in Figure 5.6.

Figure 5.6. *Photo of water-filled tube concept utilizing two tubes anchored to either side of a breach in the 1:50 scale model basin.*

Although the small-scale tests functioned as an extremely good learning tool, it soon became obvious that many of the concepts that were simple to deploy and functioned well at the 1:50 scale would likely not work well at larger scales. For this reason, we terminated testing in this basin and began preparation of a larger facility for subsequent tests.

Chapter 6

Intermediate-Scale (1:16) Testing and Development

Intermediate-Scale (1:16) Model Facility

The early phase of this project investigated a wide range of ideas of potential value to rapid levee repair; but many of those ideas were soon recognized as either impractical or beyond the state of the science that exists today. We knew that we could not continue to devote extensive amounts of time to all of these different ideas and still meet our specified timelines for large-scale demonstrations. To assist us with our down-selection, we knew that it would be extremely useful to have a physical basin that was substantially larger than the 1:50 scale flume described previously in this report. An existing physical model facility within ERDC was identified as having the best potential for providing a suitable basin for such testing of RRLB concepts. This basin was modified from its initial purpose to provide a flow capacity consistent with a 1:16 scale along a levee section (Figure 6.1). The model levee was constructed at an undistorted scale and represents a levee with a crest elevation of 20 ft (note: all dimensions are reported in prototype scale unless otherwise stated), side slopes on both faces of 1:3 (vertical:horizontal), and a crest width of 16 ft. The breach was 80 ft wide with 2:1 side slopes the full depth of the levee. Both the model basin and the levee were constructed of a concrete cap poured over a sand fill with inset aluminum templates to insure the accuracy of the bathymetry and topography.

Figure 6.1. *Test basin for 1:16 scale physical model tests.*

This model represents a fairly extreme test for breach closure, since the breach is 80 ft wide and 20 ft deep, the still water level is 18.7 ft deep, and there is as a significant riverine current flowing along, past, and through the breach (Figure 6.2).

Figure 6.2. *Flow through the breach with upstream depth at 18.7 ft.*

Concepts considered for detailed intermediate scale testing

As can be seen in Appendix B, a number of different concepts were investigated during the early part of our 1:16 model testing. As was briefly mentioned at the end of Chapter 2, our metrics, analyses and tests indicated that the conventional methods of construction (using rigid members or fabric elements) did not appear to offer a good solution for stopping flows through a large breach. Unlike our tests in the 1:50 scale flume, our tests in the 1:16 scale basin had to be much more focused. In this context, although there are some diversions described in Appendix B, we decided to concentrate our effort on testing the new concept that was introduced at the end of Chapter 2. In this concept, the bending of the fabric tube (or more generally any fabric chamber) is not determined by the beam equation but by volumetric constraints within the tube.

To illustrate this concept, let us examine the deformation of a simple cylinder with flat, non-deformable rigid ends as shown in Figure 6.3. Hypothetically, if we fill this tube's interior volume with 100% water, the volume of the tube cannot be increased without a net increase in the surface area of the fabric (i.e. the fabric stretches). Conversely, if we attempt to bend this tube along the axis of the cylinder and the fibers along the outer curve are assumed to be incapable of stretching, such a deformation will require a buckling of the fabric on the interior curve, leading to a loss in volume. However, since water is essentially incompressible, the volume cannot decrease. Thus, the tube would resist deformation. Of course, actual fabrics do stretch and there will be some elongation (stretching) of the fibers along the outer curve. This elongation will be consistent with the total pressure force pushing outward on the surface of the fabric. This stretching of the fiber on the outside curve will allow a slight deformation in the overall shape of the cylinder, leading to bending. If the material can be stretched easily, an initially straight cylinder can be curved to any degree desired; however, if we use typical construction fabrics, the amount of stretching will be only about 5-7% before the fabric fails (tears).

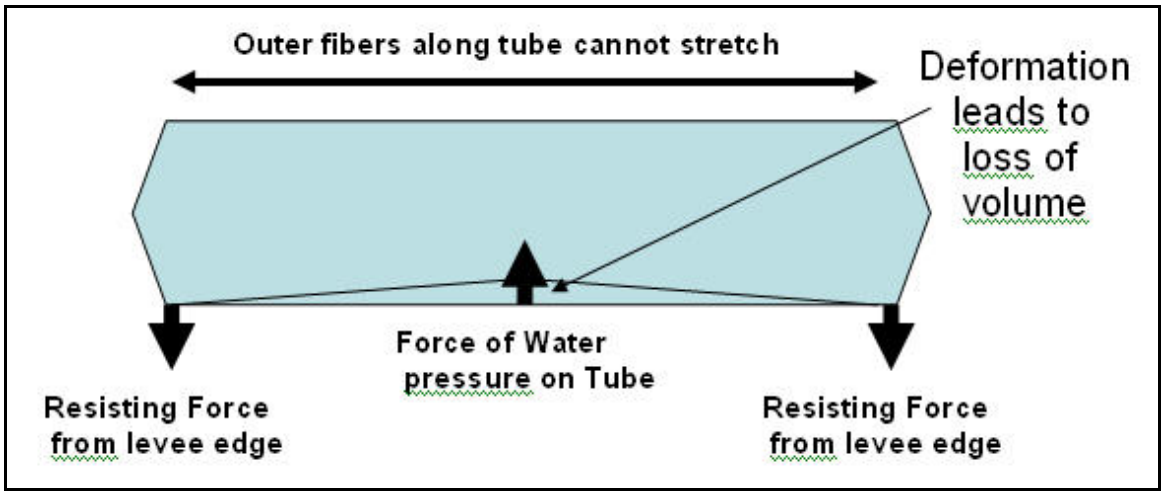

Figure 6.3. *Idealized forces on a tube at a breach.*

Since the results are not very dependent on the neglect of the 5-7% stretch, we will neglect this and assume that the deformation can be represented in a simple sense by a situation in which we have only filled the tubes with water equal to 80% of the total of the tube. In this case, we can decrease the interior volume by 20% before any resistance to further deformation would occur. For the simplistic case where the tube shapes are maintained outside of the folded region, the bending would persist to the point where the volume within the shaded areas is equal to the 20% of the volume that was missing from the tube. Once this happens, the tube would again begin to resist further deformation.

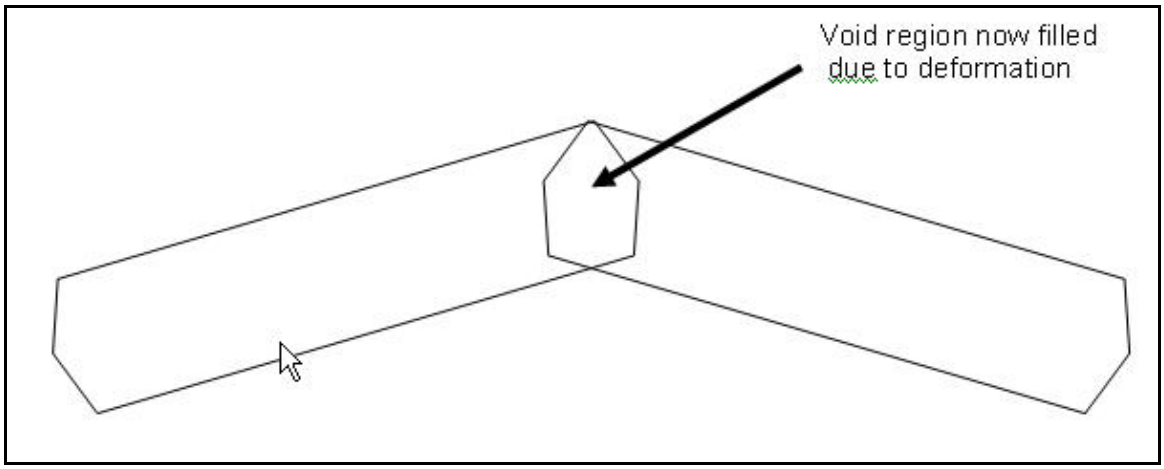

Figure 6.4. *Deformation of a tube leading to loss of volume.*

In an actual fabric, the situation is a bit more complicated, but the basic concept remains the same – a water-filled fabric tube will begin to resist deformation once the interior volume is compressed to a 100% fill level. Figure 6.4 shows an idealized concept for a situation in which a tube has deformed to the point where the interior is 100% filled. Once the compression reaches this level, resistance to additional deformation will be proportional to the pressure distributed over the entire surface of the tube, which can be a very large force. Unlike the idealized case described here, the actual shape of the fabric will be a smooth curved surface which distributes the force and response to the deformation over a wider area rather than the localized deformation shown in Figure 6.4; but the general principle will remain the same.

It is also possible to glean some general scaling principles from the simplified situation discussed here. One can see that the amount of deformation will depend on the ratio of the void volume to the diameter of the tube, giving us

$$\alpha = \tan^{-1}\left[\frac{\delta V_e}{\zeta \delta D_t^3}\right] \qquad 6.1$$

where

α is the angle subtended by the two cylinders in Figure 6.4;
δV_e is the volume of the tube that is empty;
ζ is a dimensionless coefficient of proportionality; and
D_t is the diameter of the tube.

Although the exact point of failure will be determined by physical model tests, this equation should provide a good indication of the failure mode that occurs when a tube collapses onto itself to a point where it can pass through a breach opening. For breach widths less than twice the tube diameter, a conservative approximation for the failure point can be taken as 45^o in estimates based on this equation. It is difficult to specify a functional relationship for this scaling behavior for wider breaches; so instead, we will simply rely on the physical model results.

It is likely that a numerical model can be developed to estimate the behavior of a tube undergoing deformations of the type being investigated here; however, this is well beyond the scope of the work conducted in this first year's effort. A complicating factor is the relatively unknown coefficients of drag for the fabric sliding past the periphery of the breach. Analytical solutions are also difficult for a situation such as this by the fact that we have two additional factors that much be considered besides only the ability of the tube to avoid being swept through the opening, 1) the ability of the tube to conform to a irregular shaped opening and to be able seal the flow through it and 2) the ability of the tube to achieve and maintain sufficient freeboard to block the flow up to the water surface. As will be seen in Chapter 7, when the actual large-scale model tests were conducted considerable "trial and error" effort was expended on getting a solution that met all three of these constraints.

When a tube passes over a vertically raised perturbation (levee remnant) it can be seen that a resistance to passing over the remnant can be obtained by a combination of resistance to deformation and the weight of the water within the tube when it is lifted. Such a system is ideal for sealing wide, shallow breaches and might be very effective in helping prevent overtopping in areas such as Braithwaite, Louisiana, shown in Chapter 2.

Intermediate-Scale Model Tests and Results

As noted earlier in this chapter, the breach tested in our model basin provided a substantial challenge, since it represented an opening that was 18.5 feet deep and 80 feet wide. The primary successful tests of note for sealing this breach in the 1:16 basin involved variations with a single tube that would have a prototype length of 195 feet. Once we learned that the volume fill proportion for the tube could not be much less than 60%, in this tube, essentially all tests managed to close all or close to all of the flow through the breach. Figure 6.5 shows a typical result obtained for a tube filled to a 60% capacity. As can be seen here, the performance is quite remarkable, with very little water passing through the breach after emplacement of the tube.

Figure 6.5. *Deep-breach closure with large tube filled to 60% fill volume.*

The deployment method in the tests in the 1:16 scale basin were all complicated (probably realistically) by the relatively fast currents passing by the breach, parallel to the breach, similar to the case of a breach in a levee along a large river. It was noted that the tubes always had a very strong tendency to start rolling toward the breach once part of the tube came in contact with the bottom. As described in the next Chapter, this tendency combined with the prolonged deformation of the tube plays a very positive role in reducing the dynamic forces on the remaining levee sections. However, a negative aspect of this rolling within the complicated flow field was that the tube sometimes began to twist differentially before it reached its final stopping position within the breach. This twisting appeared to provide additional avenues for water to pass through the breach after the tube was in place. Within the lab, it was relatively simple to execute techniques which could minimize this twisting, but the ability to accomplish this in similar situations at prototype scale will still have to be demonstrated.

Figure 6.6 shows the performance of the wide, shallow breach system in an application. This tube represents a tube that is 256 feet long and 8 feet in diameter at prototype scale. We originally performed a number of tests with a secondary (simulated air-filled) floatation tube attached to the 8-ft tube; but we found that removing the secondary tube improved our test results. Also during these tests, we realized that a major mistake had been made in the design of the facility which we did not have time to

correct before the testing at Stillwater was to commence. The problem was that the wide, shallow breach vicinity was designed to also serve as a movable-bed test site. This co-location created continual problems with secondary flow through the submerged (remnant) levee throughout our tests. Although it is very difficult to see in this photo due to difficulties with the lighting and the secondary flow passing through the unconsolidated underlying materials, a near-zero flow conditions was achieved in significant number of tests. The problem with "underflow" was corrected in the testing facility at Stillwater and as will be seen there the results confirmed our interpretation of the 1:16 scale results.

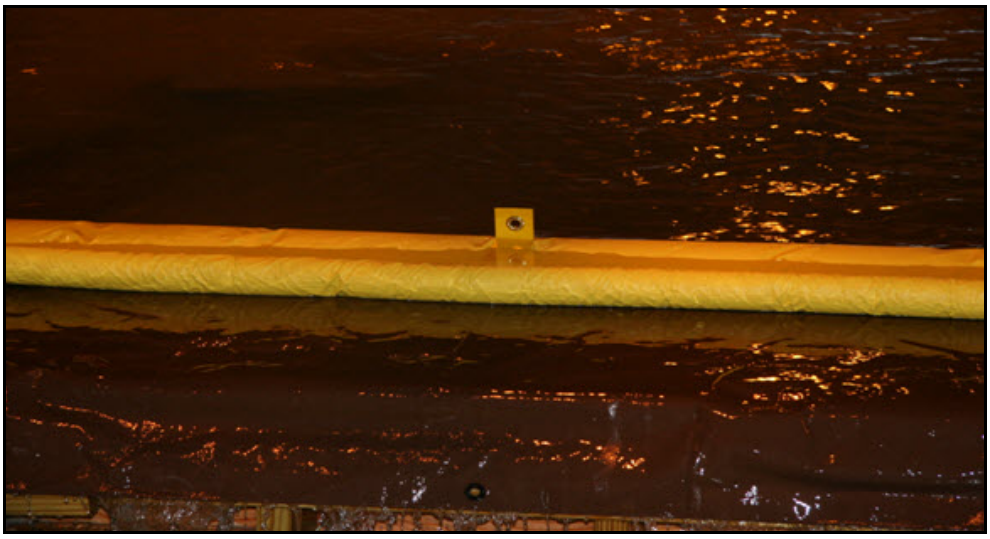

Figure 6.6. *Performance of a very long water-filled fabric tube in a wide, shallow breach test in the 1:16 scale model.*

Chapter 7

Large-Scale Model Testing and Demonstration

A review of available facilities which can generate large flow rates suggested that the optimal site for testing concepts at a larger scale than possible within in-house facilities at ERDC was the Hydraulic Engineering Research Unit (HERU) of the Agricultural Research Service in Stillwater, Oklahoma (Figure 7.1). This facility can maintain a flow rate of 125 cfs for prolonged periods of time. Dr. Greg Hanson from the HERU functioned as our primary point of contact; and he and his colleagues at this facility provided invaluable assistance with our work at this location.

Figure 7.1. *Aerial photo of facility at ARS-HERU facility in Stillwater, Oklahoma.*

Since the facility for large-scale model testing was offsite from ERDC and the HERU staff could not provide all of the services required, a decision was made to utilize

our primary contractor for this project (Oceaneering International, Inc., OII) to assist with all of the heavy equipment operations as well as the model testing at this site. Appendix C contains a report provided by OII describing details of the execution of tests at this site.

Three different concepts were tested in the ARS facilities: 1) an expedient fabric spillway; 2) a wide, shallow-breach closure system; and 3) a moderate-width, deep-breach closure system. Concepts 2 and 3 were tested in the 1:16 scale tests at ERDC, while concept 1 was not tested at the smaller scale. Since details of the tests can be found in Appendix B, this chapter will focus on a summary of the testing and lessons learned here.

Expedient Fabric Spillway

In many situations, earthen dams can be endangered by high flows over unprotected surfaces. In these situations, it is often not advisable to attempt to block the entire flow, since this will simply produce an additional rise in the water level behind the dam which would then threaten still other areas. Instead, if the water is still allowed to pass over the surface but the surface is protected from erosion, catastrophic erosion could potentially be avoided. Figure 7.2 shows the system being tested at the Stillwater site. The longitudinal tubes provide adequate ballast to prevent the tarp from lifting off of the surface and washing away. The system shown here was constructed by Kepner Plastics, a fabricator of many marine applications of fabric construction located in Torrance, California, using PVC coated polyester material. The material used here weighs approximately 27.5 ounces per square yard, which made the entire system able to be moved manually by a relatively small crew of three persons. It is envisioned that the type of system shown in Figure 7.2 can be installed by hand in connectable sections, even over fairly large areas (100's of feet across); however, the scale tested and shown here was designed for functionality only up to a flow that is approximately 1 foot above the surface. The performance of this system was clearly a success in terms of both its ease of

deployment, ability to maintain its position, and its ability to prevent erosion of the underlying cover.

Figure 7.2. *Demonstration of REPEL system with 0.5-ft of water passing over the top of the breach.*

Wide, Shallow-Breach Closure System

The 17th Street Canal breach in New Orleans attained a width of about 400 feet during Hurricane Katrina. This type of breach represents a particularly difficult challenge to any solutions which rely on remaining levee sections to either side of the breach for support, since the span distance becomes so large. It should be recognized, however, that the breach did not cut down to the base level of the canal anywhere along this 400-foot opening; thus, a remnant structure existed below the crest of the breach that affords an effective support that can be utilized by a system which resists vertical deformation (as described in the previous section on the 1:16 scale testing). Figure 7.3 shows a picture taken of the performance of the shallow, wide breach closure system during the Stillwater demonstration. The lack of curvature of the tube along the breach in this photo indicates that the tube is not depending on the sides of the breach for support.

Figure 7.4 shows a contrasting concept which does depend on the sides of the breach for support; and as can be clearly seen in this second photo, a catenary shape forms. The performance of this system was deemed to be very successful in terms of its ability to adapt to the bottom shape and shut off essentially all of the flow through the breach.

The ability of this system to prevent flow through a wide, shallow breach could be very important in many applications throughout the world. It should be recognized that such a system could be pre-positioned along low lying areas or deployed in a situation such as occurred at Braithwaite, Louisiana during Hurricanes Gustav and Ike (Figure 7.5). In both of these situations, weather conditions would have permitted the deployment of a water-filled fabric system, such as demonstrated here. Another interesting aspect of this class of system is that, by placing individual systems next to each other, very long reaches of exposed levee might be protected.

Figure 7.3. *Demonstration of shallow, wide breach closure system at ARS facility in Stillwater.*

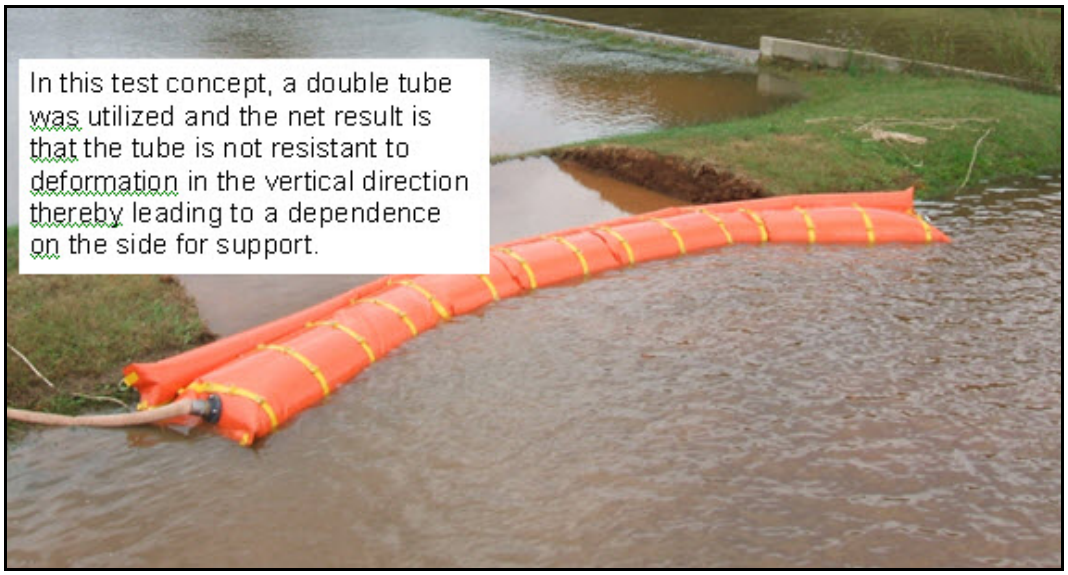

Figure 7.4. *Example of wide, shallow test at Stillwater for a system which was not resistant to deformation in the vertical dimension. The catenary shape is indicative of tension support along the tube from the edges of the breach.*

Figure 7.5. *Two photos from overtopping in Braithwaite, Louisiana during Hurricane Gustav. The left-hand panel shows a close-up of flow over a low area along the levee crest, while the right-hand panel shows a wider perspective of this flow.*

Moderate-Width, Deep-Breach Closure System

The final test at the ARS facility in Stillwater was perhaps the most exciting due to the flow velocities involved. In this test, a breach that was about 8 feet wide at the top of the levee and tapered to about 6 feet wide at the bottom of the levee had approximately 125 cfs passing through it, with maximum velocities estimated to be about 6 feet/second passing in through the central portion of the breach. The estimated static load for this situation, with a water level 5 feet above the bottom of the breach is approximately 4700 pounds. The dynamic load for a fast shutdown of such a flow (consistent with allowable deflections across a 6 foot-wide span) would have been in the neighborhood of 200,000 pounds.

As had been observed during the 1:16 testing, the tube began to roll a considerable distance away from the breach opening, indicating an interaction with the bottom. In all tests conducted, the total time between the initiation of rolling and the final quasi-stationary position of the tube was consistently around 10 seconds. If we assume approximately linear deceleration, the maximum dynamic force is only about 20,000 pounds, which is far less than the total static force. This slow deceleration and deformation of the tube represents a significant advantage of a highly compliant system (such as an unconstrained, partially filled fabric tube) to reduce impacts on adjacent levees and to minimize the risk of adding to the damage at the breach. It should also be noted that the contact surface between the tube and the peripheral areas of the levees and breach distribute the forces acting on the tube over a relatively wide area. Since this first year's test was a concept demonstration, we did not have measurements of forces on the surrounding levees, but such measurements are planned for subsequent studies.

Figure 7.6 shows the tube in its final location from one of the dozens of large-scale tests conducted with this tube. Consistent with the performance of this system concept in 1:16 scale testing, the tube blocked almost all of the flow in these tests. In some of the tests a small residual flow was observed along at locations along the periphery of the breach, typically either at the top outside edges of the breach or the lower outside edges of the breach. However, these flows were usually very small (less

than 1 cfs). As shown in Figure 7.7, the addition of two small tubes on either side of the breach opening usually provided a very effective seal for all flow.

Figure 7.6. *Sample deployment of deep-breach closure system, with a small residual flow still persisting along the upper edges of the breach opening.*

Figure 7.7. *Sample deployment of deep-breach closure system including the addition of two small tubes along the upper edges of the breach opening which produced essentially zero-flow conditions through the breach.*

As was the case with the 1:16 tests, the large-scale tubes maintained a good seal for extended periods of time (several hours) with no apparent degradation in performance. A spurious effect of blocking the flow through the main breach was that

the water in front of the breach slowly rose over a period of several minutes while the flow in the test basin adjusted to convey the 125 cfs flow over the side weir. In these cases, the side tubes illustrated in Figure 7.7 played a valuable role in helping seal the breach from additional flow around the top portion of the tube. It is possible that the same degree of "flow-blocking" could be achieved by using a higher proportion of air within the tubes combined with a reduced proportion of water, but we did not have time to test this modification during the testing phase in Stillwater.

The performance of the deep-breach closure system was deemed to be very successful in terms of its ability to adapt to the bottom shape and shut off essentially all of the flow through the breach. As noted above, it was also quite resilient in terms of its ability to continue to block the flow even in situations when incident water levels varied. Two different methods of deployment were investigated during these tests, one with the tube only and a second with the tube attached to a barge. Clearly the first of these methods is more suitable for very austere areas, while the second might be preferable in some areas where barges are readily available in the vicinity of a breach. There was no discernable difference in the performance of the systems related to the deployment method.

Chapter 8

Extrapolation to Larger Scales

Fabric Strengths Required for Larger Breaches

Interpreting model scales is always something that should be done within the perspective of a particular application. The tests conducted in Stillwater can be considered full-scale if one is dealing with a small breach or the very early stage of breaching of a potentially large breach. On the other hand, as discussed in Chapter 3, a mature breach in a large levee can easily be 18-20 feet deep and 100 feet across. In the context of breaches such as those, one must understand the scale factors which control the forces within the dynamic and static systems in order to be able to specify an objective model scale.

In general, there are two different spatial scales that can influence the forces on an RRLB system, the depth and the width of the breach. For simplicity, let us consider here the case where the levee breach dimensions retain the same relative proportion as the test case in Stillwater. In this situation, the scale of the forces should be governed by the ratio of the dimensions of the breach in Stillwater to the dimensions of the larger breach, which will be a single number.

For a tube of the type we tested in Stillwater, there are at least two constraints that must be met in order for the system to seal the breach. First, as discussed in Chapter 5, the tube must contain the correct proportions of water and "void" to enable the tube to block the flow without being forced through the breach. Second, the fabric must be sufficiently strong to contain the pressure within the tube without failing. The first of these constraints scales geometrically, so as long as a tube follows the same proportions for a larger size, it is expected to behave quite similarly to the smaller tube, as was noted in similarities between tube performance in the 15-inch and 4-foot model tests. The second of these constraints will depend on the fabric strength required to support the

"hoop" tension around the diameter of the tube. Given a simplified situation with water all the way to the top on the "upstream" side of the tube and no water on the opposite site, the pressure integral around the surface can be approximated as

$$\tau_H(x) = \Lambda \oint \Delta p(s) ds \qquad 8.1$$

where

Λ = the expected ratio of the dynamic forces to the statis forces;

$\tau_H(x)$ = the hoop tension for unit longitudinal distance along the tube;

$\Delta p(s) = p_{inside}(s) - p_{outside}(s)$;

$p_{inside}(s)$ = the outward pressure on the inside of the tube;

$p_{outside}(s)$ = the inward pressure on the outside of the tube; and

s = the location around the tube.

Assuming that the pressure differential ($\Delta p(s)$) on the "upstream" side of the tube will be approximately equal to zero and that the pressure differential on the "downstream" side of the tube will be approximately hydrostatic, we can allow Λ to remain an unknown constant for the moment and can evaluate this integral as

$$\tau_H \approx \frac{\Lambda \pi \rho g D^2}{4}. \qquad 8.2$$

Thus, we see that the hoop tension will scale as the square of the depth. For the tests in Stillwater, where the fabric performed well, we had a total depth of about 5 feet in some of the tests. For this case the hoop tension is expected to be $\Lambda \times 306.3$ pounds per linear foot of fabric. Since most fabrics have breaking strengths rated in pounds per inch, we can divide this by 12 to get a final estimate of $\Lambda \times 25.5$ pounds per inch. For the design at Stillwater, using a value of Λ = 10, we get a final estimate of 255 pounds per inch required for the tube to remain intact under the pressure loading. The fabric used was from Mehler Texnologies, Inc. (Style 8556). It consisted of a basic polyester fabric, with a PVC coating and a top coat of acrylic on both sides. The rated breaking strength was 400 pounds per inch, so we actually had some additional safety factor above the safety factor implicit in the relatively conservative value of Λ used here.

We know that the fabric selected for Stillwater worked well for many tests and did not show any undo signs of fatigue, so this should serve as a realistic guide for future fabrics in larger tubes. If we now want to design a fabric for a 15 foot-deep breach, we have to use a fabric with a breaking strength that is given by

$$8.3 \qquad \frac{\tau_{H-New}}{\tau_{H-Stillwater}} = \left(\frac{D_{new}}{D_{Stillwater}} \right)^2 = \left(\frac{15}{5} \right)^2 = 3^2 = 9$$

Thus, our requirement for the breaking strength of the fabric would be 2295 pounds per inch. Even with our conservative estimate for Λ used here, this is a value that is well within the strengths of conventional fabrics such as polyesters; and if some problems were anticipated at even larger scales, a system of reinforcing straps can be included. These straps can be made by just additional layers of fabric over the top of a single layer, forming a multi-layer fabric. Equations exist for estimating the proportionate load sharing of the straps and the fabric, given that the two materials have a roughly similar elasticity.

Full-scale deployment in "real-world" environments

The expected forces on these massive tubes during deployment will probably have to be managed by high strength lines connected to anchored winches. The overall plan will be similar to the type of executions (concept of operations – CONOPS) performed in the demonstrations at Stillwater. It is extremely important that we develop CONOPS that minimizes any attempts to work against natural forces and instead use these forces to aid us in getting the tubes into its final position, since the mass contained within these tubes will increase by a cubic factor over the mass within the tubes at Stillwater. In Stillwater, we only used lines controlled manually to manipulate the tubes into place – by allowing the current to carry the tube into place. If we assume that the manual forces were less than 100 pounds on each of the two lines connected to the ends

of the tubes, the forces in a 15-ft tube would require winches with holding/pulling force of about 2700 pounds (100 x 3 cubed) on each line.

As noted previously in this report, situations such as flow in rivers past breached levees, where currents move transverse to the breach opening (similar to the 1:16 model tests), may require some special attention to develop protocols which allow the tubes to roll into the breach without too much twisting in the fabric (due to differential rotation). Several methods for achieving this have been discussed and will be pursued in subsequent development efforts.

The effect of wave forces during positioning of a tube and on a deployed tube

Dynamic wave forces acting on a tube can be evaluated theoretically from conventional wave theories. In rivers and during situations where conditions will permit deployment operations, waves will typically be less than 1-2 feet in height. And as seen in the photographs from Hurricane Gustav, even on the periphery of a hurricane, waves may be fairly small. Once the tube is in place, the horizontal wave forces will likely be much, much smaller than the horizontal forces of the water holding the tube into the breach. On the other hand, buoyancy effects associated waves will essentially act to raise and lower the local water level adjacent to the tube. Although it is not expected that this perturbation in the water surface will create significant problems, subsequent tests must be run to ensure the accuracy of this assumption.

The effect of wind forces during positioning of a tube and on a deployed tube

The relative magnitudes of the forces of currents and winds acting on an RRLB tube can be written as

$$\frac{F_a}{F_w} = \frac{\left(\rho A u^2\right)_a}{\left(\rho A u^2\right)_w}$$

where the subscripts "a" and "w" refer to air and water, respectively, and

8.4

F is the force acting on the tube;

ρ is density;

A is the (projected) area normal to the flow; and

u is velocity.

Since the density of water is approximately 1000 times greater than that of air and the tube remains almost completely in the water at all times, we see that a reasonable upper limit for this ratio will be

$$8.5 \qquad \frac{F_a}{F_w} < 1.0 \times 10^{-4} \frac{u_a^2}{u_w^2}.$$

Even for a 40 meter per second wind and only a 1 meter per second water current, the wind forces will only be about 16% of the water forces acting on the tube.

Post emplacement operations

As was noted previously, at the Stillwater demonstration it was shown to be advantageous to deploy some secondary water-filled tubes around the large RRLB tube once the large tube was firmly seated in place. This helped to curtail flow around the upper edges of the large tube and also helped to stabilize the tube with respect to subsequent increases in the local water level. It is likely that additional, simple methods for ensuring long-term stability of the RRLB system will be required for very long intervals (possibly days to weeks) of deployment.

Chapter 9

Conclusions and "Road Ahead"

From the outset of this project it was recognized that it was not sufficient to make only small, incremental steps forward in solving the problem of rapidly repairing breached levees. We needed to develop new concepts that could be rapidly deployed in areas with essentially no available logistics support. Moreover, the magnitude of the forces acting in large breaches and their often irregular shape combined to create additional serious complications to proposed solutions. Consequently, new, innovative ideas were absolutely needed for this project to be considered successful. In particular, after consideration of the rate at which damage can occur in the lee of a breached levee and the rate at which a small breach can evolve into a large breach, we set some stringent guidelines for system deployment time. These guidelines provided the impetus to focus on solutions that were helicopter transportable and deployable by a combination of helicopter support and on-ground personnel, without any assumed availability of heavy equipment.

Following a very fast-paced study of many different concepts for the rapid repair of breached levees, we have now established a good foundation for a new method to accomplish such repairs, potentially even when massive amounts of water are flowing through the breach. This new method uses the fact that water inside a closed fabric tube will resist deformation past some limit, due to its basic incompressibility.

Next, after conducting a number of small-scale (1:50) and intermediate (1:16) model tests, we took three of the most promising ideas that had been developed and began preparation for detailed testing at the Agricultural Research Service's large-scale facility in Stillwater, Oklahoma. The three concepts down-selected for subsequent testing are as follows:

1. A manually deployable system that allows water to flow over an earthen dam or embankment while preventing erosion to the underlying surface;

2. A fabric tube system for stopping flow over a wide, shallow breach.
3. A fabric tube system for stopping flow through a deep breach.

Initial analyses of the fabric strength requirements have now been performed. These analyses show that the forces acting on the RRLB tubes should scale approximately in proportion to the depth of the breach squared. Furthermore, since the fabric strengths used in the Stillwater tests were quite minimal, it appears very feasible to extrapolate the results from the Stillwater demonstration to significantly larger breaches (15-20 feet deep).

All of our results to date have been very encouraging, demonstrating the capability of new water-filled fabric designs for closing breaches through which large volumes of water are flowing. We believe that we are very close to being able to rapidly repair breaches of the type shown in Figure 9.1. However, it is very important to develop efficient operational guides for deploying these levee closure devices and to test this new class of rapid levee repair technology very thoroughly to verify such claims before they can be considered totally operational.

Figure 9.1. *Breaches during Katrina.*

REFERENCES

Bromwell, L.G. Dean, R.G. and Vick, S.G. (2006) Report of Expert Review Panel Technical Evaluation of Herbert Hoover Dike Lake Okeechobee, Florida. Prepared for South Florida Water Management District. BCI Engineers and Scientists, Lakeland, Florida.

Bulson, P., "Design Principles of Pneumatic Structures", The Structural Engineer, Vol. 51 (6), June 1973.

Cavallaro, P.V, Sadegh, A.M., Quigley, C.J, "Contributions of Strain Energy and PV-work on the Bending Behavior of Uncoated Plain-woven Fabric Air Beams", Journal of Engineered Fibers and Fabrics, 2007, Vol. 2, pp. 16-30.

Hanson, G.J., Cook, K.R., Hunt, S. 2005. Physical modeling of overtopping erosion and breach formation of cohesive embankment. Transactions of the ASABE 48(5):1783-1794.

Main, J.A., Peterson, S.W., Strauss, A.M., "Load-Deflection Behavior of Space-Based Inflatable Fabric Beams", J. of Aerospace Engineering, 1994, Vol. 7 (2), pp. 225-238.

Mount, Jeffrey and Twiss, Robert 2004. "Subsidence, Sea Level Rise, Seismicity in the the Sacremento-San Joaquin Delta: Report to the Levee Integrity Subcommittee of the California Bay- Delta Authority Independent Science Board", December.

Scientific Assessment and Strategy Team (SAST) 2007, Science for Floodplain Management into the 21st Century, A Blueprint for Change, Part V", Interagency Floodplain Management Review Committee.

URS Corporation/Jack R. Benjamin and Associates, Inc. 2007. "Delta Risk Management Strategy Phase 1", Topical Area Levee Vulnerability, Draft 2, Technical Memorandum, prepared for California Department of Water Resources.

U.S. Army Corps of Engineers, 2006a. Performance evaluation of the New Orleans and southeast Louisiana hurricane protection system draft final report of the Interagency Performance Evaluation Task Force. U.S. Army Corps of Engineers Report, 259 pp.

Von Thun, J. L., and Gillette, D. R. (1990). "Guidance on breach parameters." Internal Memorandum, U.S. Dept. of the Interior, Bureau of Reclamation, Denver, 17.

Wahl, T. L. (1998). "Prediction of embankment dam breach parameters—A literature review and needs assessment." Dam Safety Rep. No. DSO-98-004, U.S. Dept. of the Interior, Bureau of Reclamation, Denver.

Wielgosz, C., Thomas, J.C., Le Van, A., "Mechanics of Inflatable Fabric Beams", ICCES, 2008, Vol 5, No.2, pp. 93-98.

Zech, Y. and Soares-Frazao, S. (2007). “Dam-break flow experiments and real-case data. A database from the European IMPACT research”, Journal of Hydraulic Research, Vol 45 Extra Issue, International Association of Hydraulic Engineering and Research.

Appendix A

DEVELOPMENT OF A RAPIDLY INSTALLED BREAKWATER FOR ARMY FORCE PROJECTION

D. T. Resio*, J. E. Fowler, and J. A. Melby
U. S. Army Engineer Research & Development Center
Vicksburg, Mississippi 39180

ABSTRACT

A theoretical foundation for a floating breakwater is given along with results from both lab and field tests which provide validation for this theory. An extension of these equations to the case of a structure made from pressurized, water-filled tubes shows that this type of structure should be extremely effective in enabling ship discharge in JLOTS operations to continue through Sea State 3.

1. INTRODUCTION

In 1944, during the Normandy Invasion, large breakwaters brought from England were credited with significantly improving Allied force projection capabilities during the first few weeks of this critical operation. Unfortunately, a large storm decimated the breakwaters after only a few weeks of operation. However, the early success of these breakwaters motivated considerable research into the development of rapidly transportable breakwater systems for military force projection in the decades following World War II. Little if any progress was made in this area during these years; and as documented by Jones (1971), such research served more to demonstrate the inherent in developing such systems than to produce working military assets.

Since the end of the Cold War, US forces have become increasingly reliant on CONUS-based rather than OCUNUS-based force projection. This has placed a growing emphasis on the development of effective force Projection technologies. Sealift, due to its inherent capability to efficiently transport large volumes and tonnages, has played a crucial role in essentially all past military operations conducted by US Forces. However, the lack of deep-draft ports in many areas of the world (combined with the likelihood that existing deep-draft ports will be denied or destroyed during times of war) has necessitated the development of alternative means for linking Sealift into the force projection logistics chain. When such ports are denied or do not exist, today's alternative is through operations collectively termed Joint Logistics Over the Shore (JLOTS). JLOTS operations are typically configured as shown in Figure 1, and are reasonably productive during calmer conditions

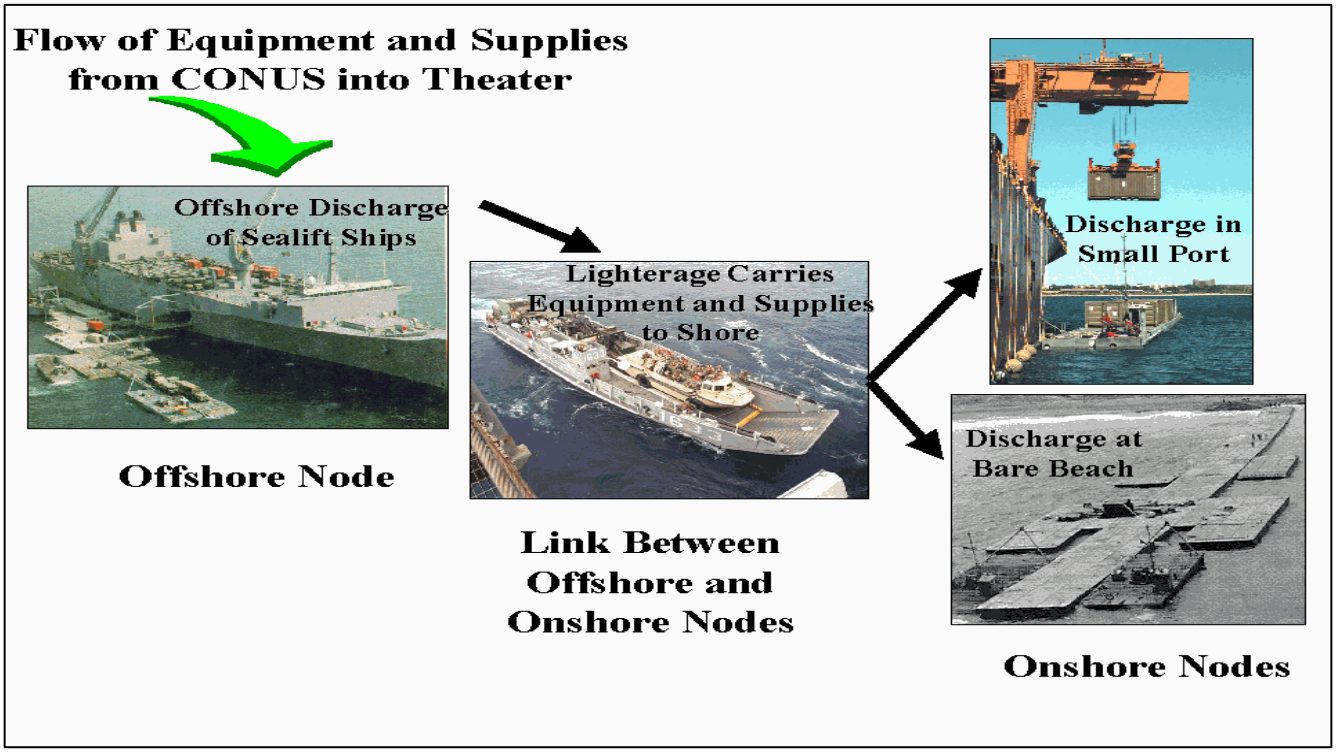

Figure 1. JLOTS operational nodes and links.

of Sea State. Unfortunately, present limitations associated with JLOTS assets effectively shut down these operations when significant wave heights become larger than 3 feet. Since waves of this size occur more than 50% of the time in coastal areas around the world (Committee On The Navy And Marine Corps In Regional Conflict In The 21st Century, 1996), this lack of capability represents a serious threat to US force projection capabilities around the world. This has sparked a large effort to develop technologies which can extend JLOTS functionality at least through the upper range of Sea State 3 (significant wave heights in the 3-foot to 5-foot range). Such an extension would increase throughput rates by amounts ranging from 50% to 200% in virtually every military area of operation around the world. One such effort, known as the Rapidly Installed Breakwater (RIB) is presently underway at the US Army Engineering Research and Development Center's Coastal and Hydraulic Laboratory (CHL). This paper discusses key aspects of the development of the RIB system for JLOTS applications.

Two classes of breakwaters have been extensively studied for military applications, floating and gravity-based. The first of these is suitable for offshore operations, while the second is used primarily in coastal applications. As shown in Figure 1, JLOTS consists of two transportation nodes, one offshore and one at the coast, with a link between these nodes. The major problem noted in past operations and exercises has been the inability to continue JLOTS operations at the offshore node in Sea State 3; hence the initial motivation for the Army has been to develop a breakwater of the first class, i.e. a floating breakwater. The effort to develop the RIB is presently part of an Army Advanced Technology Demonstration (ATD) and is a four-year effort presently scheduled for completion in FY 2002.

2. HISTORICAL PERSPECTIVE

According to Jones (1971), an optimal breakwater for military applications should have the following characteristics: a) be able to effectively reduce wave heights (performance metric), b) be highly transportable (deployability metric), c) be able to be installed quickly (employability metric), d) be able to survive storms (survivability metric), and e) be reusable (utility metric). In recent years, affordability has also become a key development issue for new systems and should probably be added to this list. Another factor that should be explicitly recognized here is the size of the area that must be sheltered from the waves in a typical JLOTS operation. Modern Sealift ships can have lengths of more than 900 feet; thus, breakwaters must be designed such that those ships can be accommodated.

Unfortunately, several of the above characteristics tend to be of a conflicting nature. For example, performance, survivability, and ship size typically imply a massive structure, while deployability and employability issues dictate that the structure be as small as possible. The state-of-the-art at the beginning of the project described herein was such that only very massive floating structures had been found capable of significantly reducing wave heights and even these tended to function well only for short wave periods (about 3-4 seconds). Since it is not presently feasible to deploy massive breakwaters from CONUS and since wave periods in Sea State 3 are typically in the range 4-6 seconds, no existing floating-breakwater technology was deemed suitable for military applications at the start of the present effort.

To be successful, a development project of this size and complexity must follow a well-conceived development plan. In this case, a workable concept was first developed, followed by an in-depth theoretical analysis, laboratory experiments, and finally field tests. Early on it was realized that a new concept would be necessary to meet military force projection needs. A new "V-shaped" design for the RIB (Figure 2), originated in the early phase of this effort (patent # 5,702,203) and appeared to offer the best chance of meeting these needs. This design, unlike previous

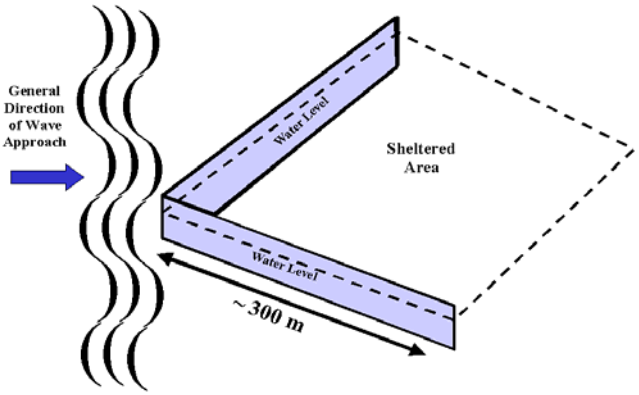

Figure 2. V-shaped design of RIB showing reduced wave height area.

designs that depended on their breadth in the direction of wave propagation, used a unique principle of wave reflection to significantly reduce wave energy (heights) in its lee.

3. THEORETICAL DEVELOPMENT

The performance of a breakwater is typically given in terms of the ratio of the wave height in the lee of the breakwater to the incident wave height

$$R = 1 - \left(\frac{H_{sh}}{H_{in}} \right) = 1 - K_T \qquad (1)$$

where R is the fraction of wave height reduction in the RIB interior, H_{sh}, is the wave height in the interior, H_{in} is the incident wave height, and $K_T = H_{sh}/H_{in}$ is the transmission coefficient.

In nature, ocean waves are made up of a continuous distribution of waves distributed in frequency and direction, i.e. a wave spectrum. Due to the dispersion relation governing wave propagation and their relatively broad spread in direction, waves can be considered to have random phases relative to each other. In this context, energy content of the waves is represented by

$$E_o = \int_0^{\infty} \int_0^{2\pi} E(f,\theta) df d\theta \qquad (2)$$

where E_{mo} is the total energy in the wave field, and $E(f,\theta)$ is the wave energy at frequency f and direction θ. A representative wave height can then be computed from a fixed relationship with the square root of the total energy, given by

$$H_{mo} = 4\sqrt{E_o} \qquad (3)$$

where H_{mo} is the zero-moment wave height, once termed the "significant" wave height. For deep-water waves, significant wave heights are the same as $H_{mo.}$

In order for the RIB to be effective for military Sealift operations involving JLOTS, it must reduce the entire range of waves associated with Sea State 3 conditions (with an upper limit of 5 feet) to Sea State 2 or less (i.e. less than 3 feet). For this reason, a criterion of a minimum of 50% reduction of wave height, for wave periods up to 6 seconds, was established as a development guideline. Additionally, for comparability with other JLOTS assets, it was determined that the RIB should be capable of surviving Sea State 5 (significant wave heights up to 12 feet). Additional constraints pertaining to size, weight, and flexibility of the RIB were recognized in terms of thresholds of available vessels and handling equipment, as well as in terms of the resilience of the structure; however such criteria were not easily quantifiable. It was also recognized that it was critical to be able to employ the RIB rapidly upon arrival at the site. A major portion of this employment is the establishment of a secure mooring system; however, mooring analyses are not included within this paper since they are the topic of another paper presented in this conference.

Wave energy enters the interior of the RIB via one of three primary mechanisms, a) propagation under the RIB, b) propagation through the RIB, and c) propagation around the ends of the RIB. Although there are other mechanisms which can contribute to wave energy being transmitted into the interior of the RIB (wave overtopping, energy passing through small openings, mooring resonance etc.), theoretical analyses and laboratory studies have shown that these are all quite small compared to the primary mechanisms enumerated here. Briggs et al. (1998) performed an extensive analysis of the first of these mechanisms; but, since comparable amounts of energy are expected to pass into the interior region via propagation through the RIB, these results were not very conclusive.

3.1 Energy propagation under RIB

A firm theoretical foundation for energy passing under a thin floating breakwater was first established by Wiegel (1960) and extended by Kriebel and Bollman (1996). This work was extended to the RIB by Kobayashi (1998). Based on their work, the proportion of wave height passing under the RIB can be written as

$$K_T = \frac{2T_F}{1+T_F} \qquad where \qquad (4)$$

$$T_F = \frac{\sinh\left[2k(d-h)\right] + 2k(d-h)}{\sinh(2kd) + 2kd} \qquad (5)$$

For the above equations K_T is the transmission coefficient, $k = 2\pi/L$ is the wave number, L is the wavelength, h is the total water depth, and d is the depth of penetration of the RIB into the water. Wiegel (1960) and Kriebel and Bollman (1996) have verified this equation in laboratory studies for the case of a narrow, rigid breakwater. Calculations for the case of an infinitely long RIB show that to reduce wave heights by 50% for 6-second waves it must occupy a significant portion of the water column (on the order of 50%) in its planned depth of operation (nominally 50 feet).

3.2 Energy propagation through RIB

Previous studies of waves interacting with breakwaters have focused on the case where the breakwater can be considered to be perfectly rigid and no deformation of the structure is produced by the wave forces acting upon it. However, this is not a reasonable assumption for the RIB. Waves propagating along the side of the RIB create very large differential forces (and resulting moments) along the RIB. For any realistically achievable material strength, the RIB will bend to some

degree in response to this forcing. In this mode, RIB motions act as a wave generator for the interior region of the RIB. If the excursion distance of the RIB over a single wave period is comparable to the excursion distance of the wave orbital motions, essentially 100% of the wave energy will pass through the RIB into the interior. As shown by Melby et al. (1998), the excursion distance of the RIB can be related to the incident wave conditions via the relationship

$$\delta_{y\max} = \int_0^L \int_0^L \frac{M}{EI}\, dxdx \qquad (6)$$

where *x* and *y* are the horizontal coordinates along and normal to the RIB leg, respectively, *EI* provides a measure of the structures overall "stiffness", *E* is Young's Modulus of Elasticity (determined by material properties), *I* is the moment of inertia, and *ymax* is the maximum exercusion normalized by the incident wave amplitude. *M* is the moment of inertia created by the wave forces given by

$$M = \iiint p(x,z)\, dzdxdx \qquad (7)$$

where *p (x,z)* is the wave pressure which varies along the RIB (x-direction) and vertically (z-direction). Results from numerical evaluations of these integrals were made for an infinitely long RIB section. Data from these calculations provided extremely valuable insights into design specifications for the RIB. First, as shown in Figure 3, the performance of the RIB is shown to be a strong function of both the bending resistance of the RIB (the *EI* term in equation 5) and wave length. In theory, it

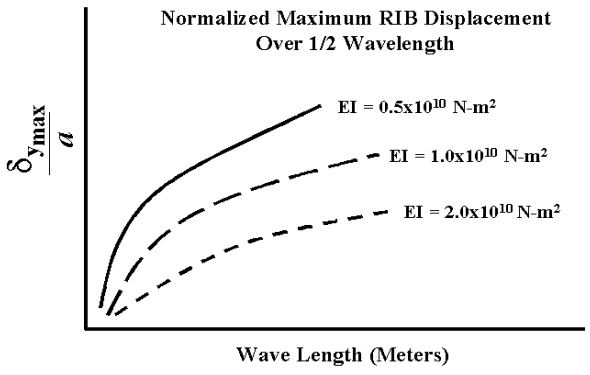

Figure 3. Normalized maximum RIB displacement versus wavelength

is only a very weak function of wave height (mainly due to weak nonlinearities), which has been confirmed in subsequent laboratory and field tests. The magnitude of the energy propagation via this mechanism clearly demonstrates the importance of having a very large value for *EI* in the design of the RIB.

3.3 Diffraction around ends of RIB

Since the RIB does not extend to a fixed boundary, wave energy can propagate around the tips of the "V" via diffraction. Diffracted waves appear to observers as circular waves emanating from these tips. Foundations for diffraction theory date back well into the 19th century. For the case here, a numerical solution to the diffraction equation of the form

$$a_b = a_i \int_0^\infty \frac{\Lambda}{\sqrt{r}}\, e^{-i\rho}\, dx \qquad (8)$$

where a_b is the wave amplitude at point b, a is the incident wave amplitude along the line source along the x-axis, r is the distance points along the line source, Λ is the so-called obliquity factor, and ρ is the wave phase at point b. Results from these calculations show that diffraction only contributes 2-5% of the wave height in the interior of the RIB for angles +/- 60 degrees within the centerline of the RIB (Figure 4). Given all the other

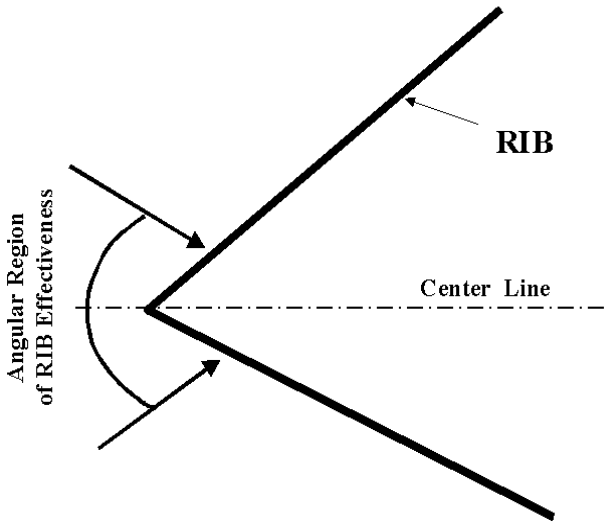

Figure 4. Range of effectiveness for incident wave angles on RIB.

design uncertainties in maritime wave-structure interactions, the contribution due to diffraction can probably be neglected for practical purposes.

3.4 Summary of analytical analyses of performance

Based on calculations of the three major means by which wave energy propagates into the RIB interior region, it was determined that both the depth of

penetration of the RIB into the water column and the bending resistance were of critical importance to optimal RIB design. On the other hand, as EI increases, the effective "brittleness" of the structure increases, leading to the potential for catastrophic structural failure, if not circumvented. Additional discussion of this design consideration is presented in a later section of this paper.

4. LABORATORY EXPERIMENTS

To verify the theoretical formulation for RIB performance and to improve our understanding of expected behavior for realistic RIB lengths and mooring configurations, extensive laboratory experiments were conducted in laboratory facilities located at the Coastal and Hydraulics Laboratory in Vicksburg, Mississippi. These experiments were run at a 1:16 scale in a wave basin using spectral waves. Results of these experiments were found to be in excellent agreement with the analytical results, showing that a) wave height does not significantly affect performance, and b) wave period, depth of penetration, and structural stiffness are all critical design parameters.

5. FIELD TESTS

Although it was possible to formulate a general theory for RIB performance, many practical considerations associated with handling of the RIB, mooring the RIB, overall survivability of the RIB, and structural fatigue could only be addressed by way of field tests. In order to keep the cost of these tests as low as possible, many of these tests were conducted at intermediate scales (1:4 – 1:3). Figure 5 shows an aerial photo of the RIB from its first field test (1:4 scale) conducted in Currituck Sound in North Carolina. The

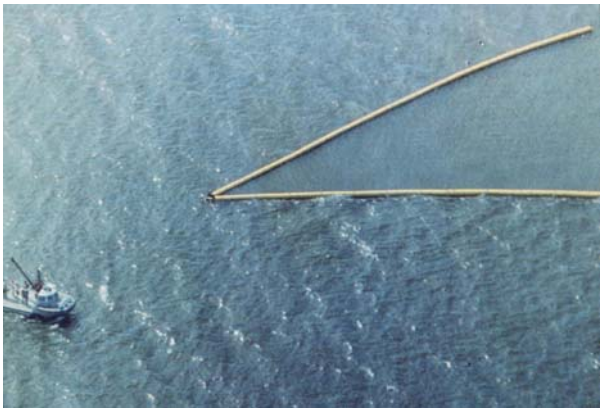

Figure 5. RIB used in FY 96 field study.

RIB in this test was fabricated of lightweight metal sections with welded seams between the sections. RIB performance in these tests was superb, reducing incident wave heights by 70% or more (consistent with both analytical and laboratory results); however, a major finding from the study was that excessive bending moments caused structural failures at the welded junctions between sections. Subsequent analysis showed that major modifications to the RIB design were required if this type of failure were to be avoided in the future.

In order to expedite RIB development, two classes of structures were tested in the field in 1997, a metallic RIB with flexible joints added to alleviate local stresses, and a hydrobeam RIB. Individuals from CHL and the U.S. Army Natick RD&E Center originally discussed the potential of the latter structure during the summer of 1996. Kepner Plastics Fabricators completed its final design and fabrication in the spring of 1997. Basically, such a structure is a pressurized tube that attains its structural stiffness by using high-strength fabrics in the lateral direction along the sides of the "V." Wave height reductions for both structures were in the range of 50-60% (again consistent with analytical and laboratory results). Unfortunately, both structures again encountered difficulties in areas of local stresses and where materials of different properties were joined.

Due to the vastly superior handling and fatigue characteristics of the hydrobeam RIB, a detailed analysis of construction cost was made. At that time, this analysis indicated that the manufacturing cost was prohibitive, given our understanding of the governing equations for the amount of fabric required and the cost of producing appropriate high-strength fabrics. Consequently, when design of the first prototype-scale RIB began, it was decided to construct a hybrid structure that combined multiple layers of steel bridging panels for stiffness & strength and marine textile fabric to connect the panels and make the sides, rather than completely constructed from fabrics. Figure 6 shows an aerial photo of this structure from field tests conducted off the coast of Cape Canaveral in late spring of 1999. Once again the

Figure 6. RIB used in FY 99 field study.

structure performed as designed in terms of wave height reduction (50-55%), but encountered problems with fatigue and large-wave survivability.

6. FINAL DESIGN FOR THE ATD RIB

Following the full-scale field test in 1999, it became apparent that failure modes in steel structures of the RIB class were going to be extremely difficult to circumvent in any prolonged employment. In each case that a steel-fabricated RIB was tested, the effective "brittleness" of steel led to catastrophic bending and/or breaking of sections. Flexible joints afforded some relief to this design dilemma, but constant wave motions seemed to inevitably produce fatigue, and ultimately, failure in such joints. Thus, fabric-based RIB designs were reconsidered as an alternative to the steel-based designs.

Two fundamental problems had to be resolved to make fabric-based designs feasible; high basic fabric costs, and required internal pressures within the RIB. The first of these problems essentially solved itself, primarily due to advances in manufacturing technologies that allowed a cost reduction of about a factor of 10 in the types of materials required for the RIB. The second problem relates to the amount and strength of material required for the RIB to be pressurized to its design value. Initial estimates for RIB pressures were based on the concept of dynamic similitude. In this context, pressures used in laboratory-scale models had to be increased in proportion to the scale factor when design values for a prototype-scale RIB were obtained. For example, experiments run at a scale of 1:16 using pressures in the range of 2-5 psi would require internal pressures ranging from 32-80 psi for a prototype scale RIB.

Hoop tension, or tension in the material around the circumference of a tube is given as

$$T_H = \pi\, D\, p \tag{9}$$

where T_H is the hoop tension in terms of force per length, D is the diameter of the tube and p is the pressure. Internal pressures in the range of 32-80 psi would require materials with breaking strengths in the 10's of thousands of pounds per lineal inch along the RIB. Such a fabric would be prohibitively thick and bulky and its cost would also be prohibitive in a structure the size of the RIB. Fortunately, subsequent detailed analysis indicated that it was not critical that internal pressures be scaled dynamically. Instead, it was determined that the appropriate design parameter linked to internal pressure is the "wrinkle moment" for the fabric beam. Brown (1996, 2000) showed that this parameter was linked to the internal pressure by

$$M_w = \frac{\pi}{16}\, pD^3 \tag{10}$$

where M_w is the wrinkle moment. Using this equation as the basis for estimating design values for the internal pressure, it was determined that a value in the range of 1-3 psi should suffice for the prototype-scale RIB design. This finding was the key to allowing a successful design for this class of structure, since it reduced fabric strength requirements for materials around tube circumferences by a factor of 100 or more. It also enabled a wide class of available fabrics from polyurethanes through vulcanized rubber products to be considered.

Both laboratory and field experiments have indicated that the primary stiffness requirement for the RIB is in the lateral direction. Consequently, the main design requirement for stiffness is along the length of the RIB at the 3 and 9 o'clock positions on the surface of the RIB. Therefore, only in the lateral direction are the very-high values of fabric strengths required. In light of this, the final tube design emerged as shown in Figure 7, with

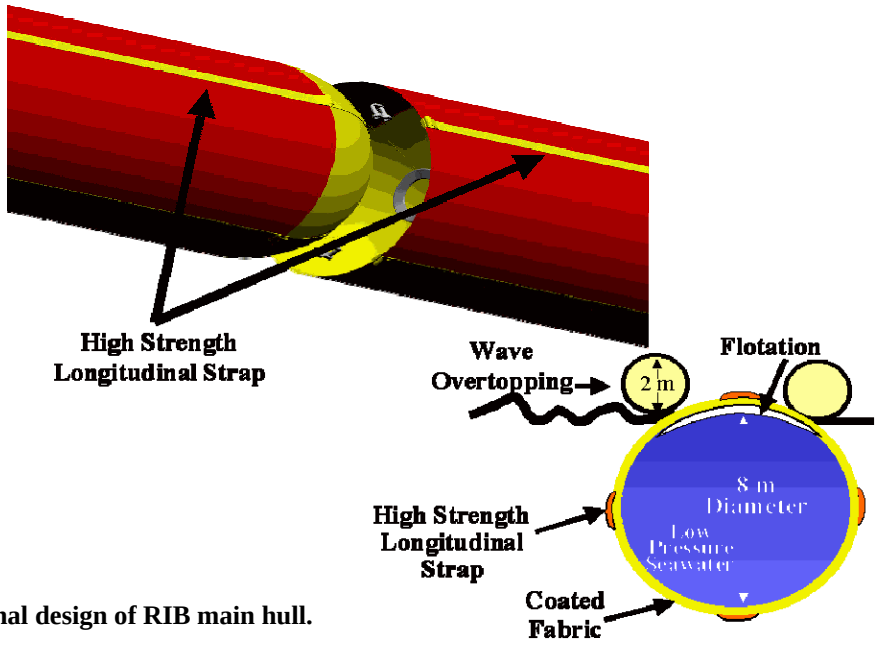

Figure 7. Final design of RIB main hull.

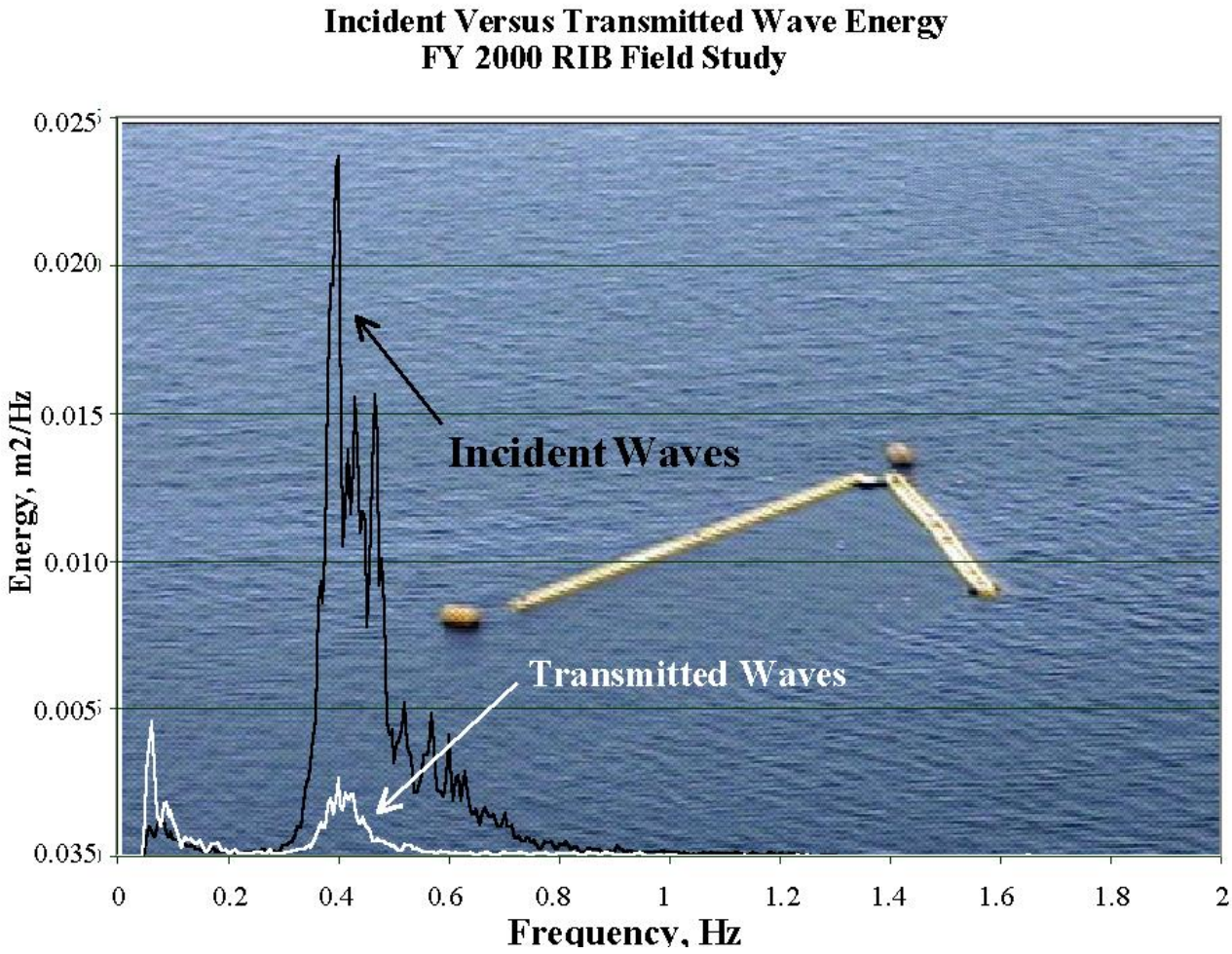

Figure 8. Incident and transmitted wave energy plots superimposed on a photo of the RIB used in the FY 2000 field study.

high strength materials of the Kevlar-Vectran class (high molecular weight polymers) used as straps along the sides of the fabric tubes. The number, size, and strength of the straps were determined based on strength and stiffness requirements identified in Equations 6, 7, and 10 along with mooring loads to be transmitted through the structure. In this design concept, arbitrary-length tube sections can be fabricated and joined together to form a continuous strength beam for wave deflection. Furthermore, the basic failure mode of this type of structure is for the fabric to locally wrinkle and under extreme loads to buckle. Unlike the case for steel structures, this type of failure is not detrimental to subsequent performance of the RIB. Figure 8 shows an aerial photo of a 1:4-scale hydrobeam RIB tested in Pensacola Bay, Florida in the summer of 2000, along with a sample of wave spectra measured simultaneously inside and outside of the RIB. This structure performed very well with wave height reductions in the range of 50-70% for incident waves within +/- 60 degrees of the centerline of the RIB. Moreover, its performance did not degrade over the 5-week test interval. The RIB was recovered at the end of the field test and could be redeployed if necessary.

6. SUMMARY AND CONCLUSIONS

Following the development of a strong theoretical foundation for a new class of floating breakwater, a series of laboratory and field tests have been used to aid development of Rapidly Installed Breakwater (RIB) for military applications. Field tests conducted this past summer have shown that this new class of structure is capable of meeting all key metrics for such a system: performance, deployability, employability, survivability, utility, affordability, and size. Based on results such as those shown in Figure 8, the RIB system developed at WES appears to hold great promise for alleviating force projection concerns related to offloading problems associated with higher sea states during JLOTS operations.

ACKNOWLEDGEMENTS

Permission of Headquarters, US Army Corps of Engineers (USACE), for permission to publish this paper is acknowledged with appreciation. This research is being conducted as part of the USACE Military Engineering RDT&E Program of the US Army Engineer Research and Development Center's Coastal and Hydraulics Laboratory. Kepner Plastics Fabricators, Inc., Torrance, California, fabricated the RIB Systems deployed during the field studies. Quantum Engineering Design, Inc. Corvallis, Oregon, and Vertigo Inc., Lake Elsinore, California assisted in the design of the RIB models used in various laboratory and field studies. Strait Moorings International Inc., Shediac, New Brunswick, Canada, and PCCI, Inc., Alexandria, Virginia assisted in the design of the mooring system used in the FY 2000 field study.

REFERENCES

Briggs, M.J., Demirbilek, Z., and Matheu, E.E. (1998). An Integrated Study of Wave Phenomena Affecting Floating Breakwater Design for JLOTS, *21st Army Science Conference*, Norfolk, VA, June 15-17.

Brown, G. (1996). "Braided airbeams in bending". Report for contract DAK-60-94-C-1051, Vertigo, Inc., Lake Elsinore, CA.

Brown, G. (2000). "Reinforced Fabric Beams for RIBS". Report for contract, Vertigo, Inc., Lake Elsinore, CA.

Committee On The Navy And Marine Corps In Regional Conflict In The 21st Century, 1996. The Navy and Marine Corps in Regional Conflict in the 21st Century, National Academy Press Washington, D.C. , pp. 69-70.

Jones, D. B. (1971) Transportable breakwaters : A survey of concepts; sponsored by Naval Facilities Engineering Command. Technical report Number R727. Port Hueneme, Calif. : Naval Civil Engineering Laboratory

Kobayashi, N. (1998). "RIB wave field model development". Report for contract DACA39-98-M-0279, Center for Applied Coastal Research, Univ. of Delaware, Newark, DE.

Kriebel, D.L. and Bollman, C.A. (1996). Wave Transmission Past Vertical Wave Barriers, *25th International Conference on Coastal Engineering*, Ch 191, 2470-2483.

Melby, J.A. (1998) "Wave Transmission characteristics of RIB". Unpublished RIB report. USAE Engineer Research and Development Center, Vicksburg, MS.

Wiegel, R.L. (1960). Transmission of Waves Past a Rigid Vertical Thin Barrier, *Journal of Waterway, Port, Coastal, and Ocean Division*, 86(WW1), March 1-12.

Appendix B

1:16 Scale Model Tests

Test Facility

An existing physical model facility was modified to include a breached levee on which a series of experiments could be conducted to test methods for sealing the breach. The model levee was constructed at an undistorted scale of 1:16 (model:prototype) to represent a levee with a crest elevation of 20 ft (note: all dimensions are reported in prototype scale unless otherwise stated), side slopes on both faces of 1:3 (vertical:horizontal), and a crest width of 16 ft. The breach was 80 ft wide with 2:1 side slopes the full depth of the levee. Both the model basin and the levee were constructed of a concrete cap poured over a sand fill with inset aluminum templates to insure the accuracy of the bathymetry and topography.

Figure 1. Test basin for 1:16 scale physical model tests.

The model represented a fairly extreme test as the breach was 80 ft wide and 20 ft deep, the still water level was 18.7 ft deep, and there was as a significant riverine current flowing along the levee and past and through the breach (Figure).

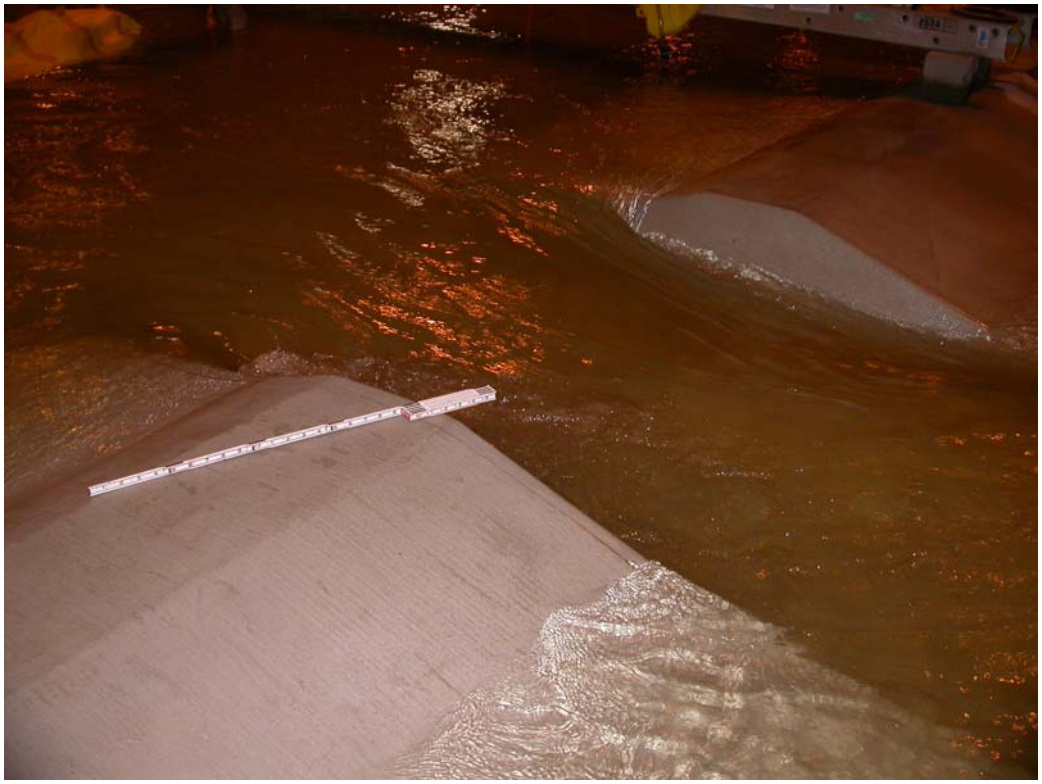

Figure 2. Flow through the breach with upstream depth at 18.7 ft.

195-ft-long Fabric Bags

Tests were conducted to determine the feasibility of stopping the breach with a fabric bag or bags while flood waters were still flowing through the breach. Fabric bags in a variety of sizes were constructed for the study by Kepner Plastics, Inc., in California. The bags were constructed of polyvinyl chloride-coated fabric weighing 10 oz per square yd. Initial bags constructed of heavier fabric appeared to be unrealistically rigid, and Kepner Plastics advised that bags lighter than 10 oz per square yd had a tendency for D-rings and other fasteners to pull off by separating the polyvinyl chloride coating from the underlying fabric. The 10 oz per square yd bags exhibited a reasonable level of rigidity.

The most promising tests used a bag designed with the same length as a standard hopper barge (195 ft). For a 20 ft high breach, a 30-ft-diameter bag was chosen to insure the bag would be at least 20-ft high when sitting on the substrate and distended into an oval shape. It was necessary to have the bag not only extend from the water surface to the floor, but when the bag rolled up on the levee the bag had to sit high enough above the water level to exert a downward force with the portion of the bag above water to create a watertight seal beneath the bag.

Fill level

Before filling the bag, the bag was submerged starting at one end to force any air out of the bag. A flow meter was used to measure the volume of water placed in the bag.

As the bag is filled, it becomes rigid and cylindrical. If the bag is under-filled, it will buckle when placed across the breach, the ends will fold in, and the bag will get pushed through the breach. If the bag is over-filled, it spans the breach as a cylinder and does not provide a good seal. The ideal fill level allows the bag to bend enough to penetrate into the breach yet have sufficient rigidity to prevent the bag from buckling. Figure 2 shows the breach filled with the 195-ft-long bag filled to 70 percent of its capacity. The bag has rolled up the side of the levee so that the ends are elevated higher than the section within the breach. Water is leaking at the corners where the bag does not fit snugly into the angle between the floor and the side of the breach. It is expected that a real breach would not have as abrupt an angle and that the prototype bag would provide a better seal in the corners.

Figure 2. Breach sealed by 195-ft-long bag with 70% fill.

Figure 3 shows the same bag filled to 80 percent capacity. Compared to Figure 2, the 80%-filled bag is more rigid and does not extend into the breach as far. The seal is poorer with more water flowing through the breach. Water can be seen flowing around the ends of the bag and entering the breach above where the bag is resting on the levee face.

Figure 3. Breach sealed with 195-ft-long bag with 80% fill.

Filling the bag to 70 percent capacity worked well for the breach in the experiments, but it is expected that the optimum degree of fill will be dependent on the width and depth of the breach, which will not be adequately known during deployment of the bag. A solution was to overfill the bag, place the bag into the breach so that it spans the breach as a rigid cylinder, and then drain water from the bag until the bag starts to fold and extends into the breach to form the optimum seal.

Deployment

The bag was held in place offshore of the breach during filling by lines attached to each end of the bag. When the bag was filled to the desired level, the bag was maneuvered to the breach in a manner to simulate a tow boat fastened by a line to

each end of the bag. It is obvious that a tow boat would not wish to get too near the breach, nor between the bag and the breach, and that the tow can only pull the bag and not push it. It was therefore necessary to hold the bag in the current such that the combination of riverine current and flow through the breach would pull the bag into the breach while the lines were used to maneuver the bag into position.

A problem with deployment was that the bag would roll along the floor rather than slide. By rolling, it was difficult to maneuver and needed to be lined up correctly at the start of the deployment as it tended to roll in a straight line. The bag needed to have sufficient length that it would still span the breach when the bag did not line up correctly. Using a 195-ft-long bag for an 80-ft-wide breach provided sufficient length that the bag was always deployed into the breach in the laboratory experiments, but it is expected that prototype deployments will be more difficult to align.

To keep the bag from rolling, tests were conducted where the air in the bag was not removed prior to filling the bag with water. The volume of air was not measured.

Figur shows the breach sealed with air left in the bag, then the bag was filed with 65 percent capacity water. The bag slid along the flume bottom during deployment, as desired. When the bag reached the levee, the bag rolled up the sides of the levee and all the air went to the ends of the bag. The portion of the bag within the breach therefore had the full weight of water to seal against the bottom of the breach. The option of leaving some air in the bag seemed to work well.

Figure 5. Breach filled with 195-ft-long bag with 65% fill and air left in bag before filling.

Another method tried to prevent rolling during deployment was to fasten an outside air chamber along the length of the bag. Six-in.-diameter orally-inflated tubes used in SCUBA diving as emergency signal devices were fastened along the length of the bag (Figure 4). The outside air chamber was successful in keeping the bag from rolling along the bottom of the test basin, but got in the way when the bag rolled up the face of the levee. However, the bag was able to roll over the air chamber and successfully sealed the breach (Figure 5). An internal air chamber could be built into the bag to prevent the outer chamber from interfering with the roll of the bag up the side of the levee.

Figure 4. SCUBA signal tubes fastened along 195-ft-long bag.

Figure 5. 195-ft-long bag deployed with outside air chamber.

A third option for keeping the bag from rolling was to change the shape of the bag from a cylinder to a wedge. A beam was fastened to the ends of the bag to force the bag to fold in the middle, and rope ties along the length of the bag helped to maintain the wedge shape. A "sea anchor" was fastened to the middle of the bag at the fold to direct the point of the wedge into the breach. Air was not removed from the bag, and the bag was filled with 60 percent capacity water. In Figure 6 the wedge had entered the breach crooked and off-center, but still made a good seal. An extension of the wedge idea is to try a doughnut-shaped bag so that it could enter the breach at any angle. As a doughnut-shaped bag was not available, this option was not tested.

Figure 6. Beam and ties used to force 195-ft-long bag into a wedge shape.

Deployment by barge

Another method of deploying the bag without allowing the bag to roll was to deliver the bag to the breach attached to a barge. A scale model of a standard hopper barge was constructed to reproduce the outside dimensions, weight, and draft of a prototype barge. The barge was 195 ft long (prototype), 35 ft wide, 12 ft high sides, then a partial deck with inner walls extending up another 2 ft. Draft of the barge was approximately 6 ft.

Because the sides of the barge were 12 ft high, the bag was tied to the barge with 12 ft lines such that it hung at the bottom of the barge. In a manner similar to the

bag only deployment, the barge was held in place by a line attached at each end to simulate a towboat fastened by line to each end of the barge. The barge was held in the current during filling of the bag such that the combination of riverine current and flow through the breach would carry the barge/bag into the breach.

With the bag tied with 12-ft-long lines along the length of the barge, the bag was unable to extend sufficiently into the breach to form a good seal. The bag spanned the breach in a manner similar to the bag-only when the bag was overfilled and spanned the breach as a rigid cylinder. The solution was to tie the bag to the barge with lines of varying length. By using 12-ft-long lines a the ends of the barge and extending the lines to 36-ft-long in the middle, the bag was able to penetrate into the breach further and form a better seal. Figure *7* and Figure 8 show the bag deployed into the breach while attached to the barge.

Figure 7. Barge with bag fastened by variable length lines.

Figure 8. Bag extending into the breach while attached to the barge.

80-ft-long by 30-ft diam bags

A number of tests with smaller bags were conducted but were not as successful as the tests with the 195-ft-long bag. An example of the shorter bags is the 80-ft-long by 30-ft-diam bags shown in Figur (looking upstream into the breach) and Figure *9* (looking downstream in the breach). The bags were difficult to hold in place in the breach during filling and the very high currents that formed between and around the bags during filling would cause extensive scouring.

Figure 11. 30-ft-diam bags placed side-by-side to span the breach, looking upstream into the breach

Figure 9. 30-ft-diam bags in breach, looking downstream.

Shallow-water breach

Experiments were also conducted on long shallow breach. Water flowing over the breach was only 2 ft deep (target depth, measured depth was 1.6 ft), and the

breach was 112 ft long. The breach was constructed of plywood with a 1:3 riverine-side slope (Figure *10*). The landward side of the levee was not reproduced and a tarp held in place by concrete blocks was placed on the landward side to prevent scour (Figure *11*).

Figure 10. Plywood sections used to construct the shallow-water breach. The section on the left end is elevated only to illustrate the construction.

Figure 11. Shallow-water breach with bag in place.

The bag used in the shallow-water breach tests was 256-ft-long by 8-ft-diam with an attached external floatation chamber. Although the flotation chamber is intended to be an air-inflatable chamber, for the 1:16 scale tests the flotation chamber was filled with foam. One method of deployment was to anchor the bag at the upstream end of the breach, extend the bag into the current, and let the current carry the bag around to cover the breach. Deployment by this method is shown in Figure *12* and

Figure 13.

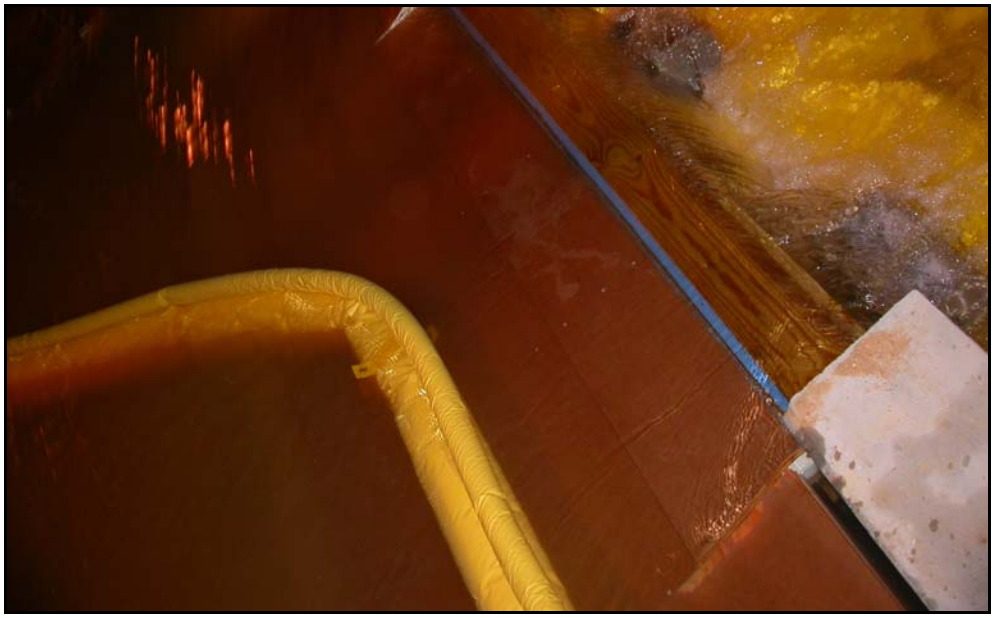

Figure 12. Shallow-water breach bag being carried into place by current.

Figure 13. Shallow-water breach bag nearly in place.

The floatation chamber was found to interfere with the bag rolling up the levee slope and into the breach. In later tests, the floatation chamber was therefore cut from the bag allowing further penetration into the breach and achieving a better seal.

Appendix C

Rapid Levee Repair System
Scale Testing Summary

TM305051
Revision A

Oceaneering International, Inc.
7001 Dorsey Road
Hanover, MD 21076

Change History

CRF #	Rev	Release Date	POC
ECO-1782	-	01/07/09	BW
ECO-1784	A	01/13/09	BW

TABLE OF CONTENTS

1.0 Introduction

The Rapid Levee Repair System (RLRS) has progressed through its initial study, conceptual design, and scale test phases. The use of water filled fabric tubes to plug breaches was explored and evaluated in scale testing due to the advantages that it offered. This document summarizes each of the concept development stages and the results that prove the validity of the concepts for testing at full scale level.

2.0 History/System Drivers

2.1 Geography

Recent large magnitude flood disasters have generated an increased focus on emergency repair of breached levees. Analysis of failed levee systems was used to characterize the causing factors and parameters of typical breaches, and served as a starting point for the development of new methods of mitigating flooding or preventing further erosion.

The size and type of body of water plays a role in determining the appropriate deployment method to ensure safety of personnel and equipment and overall effectiveness. An example of this is in the case of a sufficiently large lake or wide river with calm flow areas away from the breach. The calm area offers a safe staging area for boats or barges and "stable" standoff area for them during deployment. In cases where these calm areas may not exist such as fast-flowing rivers, alternative methods of anchoring the system and staging sequence may be required. The concepts addressed in this report were evaluated using the calm standoff area approach while noting potential factors and deployment techniques that will be affected or required in fast-flow deployment.

2.2 Breach characteristics:

Levee breaches were classified into two stages or types of failure; shallow and deep. Shallow breaches are a result of the initial overtopping and erosion of the levee and may stretch across its entire length. They differ from deep breaches in that they do no descend to the bottom of the levee or floor of the body of water. In recent events shallow breaches were found to range from just overtopping to two feet deep and spanned 400 ft of the levee.

In some cases the onset of a shallow breach results in local erosion of the nominally dry backside of the levee. Left to continue, this results in the propagation of crevices in width and eventually to the bottom of the levee or floor creating a deep breach. In recent events deep breaches occurred that were 20ft deep and 80ft wide which serve as a design goal for concept development.

With regards to using water-filled tubes to plug breaches, levee slope offers the advantage to aid in deployment and increase the systems effectiveness. In both shallow and deep breach concepts, as the tubes contact the levee and are pushed by the flow of water, they eventually roll up its sloped face to a point of equilibrium “head” above the body of water. Furthermore, in the case of deep breaches, the tube compresses as it flows partially into the breach creating additional head and stability.

2.3 Initial concept evaluation

Existing facilities at USACE-ERDC, Vicksburg, MS with levee breach simulation capabilities offered the opportunity to test at 1/16 scale. Testing at this scale allowed an efficient means of down-selecting to the most viable concepts. Parameters of the test facility such as flow rate and profiles were well-characterized in previous research activities offering a reliable starting point for design requirements. Breach models and supporting infrastructure required no new construction or modification. Special consideration was given to the performance of the 1/16 scale tube materials during testing. Maintaining strength of the tube while maintaining flexibility often resulted in a trade. Scaling materials for 1/16 scale testing resulted in less durable test articles relative to the those available for 1/4 and full scale models.

2.4 Larger scale testing

Existing facilities at US Department of Agriculture, Agricultural Research Service in Stillwater, OK, offered the opportunity to test at 1/4 scale with minimal facility construction or modification. Concepts selected based on evaluation in 1/16 testing were tested at 1/4 scale level. Materials in 1/4 scale test articles more closely resembled those anticipated for use in full-scale models. Strength and flexibility did not require compromise as in the case of 1/16 scale testing.

3.0 Concept Descriptions

The following concepts were evaluated in scale testing. General arrangements and approach along with their advantages and disadvantages are discussed. Details of test procedures and results are discussed in Sections 4.0 and 5.0.

3.1 Parallel Flow, Deep Breach Configuration

The concepts selected for initial deep breach testing were based on parallel and cross-flow configurations. Parallel flow arrangements are those in which tubes are arranged with their longitudinal axis parallel to the breach flow and do not span beyond the width of the breach. They do not take advantage of the sloped levee face in establishing equilibrium. Therefore additional means of anchoring throughout deployment and positioning is required. Figure 3.1.1 shows a parallel flow configuration that was tested on the 1/16 scale level.

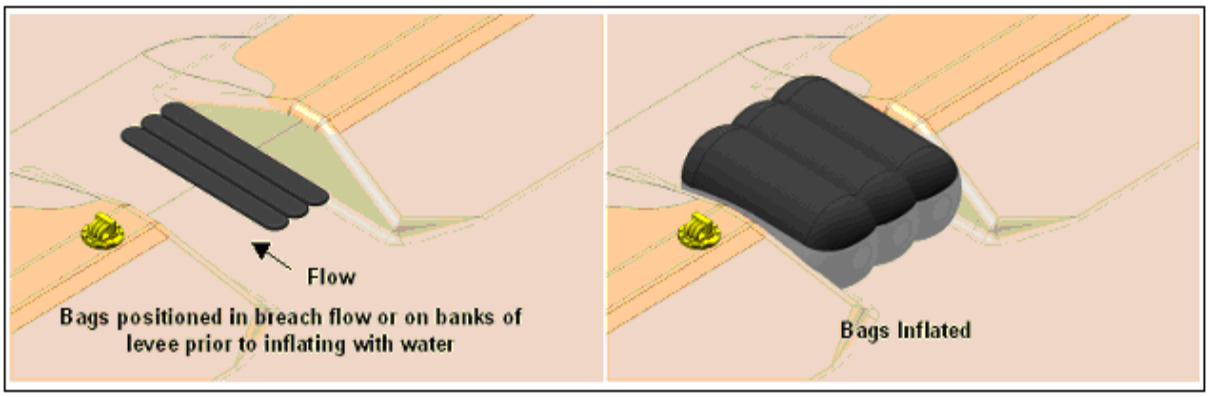

Figure 3.1.1: Parallel Flow Concept.

3.2 Cross-Flow, Deep Breach Configuration

The Cross-Flow Deep Breach configuration consists of a tube that spans and overlaps the width of the breach. Figure 3.2.1 shows an example witnessed in 1/4 scale testing. It is positioned from the calm area of flow using tag lines to "fly" it into the breach. The tag lines are managed using land-based weights or anchors. In 1/4 scale a line at each end of the tube was required and safely managed by one attendant each. As the tube approaches the levee and makes contact its sloped face, lateral motion ceases and the tube rolls into place. When the tube begins to roll the tag lines are release to allow it to build maximum momentum.

Figure 3.2.1 Cross-Flow, Deep Breach

As mentioned in Section 2.3, the slope of the levee face allows the tube to establish and maintain position during deployment and steady state holding. The tube compresses as it is drawn into the breach. Additional head pressure is established as the tube rolls up the face of the levee until the system reaches equilibrium.

3.3 Cross-Flow, Deep Breach Barge-Deployed Configuration

This approach, also referred to as Barge-Deployed Tube, uses a barge for pre-staging and deploying the equipment discussed in Section 3.2. The barge remains in the calm area mentioned in Section 2.1 while maneuvering the tube into the breach flow. When properly positioned, the barge releases the tube and the sequence of events occurs that is mentioned in section 3.2 starting when the tag lines are released. The significance of the barge-deployed configuration is that a self-contained system can be pre-staged, maneuvered into place, and effectively deploy the tube from a safe standoff distance.

3.4 Shallow Water Spillway

In some cases it may be desirable to allow the main body of water to relieve in a overtopping situation to avoid flooding in other sections of the levee. In doing so however, erosion must be mitigated to prevent a deep breach situation or compromising of the levee. The Shallow Water Spillway concept does so with the positioning of a tarp to cover the levee in the area of flow. It is held in position using chains along the front edge and a series of water filled tubes to weight it down in the flow entry region. The tarp extends to protect the back side of the levee from erosion. Figure 3.4.1 shows and example of this at the 1/4 scale level. The flow through the protected channel is 8in deep and 20ft wide, with the exception of the 15in diameter x 90in long anchor tubes.

Figure 3.4.1: Shallow Water Spillway

3.5 Shallow Water Blocking Configuration

This concept is aimed at stopping over-topping flow over long lengths of the levee. Figure 3.5.1 shows and example in 1/4 scale testing. It employs a tube that spans the width of the flow and is anchored by the sloped face and lip of the breach. Similar to the deep breach concepts, the tube establishes and maintains equilibrium by rolling up the face of the levee and developing head above the nominal water surface. Additional tubes are placed as required to address flow around the ends. Since the tube is anchored along its entire length, it can be installed for distances along the levee limited only by practical handling and deployment considerations.

Figure 3.5.1: Shallow Water Blocking Configuration.

4.0 Test Article Configuration, 1/16 and 1/4 Scale

The following drawings pertain to the test articles used in 1/16 and 1/4 scale testing and are provided for reference.

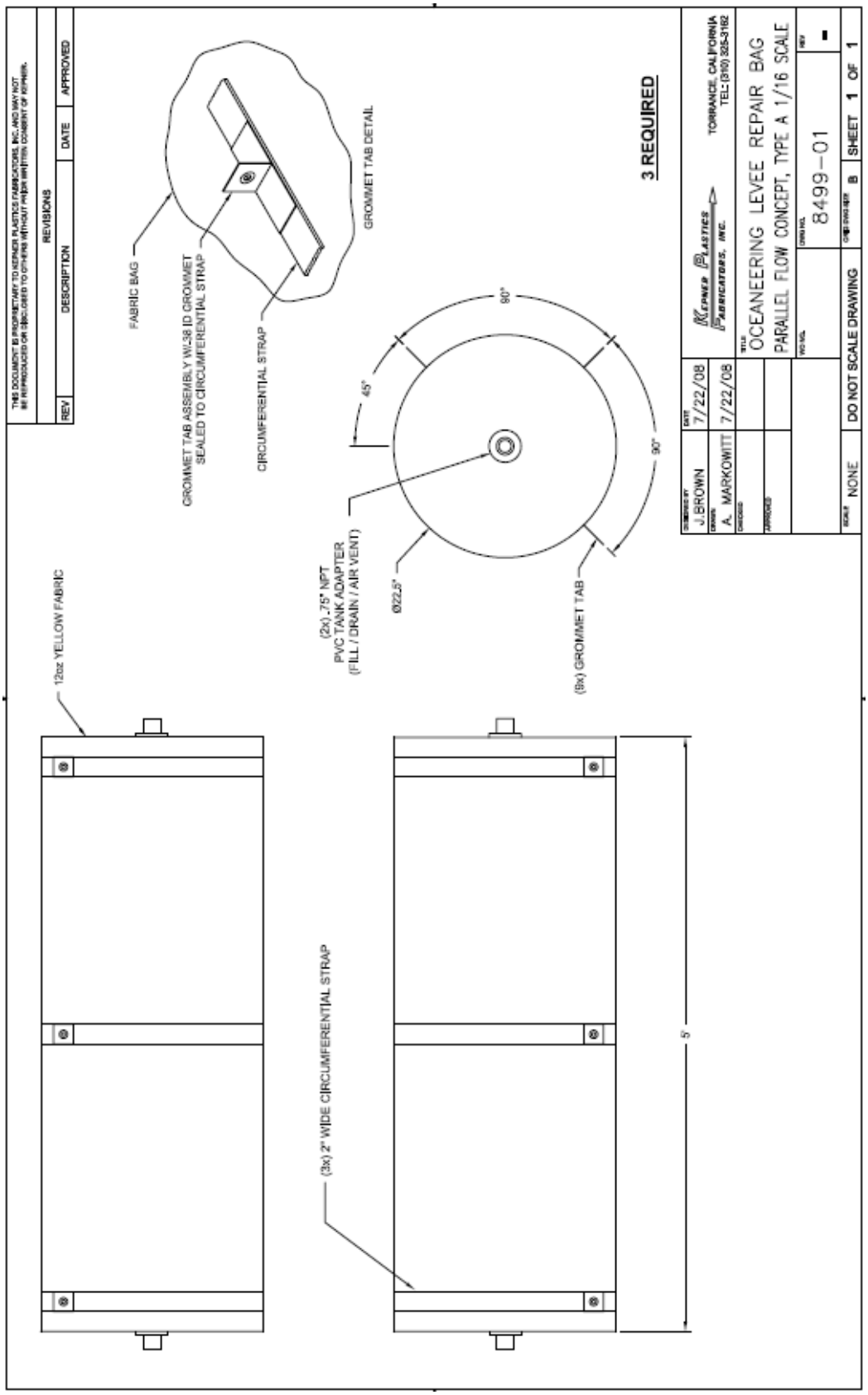

Figure 4.1: Parallel Flow Tube, Type A, 1/16 Scale

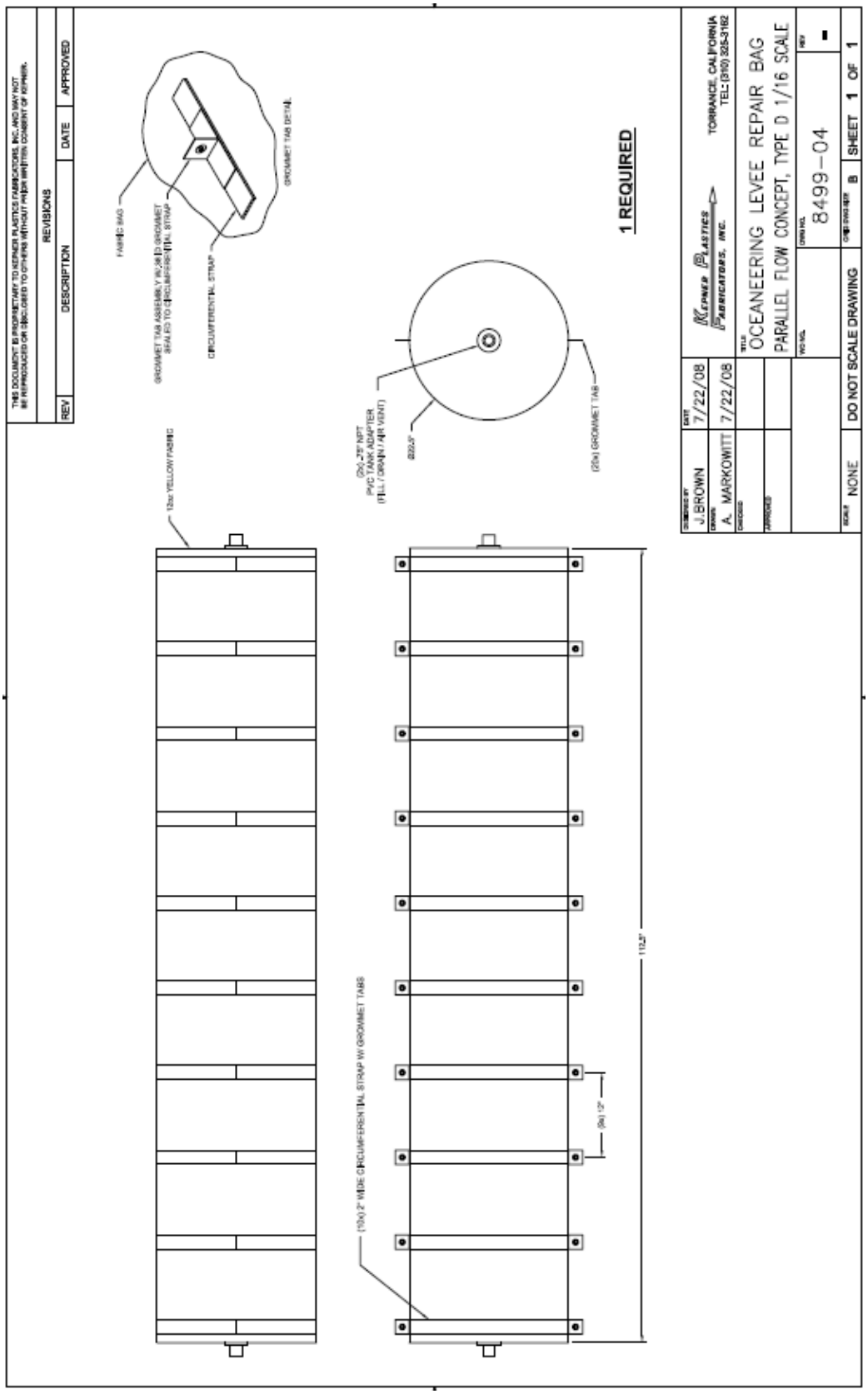

Figure 4.4: Cross-Flow Deep Breach Tube, 1/16 Scale

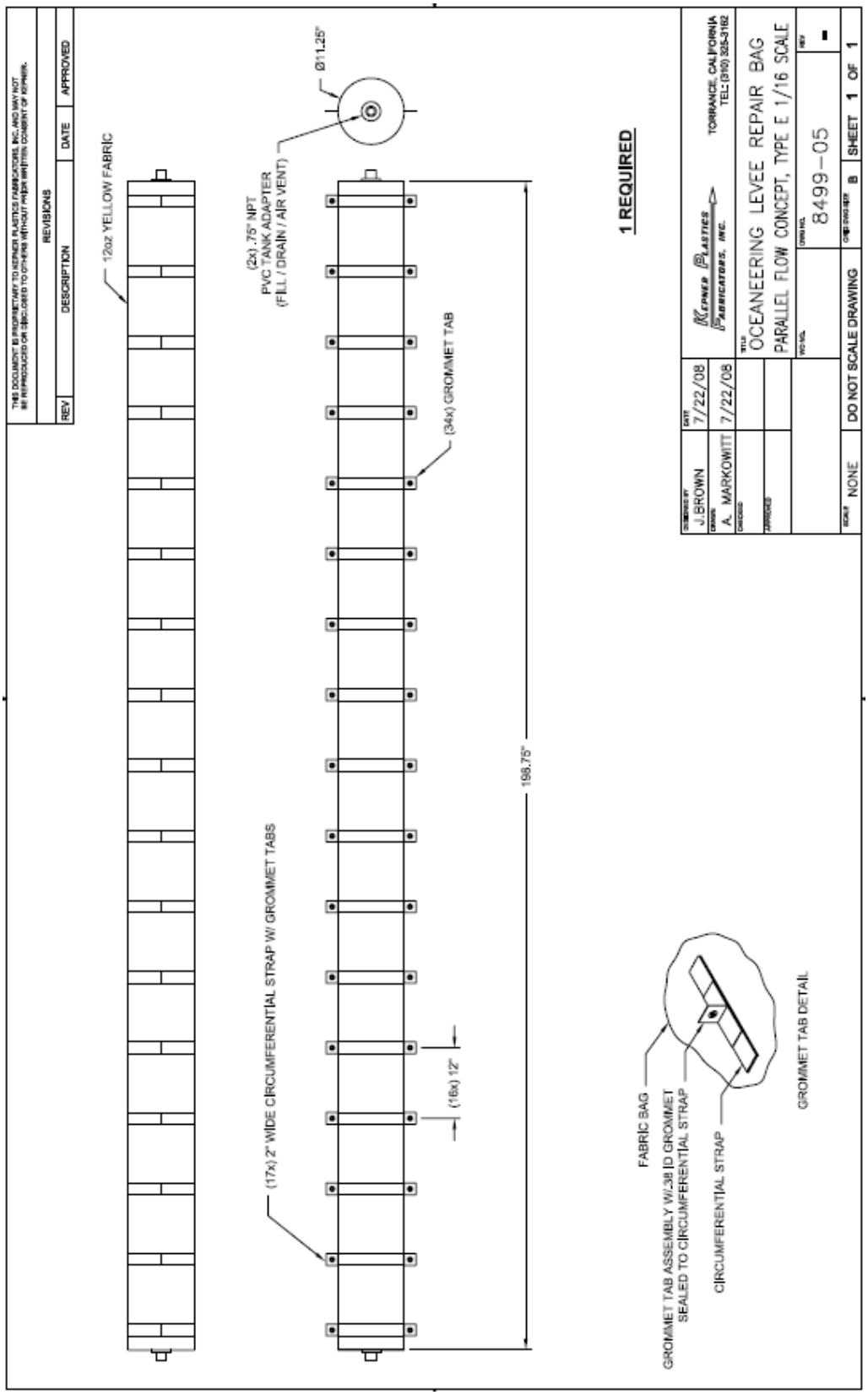

Figure 4.5: Shallow Water Block Tube, 1/16 Scale

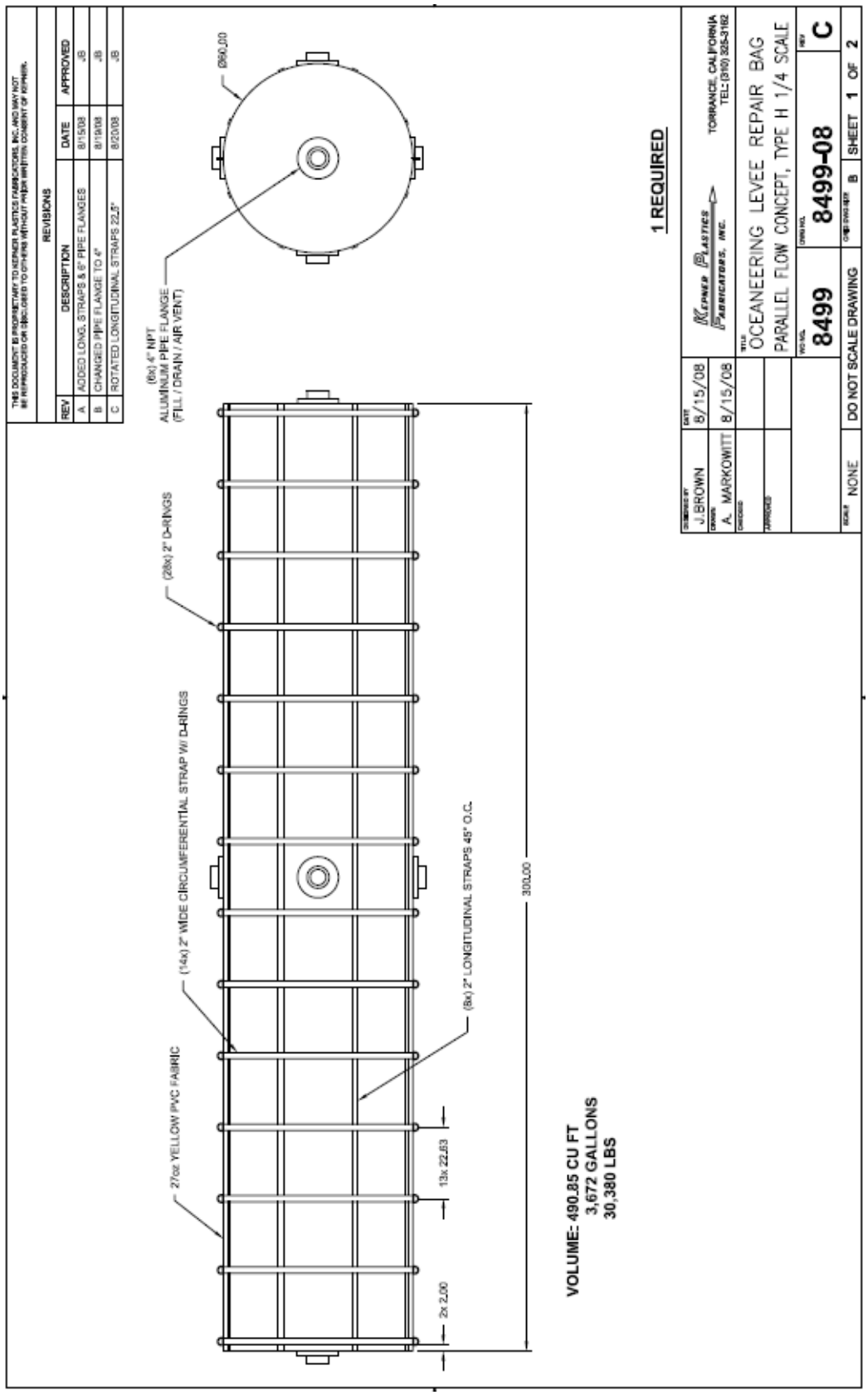

Figure 4.6: Cross-Flow, Deep Breach Tube, 1/4 Scale

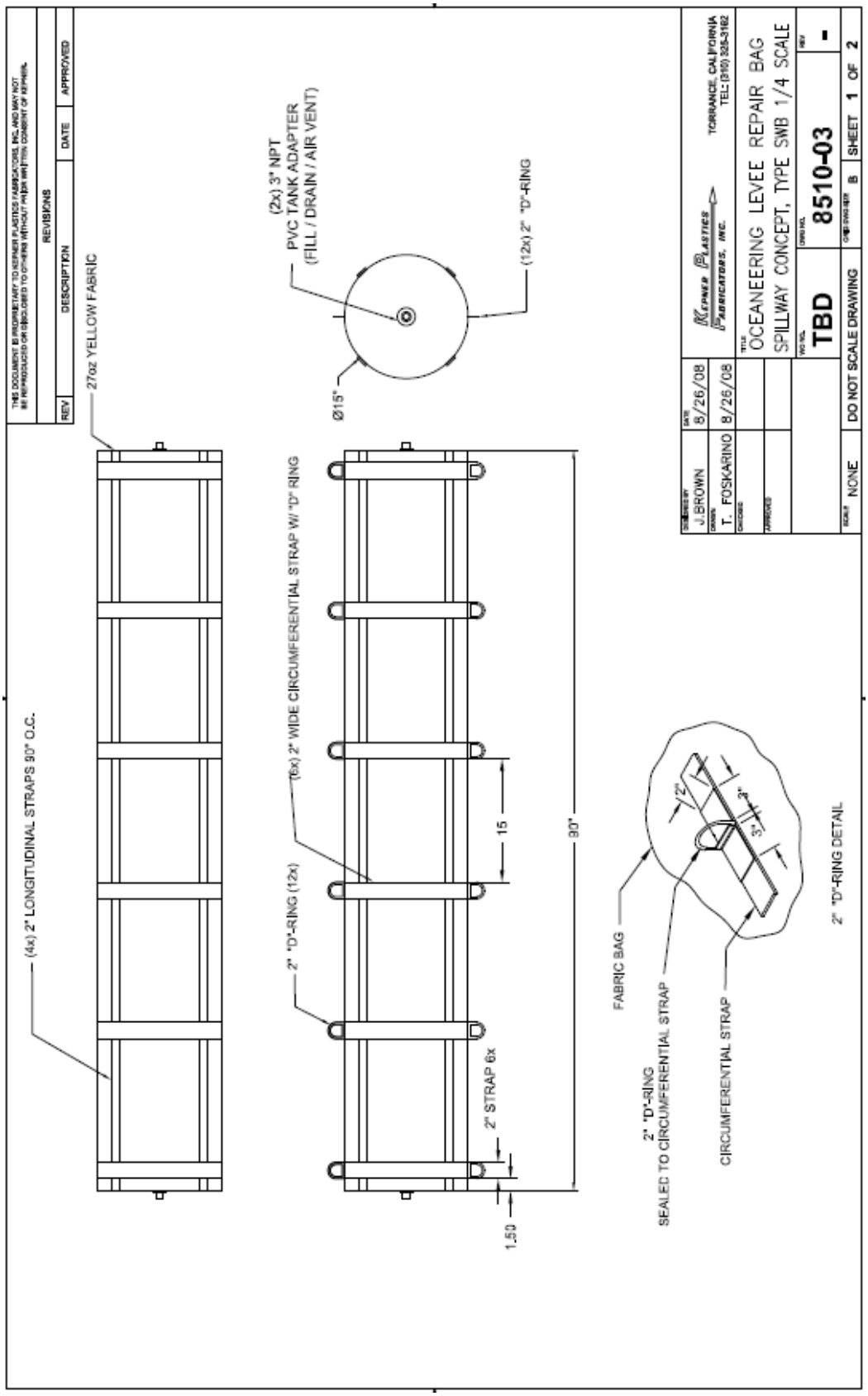

Figure 4.7: Shallow Water Spillway Tube, 1/4 Scale

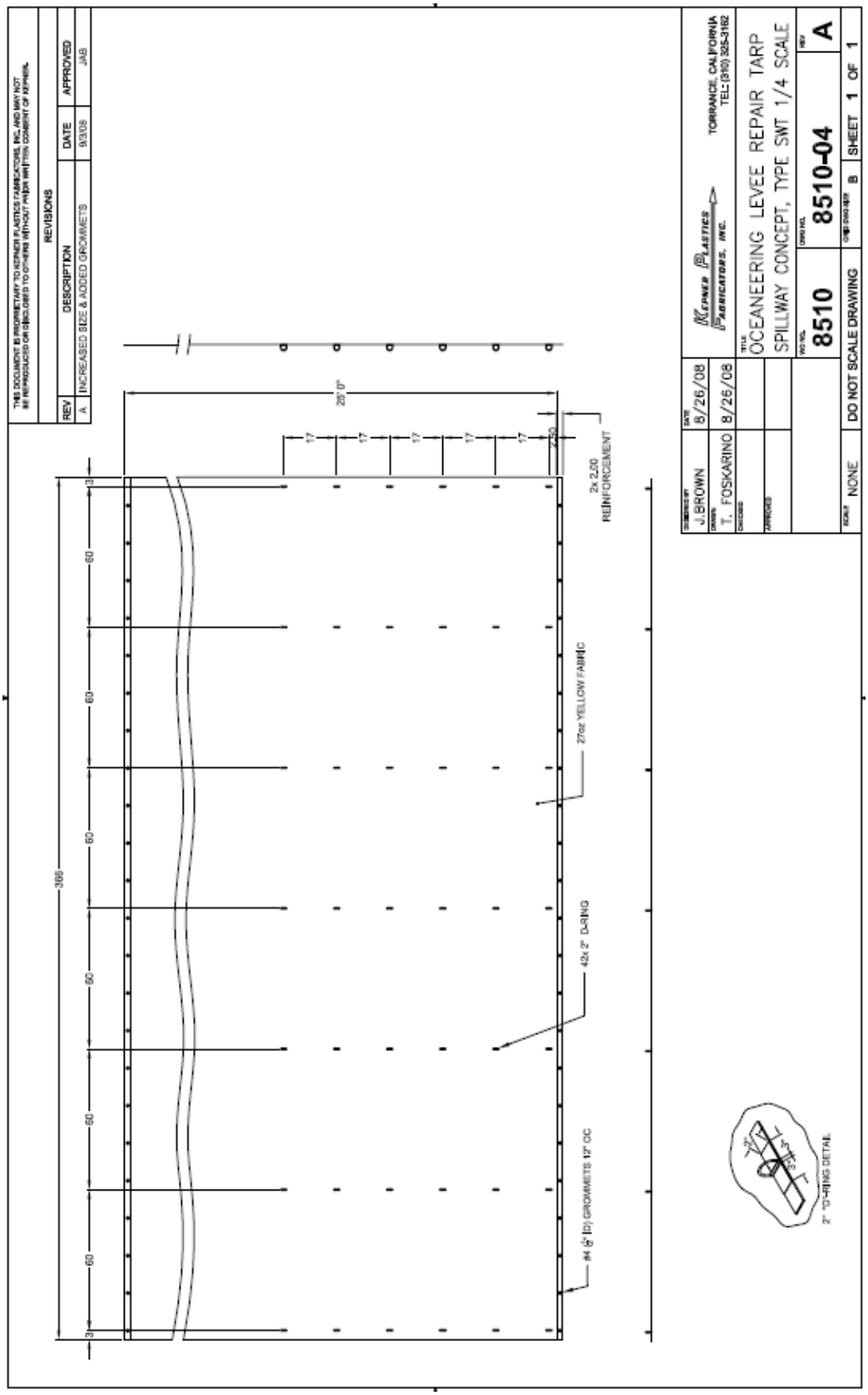

Figure 4.8: Shallow Water Spillway Tarp, 1/4 Scale

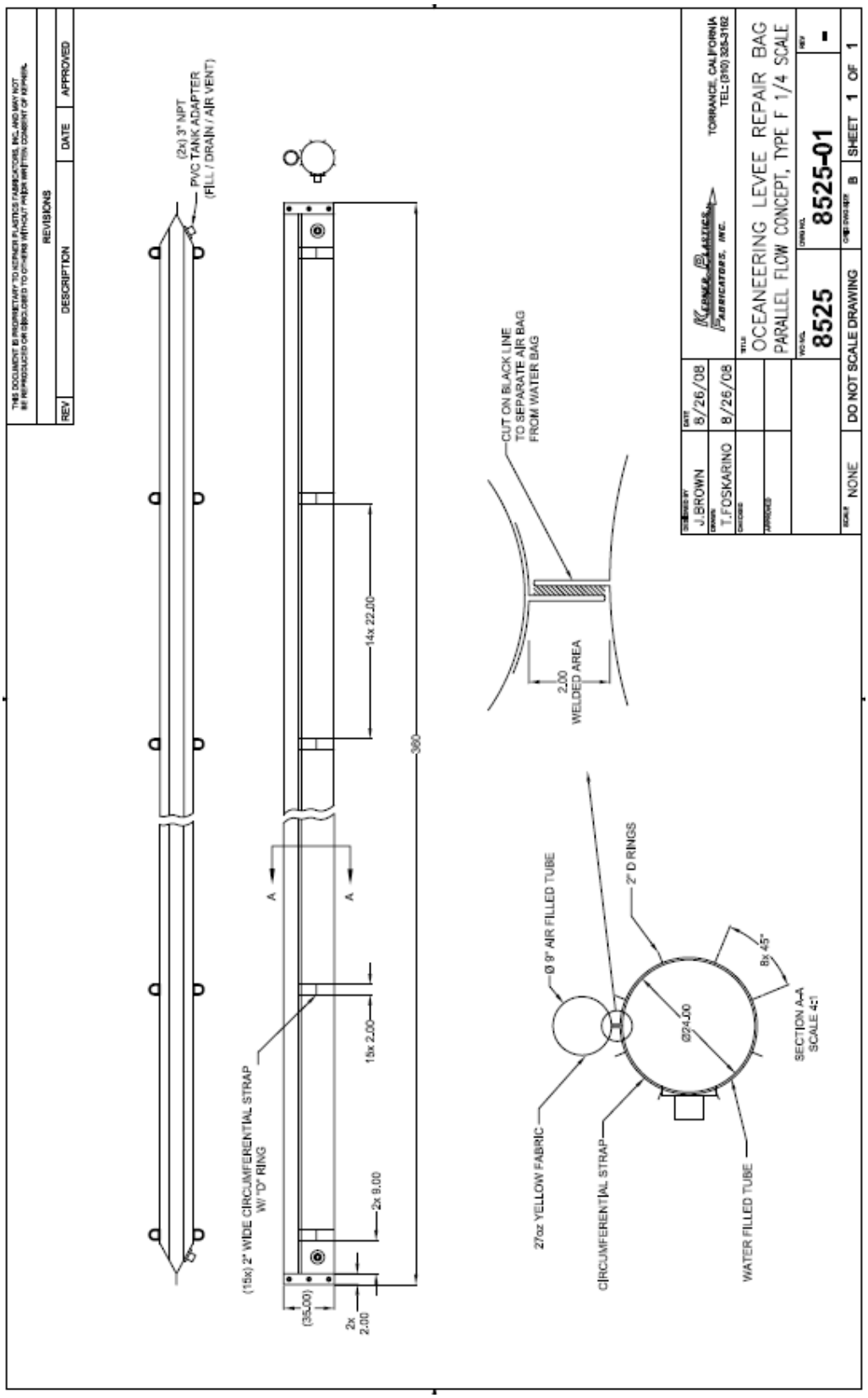

Figure 4.9: Shallow Water Block Tube, 1/4 Scale

5.0 Testing: 1/4 Scale

5.1 Test Facility Configuration:

The USDA-ARS Hydraulic Research Lab in Stillwater, OK is situated adjacent to the Lake Carl Blackwell. Water is siphoned over the dam and distributed through the supply canal to the test channel or other areas of the facility as needed. Figures 5.1.1 and 5.1.2 show an aerial of view of the lab and a view of the test channel respectively.

Figure 5.1.1: Aerial View of USDA-ARS Hydraulic Research lab.

Figure 5.1.2: Test Channel.

The supply canal is capable of delivering up to 125ft^3/s of water to the test channel. The test channel incorporates two test levee sections for shallow and deep breach applications. Figure 5.1.3 shows the deep breach section and the surrounding walkways and supporting structure. For demonstration purposes, an easily eroded filler material is shown being washed out of the 5ft wide previously excavated breach. Figure 5.1.4 shows the deep breach at 125ft^3/s full test flow.

Figure 5.1.3: Deep Breach Levee Section.

Figure 5.1.4: Deep Breach With 125ft^3/s Flow.

Figure 5.1.5 shows the shallow water breach with the Spillway concept deployed. The breach is 20ft wide resulting in a flow depth of 8in.

Figure 5.1.5. Shallow Breach with Spillway Concept.

5.2 Test Equipment

The following (not limited to) items were used to support 1/4 scale testing:

-(1) Barge 20ft x 10ft x 4ft
-(2) 8hp centrifugal pumps with 3in ports
-(1) 10,000lb capacity 50' reach all-terrain forklift
-(1) Air compressor diesel-powered high capacity
-(1) Soil auger/anchor installer
-(3) Auger/anchor
-(5) 50ft length fire hose, 3in diameter
-(1) Water meter, propeller style 3in ports, 200gpm capacity

5.3 Test Procedures and Results

5.3.1 Cross-flow, Tube Only Configuration

The test channel was set to provide 125ft^3/s flow through the 8ft wide x 3ft deep breach. A 100ft tag line was tied to each end of the tube and secured to anchor points upstream of the breach as shown in Figure 5.3.1.1.

Figure 5.3.1.1 Tube Filled, Staged for Deployment

The tube was tested at prescribed fill levels of air and water. Fill parameters for air and water and the corresponding results are presented in Table 5.3.1.1. The test was repeated for each set of parameters and followed the sequence:

1. The tube was secured in the test channel in the configuration shown in 5.3.1.1. Conditions in the calm upstream area permitted the tube to be maneuvered safely into place in the presence of full test channel flow in the interest of expediting test repetitions. Otherwise staging occurred prior to test channel fill.

Note: Steps 2 through 8 refer to tube air/water filling and are referenced in later sections.

2. A length of fire hose was connected to the end of the tube and capped.

3. The tube was filled to the prescribed amount of air by connecting the air compressor to the fire hose and capping it. This step may occur in an empty or flooded test channel.

4. Full test channel flow was developed. This was noted by monitoring the fill level of the channel.

5. The fire hose (previously used for air fill) was uncapped and immediately connected in series with the water meter to the transfer pump, and pump activated. Care was taken to minimize the loss of air pre-fill.

6. The tube was filled with the prescribed amount of water by monitoring the water meter and the pump was shut off.
7. The fire hose was removed at the tube with its port immediately capped to minimize the loss of water.

8. The hose was cleared from the deployment area as to not interfere with tag lines or personnel.

9. Under the direction of the test coordinator, one operator at each of the two tag lines payed out slack to allow the tube to be carried toward the breach.

10. The tube was steered into position holding one tag line and paying out the other to cause the tube to “kite” laterally in the current. Once in position, the lines were equalized to stop lateral motion. The process was repeated as necessary until the tube made contact with the base of the breach.

11. As the tube contacted the breach, lateral variations in position ceased and it began to roll.

12. In the proximity of breach flow the tube began to develop momentum toward the levee and the tag lines were released.

13. The tube was carried toward the breach and up the walls of the levee and settled into position as described in Section 3.2, or washed through if the fill levels were insufficient.

14. If the tube remained in position, the leak rate was estimated based on percentage of surface area of flow compared to the original breach size. These values were estimated visually since more precise measurements would have put personnel at a safety risk.

15. The tube was released by removing any of its plugs that were safely reachable. When it deflated it flowed through the breach for recovery downstream.

16. Two lifting straps were placed around the tube and the forklift was used to retrieve it from the water.

17. All plugs were removed from the tube. Using the forklift it was lifted completely off the ground to drain.

18. At this point, the tube was ready for the next repetition or storage.

Discussion and Results: Table 5.3.1.1 shows the fill quantity combinations for air and water and the corresponding results and observations. This table also encompasses the results from section 5.3.2 pertaining to tube fill amounts.

Test #	Air Fill %	Water Fill %	Estimated Flow Blockage %	Barge Delivery?	Additional Observations/Comments
1	10	60	90	N	Did not roll high enough on levee, good seal on bottom.
2	10	50	90	N	Similar to above. Tube did not roll up levee high enough.
3	10	40	0	N	Tube folded and swept through breach.
4	0	50	90	N	Tube sank, was difficult to work out of sight underwater until it reached levee. Results similar to Test 2.
5	0	45	0	N	Tube came in at an angle, was swept through breach.
6	20	50	95	N	Best seal yet.
7	10	40	0	Y	Barge twisted, one end of tube

					entered breach, swept through.
8	20	60	98	Y	Tube tangled in harness. When harness released from barge, tube rolled up levee forming good seal.
9	20	50	95	Y	Longer lines on harness, worked well but folded in middle and was close to going through breach. Needs more fill.
10	20	60	98	Y	Formed good seal after opening quick releases on harness.
11	30	65	90	Y	One side sticking too high—too much air.
12	20	65	98	Y	This worked well.
13	20	65	98	Y	Changed delivery so tube is released from barge instead of being played from barge with lines. Quick release stuck, but then good seal.
14	20	65	98	Y	Lubed quick release. Very good seal.
15	20	65	98	Y	Repeat of above. Works well.
Breach enlarged by scour during tests with Shallow Breach Tube					
16	20	65	90	N	Poor seal at bottom. Scoured corners need to be re-shaped.
17	20	65	95	N	Better, but would prefer more penetration into breach.
18	20	60	0	Y	Tube did not center in breach, was swept through.
19	20	65	95	N	Works well with larger breach.
20	20	65	90	Y	Worked well, but then hole opened at bottom when water level rose after plugging breach.

Table 5.3.1.1: Tube Fill Amount and Results

Satisfactory results were repeatedly achieved using 65% water and 20% air fill levels. Fill levels of less than 50% water yielded unpredictable results plugging and had the potential of washing through completely. Fill values in excess of 65% water successfully allowed the tube to restrain itself in the breach but allowed more leak rate. The higher fill levels reduced the ability of the tube to conform to the breach profile.

5.3.2 Cross-flow, Barge-Deployed Tube Configuration

The tag lines used to maneuver the tube in Section 5.3.1 were used to secure it to the barge. Release mechanisms were installed at the attachment points to allow the tube to develop momentum in proximity of the breach flow and maintain safe standoff of the barge. Figure 5.3.2.1 shows the staged system.

Figure 5.3.2.1: Barge-Deployed Tube Configuration

The test procedure was as follows:

1. The barge and tube were secured in the test channel in the configuration shown in 5.3.2.1. A tag line at each of the four corners was used to secure and maneuver the barge. Conditions in the calm upstream area permitted them to be maneuvered safely into place in the presence of full test channel flow as necessary. Otherwise staging occurred prior to test channel fill.

2. - 8. Refer to steps 2 through 8 of section 5.3.1.1 for tube filling procedures.

NOTE: The following steps required 7 personnel for deployment; one on each of the four tag lines, one on each of the two release mechanism lines, and one test coordinator.

9. Under the direction of the test coordinator the barge/tube were guided toward the breach using the four tag lines.

10. The barge/tube was steered into position holding one of the two upstream tag lines and paying out the other to cause the barge to “kite” laterally in the current. Once in position, the lines were equalized to stop lateral motion. Some assistance in lateral positioning was provided by the forward two tag lines. The process was repeated as necessary until the tube made contact with the base of the breach.

11. As the tube contacted the breach, lateral variations in position ceased and it began to roll.

12. In the proximity of breach flow the tube began to develop momentum toward the levee and the release mechanisms were triggered.

13. - 18. Refer to steps 13 – 18 of section 5.3.1.1.

Results corresponding to tube air/water fill amounts are included in Table 5.3.1.1.

5.3.3 Shallow Water Spillway

The procedure for deploying was as follows.

1. The anchoring chain was attached to the leading edge of the tarp prior to initiating the test.

2. Water was supplied to the test channel.

3. As the water level approached the “spillover point” of the test levee, the tarp was spread out over the area to be protected. The edge with the anchoring chain was positioned 2ft below the lip of the levee.

4. Anchoring tubes were placed at five attachment points as shown in Figure 5.1.1.

5. The tubes were completely filled with water to complete the installation of the system.

The above procedure required less than 15 minutes to complete. The system sustained 8in of overflow depth across the entire protected area and remained securely in position.

5.3.4 Shallow Water Block Configuration

The Procedure for testing this concept was as follows:

1. Secure one tag line to each end of the tube.

2. Establish flow in the test channel if not already.

3. Fill the tube with the prescribed amount of air and water.

4. Under the guidance of the test director, maneuver the tube into place across the breach as shown in figure 5.3.4.1.

Figure 5.4.3.1: Shallow Water Block Test

The tube was filled completely with water and no air. This amount was initially determined by filling completely with water and maneuvering it into place. Once seated against the levee, the tube was partially drained to increase conformance in the area near the walls and minimize leakage. Two additional tubes were placed at the ends the stop flow in the vicinity of the breach walls. The system stopped the flow through the breach as intended.

6.0 Testing Improvements

The following are suggestions that may ease testing at the next level.

- The tarp used in the spillway concept should be a rough surface to reduce the chance of personnel slipping during deployment and removal.
- For all “blocking” concepts, using an over-filled tube and releasing water after it is seated at the breach will nearly guarantee that it does not wash though. This approach is suited for real world scenarios where exact breach geometry is unknown.
- For all “blocking” concepts, definition of acceptable leakage criteria and acceptability of using additional tubes around edges should be established. Using the additional tubes eased the requirement placed on the “main” tube and reduce the number of test repetitions to achieve a successful blockage.

7.0 Design Improvements

- Reinforcement of the D-rings/line attachment points to the deep breach tube may be necessary in larger scale use. One way of accomplishing this would be to wrap the entire tube with a nylon strap. Instead of D-rings welded to the tube, weld "belt loops" that the strap can be fed through as necessary.

- Develop/analyze breach size and tube fill "formula" (or use an over-fill and drain to fit approach if applicable). Quantify the relationship of water head in tube over the plugged breach to the submerged depth both upstream and downstream (as we initially saw depth until the downstream area drained). The "wedge" shape and effective reduction in volume in the tube in the breach and compressibility effect from air pre-fill may should also be included.

- With consideration given to the effort required in maneuvering all apparatus during testing, determine where the crossover point is where machinery will be required for full scale operation.

8.0 Conclusion

Testing at the 1/4 scale level was successful at validating the effectiveness and functionality of all four concepts. Scale testing at the 1/16 level gave initial insight as to how the tubes interact with water flow in the vicinity of the breach and with the geometric profile of the breach itself. Quarter scale testing built upon this initial evaluation in that test article construction and the subjected forces were a closer replication of full scale parameters. An example of this is the flexibility of the tube material with relation to strength. In order to provide flexibility at the 1/16 scale level, thickness, strength, and durability were compromised.

The Deep Breach Tube configuration was characterized to determine the appropriate fill levels of air and water in the tube. The result of the experimentation was the set of parameters that provided reliable and repeatable deployment and breach flow blockage.

The Deep Breach Barge-Deployed configuration was used to develop and test a maneuvering and release method of the Deep Breach Tube. Once the interactions of the bag, breach, and barge flow were understood, reliable and repeatable results were achieved.

The Shallow Water Spillway allowed the upstream body of water to be relieved without erosion or compromising of the levee. Since this concept is intended to be deployed prior to overtopping, emphasis was placed on team coordination and equipment staging to provide the most efficient and

rapid response. This resulted in a fifteen-minute or less deployment time.

The Shallow Water Blocking Configuration also performed as intended and stopped flow over the breach. The focus of experimentation was to characterize the effect of varying fill levels and the amount that the tube is allowed propagate into the breach. Repeatability and reliability was demonstrated by slightly over filling the tube so that it was retained by the lip of the breach. Use of auxiliary tubes provided a reliable seal at the ends of the main tubes. The fact that the bag is retained along its entire length by the lip of the levee allows this concept to be deployed over long distances, limited only by practicality handling and deployment.

The knowledge gained and data acquired in scale testing thus far provides a necessary basis for future larger scale testing. Coupled with additional analysis and suitable test facilities, further development of the concepts to meet the requirements of full scale implementation may be achieved.